MOLECULAR AND GENETIC ANALYSIS OF PARKIN IN MICROGLIAL ACTIVATION AND INFLAMMATION-RELATED NEURODEGENERATION

APPROVED BY SUPERVISORY COMMITTEE

Malú Tansey, Ph.D.

Matthew S. Goldberg, Ph.D.

Zhijian Chen, Ph.D.

David Farrar, Ph.D.

Gang Yu, Ph.D.

DEDICATION

This is dedicated to my family for their love and support

and

to my husband (to be) Andy.

MOLECULAR AND GENETIC ANALYSIS OF PARKIN IN MICROGLIAL ACTIVATION AND INFLAMMATION-RELATED NEURODEGENERATION

by

THI ANH TRAN

DISSERTATION

Presented to the Faculty of the Graduate School of Biomedical Sciences

The University of Texas Southwestern Medical Center at Dallas

In Partial Fulfillment of the Requirements

For the Degree of

DOCTOR OF PHILOSOPHY
The University of Texas Southwestern Medical Center at Dallas

Dallas, Texas

March, 2010

MOLECULAR AND GENETIC ANALYSIS OF PARKIN IN MICROGLIAL ACTIVATION AND INFLAMMATION-RELATED NEURODEGENERATION

THI ANH TRAN

The University of Texas Southwestern Medical Center at Dallas, 2010

MALU TANSEY, Ph.D.

Parkinson's disease (PD) is a progressive, neurodegenerative disease characterized by the loss of dopaminergic (DA) neurons in the substantia nigra (SN). Genetic mutations account for only 5-10% of PD cases. Oxidative stress and inflammation have both been linked to sporadic PD. Inflammation-induced injury to dopaminergic neurons can be significantly attenuated by impairment of microglial activation. In addition, previous studies from our lab reported that *parkin*$^{-/-}$ mice are more susceptible to inflammation-induced degeneration of nigral DA neurons. Therefore, inflammatory responses are a critical determinant of DA neuronal survival.

Microglia support neuronal survival by providing trophic factors and phagocytosing debris. However, with chronic inflammation glia release chemical mediators which are toxic to surrounding neurons. Our data provide evidence that Parkin is a negative regulator of microglial activation. *parkin*$^{-/-}$ mice display increased cytokine expression in the midbrain and increased cytokines in the serum suggesting *parkin*$^{-/-}$ mice are basally inflamed.

Parkin loss-of-function mutations are linked to autosomal recessive PD. The *parkin* gene encodes an E3 ubiquitin ligase linked to mitochondrial dysfunction. Most studies on Parkin concentrate on its role in neurons, however, we hypothesize that Parkin function in microglial activation and inflammatory signaling also affect DA neuron survival. Our biochemical analyses of primary wild type microglia show Parkin expression is negatively regulated by inflammatory stimuli. Pharmacological or genetic inhibition of NF-κB, a transcription factor activated by inflammatory stimulation, blocks the inflammation-induced decrease in Parkin levels. Additionally, our data suggests that NF-κB may bind the parkin promoter, further implicating Parkin function in the inflammatory activation pathway.

These novel findings suggest that in a normal cell experiencing inflammation, the decreased expression of Parkin, which has been shown to antagonize apoptotic signaling cascades, may render the cell more susceptible to death. Additionally, sources of inflammation including environmental triggers, infection, or traumatic injury could cause a normal individual to have the same susceptibility to PD as an individual with an inherited mutation, because inflammation leads to Parkin loss of function.

ACKNOWLEDGEMENTS

During these brief years at UT Southwestern, I have learned and grown much as a scientist and as a person. I am indebted to family, friends, and peers for their support, patience and stimulating conversations about biology and life in general. First, I would like thank my mentor Malú Tansey for finding a place for me in her lab when I was struggling, and for believing in my potential. I am grateful that she provided an environment to arm me with the technical skills, critical eye and the confidence that I would need to succeed in this field. I would not have finished with a smile still on my face without her encouragement when the science was not working quite right, her beatings with the wet noodle to remind me of the caliber of excellence that was expected, and her overall enthusiasm. I would also like to thank my committee members Dr. David Farrar, Dr. James Chen, Dr. Gang Yu, and my chair Dr. Matt Goldberg for taking the time to discuss projects and share their expertise, as well as offer support and reagents to see those projects to completion. I would also like to thank Dr. Melanie Cobb, Dean of the Graduate School, and Nancy McKinney for keeping me on track, and for their sincere concern in my development.

Special thanks go out to Tansey lab members past and present for being helpful and making the lab environment so enjoyable. I am grateful for Dr. Jae Lee and Dr. Laura Alto for their patience in teaching me techniques, their valuable input on my projects, and advice on how to survive graduate school. I would also like to thank the previous graduate students Dr. Phil Wrage, Dr. Melissa McCoy and Dr. Fiona McAlpine for

paving the way in the lab, and especially Terina Martinez and Ashley Harms for their friendship and support as we journeyed together, and their willingness to make chocolate runs when the road was rough. Special thanks to our lab manager Kelly Ruhn for not letting me crowd the freezer, and teaching me about mice, soccer and how not to be so type A.

I am grateful for my friends who helped me balance work and play by sprinkling in art and music. Thank you to my former roommates for leaving the light on when I would work late, and sharing cold pizza and warm cups of coffee. Grad school would not have been the same without my graduate school classmates and peers, so thanks for all the camaraderie and karaoke. Thank you most especially to my grad school peer turned significant other, Andy, for inspiring me not only by his incredible work ethic and intellect, but by his infinite patience through this writing process.

Finally, I am here because of the unwavering love of my parents Tu and Anne, my brothers Kiet and Hieu, and my incredible aunts, uncles and cousins. Thanks Mom for packing me dinners and sending me sunshine in all the ways that you did. Thanks Dad for cultivating my curiosity in life and fostering an attitude in which I need not fear the unknown.

TABLE OF CONTENTS

PRIOR PUBLICATIONS

Tran TA, Nguyen AD, Goldberg MS, and Tansey MG. Parkin expression is negatively regulated by inflammatory signaling and loss of parkin results in chronic activation of microglia. *In Preparation for submission to Glia.*

Tran TA[#], Martinez TN[#], Frank-Cannon TC[#], Marvin M, Ruhn KA, Hong J, Trevino I, Casey B, Tansey MG, Goldberg MS. (2009) DJ-1 deficiency does not increase vulnerability to inflammation-related nigral degeneration*. In preparation for submission to Neurobiology of Disease.*
[#] Equal contribution

Lee, J.K., **Tran, T.A**., and Tansey, M.G. (2009), Neuroinflammation in Parkinson's Disease. [Review] J Neuroimmunepharmacology. 10 Oct ePub

Frank-Cannon TC, **Tran TA**, Ruhn KA, Martinez TN, Hong J, Marvin M, Hartley M, Trevino I, Casey B, Goldberg MS, Tansey MG. (2008) Parkin Deficiency Increases Vulnerability to Inflammation-Related Nigral Degeneration. J Neuroscience, 28(43):10825–10834.

Tran T[#], McCoy M[#], Sporn M, and Tansey M. (2008) The synthetic triterpenoid CDDO-Methyl ester modulates microglial activities, inhibits TNF production, and provides dopaminergic neuroprotection. J NeuroInflamm, 5:14.
[#] Equal contribution

Wrage PC[#], Tran T[#], To K[#], Keefer EW, Ruhn KA, Hong J, Hattangadi S,Trevino I, Tansey MG. (2008) The Neuro-Glial Properties of Adipose-Derived Adult Stromal (ADAS) Cells Are Not Regulated by Notch 1 and Are Not Derived from Neural Crest Lineage. PLoS ONE 3(1): e1453. doi:10.1371/journal.pone.0001453
[#] Equal contribution

Tansey M, Frank-Cannon TC, McCoy MK, Lee JK, Martinez TN, McAlpine FE, Ruhn KA, **Tran TA**. (2007) Neuroinflammation in Parkinson's Disease: Is there sufficient evidence for mechanism-based interventional therapy? Frontiers in Bioscience 13, 709-717.

LIST OF FIGURES

LIST OF APPENDICES

LIST OF DEFINITIONS

AD – Alzheimer disease

Aβ – amyloid beta

ALS – amyotrophic lateral sclerosis

APC – antigen presenting cell

ARPD – autosomal recessive juvenile Parkinson's disease

BDNF – brain derived neurotrophic factor

CNS – central nervous system

CB – cerebellum

CSF – cerebral spinal fluid

ChIP – chromatin immunoprecipitation

CFU – colony forming unit

CM – conditioned media

CX – cortex

CDDO – 2-cyano-3,12-dioxooleana-1,9,-dien-28-oic acid

CDDO-Me – 2-cyano-3,12-dioxooleana-1,9,-dien-28-oic acid methyl ester

cdk – cyclin-dependent kinase

COX – cyclooxygenase

DIV – days *in vitro*

DLBD – diffuse Lewy body disease

MTS – 3-(4,5-dimethylthiazol-2-yl)-5-(3-carboxymethoxyphenyl)-2-(4-sulfophenyl)-2H-tetrazolium, inner salt

DA – dopaminergic

EL – encephalitis lethargic

ER – endoplasmic reticulum

EEAT2 – excitatory amino acid transporter 2

FTD – Frontotemporal dementia

GDNF – glial derived neurotrophic factor

GLT1 – glutamate transporter 1

GM-CSF – granulocyte and macrophage colony stimulating factor

HPLC – high performance liquid chromatography

HO-1 – heme-oxygenase-1

6-OHDA – 6-hydroxydopamine

IKK – IκB kinase

IBR – inbetween ring

iNOS – inducible nitric oxide synthase

IκB – inhibitor of κB

IOD – integrated optical density

IFNg – interferon gamma

IL – interleukin

IL1R – interleukin 1 receptor

inTNF – intranasal tumor necrosis factor

i.p. – intraperitoneal

Iba1 – ionized calcium binding adaptor molecule 1

LB – Lewy body

JEV – Japanese encephalitis virus

KC – keratinocyte-derived chemokine

LPS – lipopolysaccharide

LM – Listeria monocytogenes

MAVS – mitochondrial antiviral signaling

M-CSF – macrophage colony stimulating factor

MPTP – 1-methyl-4-phenyl-1,2,3,6-tetrahydropyridine

MPP+ – 1-methyl-4-phenylpyridinium

MP – mononuclear phagocyte

ANOVA – multiple-way analysis of variance

NQO1 – NAD(P)H:quinone oxidoreductase

NE – nasal epithelia

NeuN – neuronal nuclear antigen

Nrf2 – NF-E2 related factor

NO – nitric oxide

NSAID – non-steroidal anti-inflammatory drug

NF-κB – nuclear factor κB

OB – olfactory bulb

OE – overexpression

PMS – phenazine methosulfate

PBS – phosphate-buffered saline

PET – positron emission tomography

PEP – post-encephalitic Parkinsonism

PINK1 – PTEN-induced kinase 1

QPCR – quantitative real-time polymerase chain reaction

RNS – reactive nitrogen species

ROS – reactive oxygen species

RING – really interesting new gene

RGS10 – regulator of G protein signaling 10

Rh-TNF – rhodamine-labeled human tumor necrosis factor

SEM – standard error of the mean

SN – substantia nigra

SOD – superoxide dismutase

tk – thymidine kinase

TLR4 – toll like receptor 4

TLCK – N-α-tosyl-L-lysine chloromethyl ketone

TBS – Tris-buffered saline

TBST – Tris-buffered saline with 0.2 % Triton X-100

TNF – tumor necrosis factor

TNF R1– tumor necrosis factor receptor 1

TNF R2– tumor necrosis factor receptor 2

TH – tyrosine hydroxylase

UPS – ubiquitin proteasome system

UBL – ubiquitin-like

UPR – unfolded protein response

MB – ventral midbrain

VTA – ventral tegmental area

CHAPTER ONE

Introduction

Parkinson's disease

Clinical features

Parkinson's disease (PD) is a chronic and progressive neurodegenerative disorder affecting approximately 3% of the adult population over 65 years of age (Lang and Lozano 1998; Fahn 2003; Whitton 2007). Clinically, PD is recognized by the symptoms of tremor, rigidity, postural instability, and bradykinesia initially described by James Parkinson in 1817 in his *An Essay on the Shaking Palsy*. In 1861, Jean-Martin Charcot expanded on these findings, and cemented Parkinson's place in history by naming the disorder after Parkinson (Goetz 1986)**.** Motor symptoms also include gait freezing or the inability to move the lower extremities for a few seconds at a time, speech disturbances and difficulties swallowing. Non-motor effects include cognitive and psychiatric disturbances such as depression and increased risk taking behavior (Jankovic 2008).

Pathophysiology

The progression of PD pathology is thought to begin in the vagus nerve and progress to brain stem, midbrain, basal forebrain, and finally to the cortex (Braak, Rub et al. 2003). However, PD is primarily characterized by degeneration of dopamine-producing neurons in the substantia nigra pars compacta (SNpc) in the ventral midbrain (Lang and Lozano 1998). Nigral dopaminergic (DA) neurons project to the striatum, the output of which

regulates motor behavior. The direct nigrostriatal pathway signals movement while the indirect pathway signals inhibition. The loss of the nigrostriatal pathway leads to inhibition of the direct pathway and excitation of the indirect pathway, the combination of which leads to hypokinesia. Additional pathological hallmarks of PD include the presence of Lewy bodies (LBs), intracytoplasmic inclusions, and Lewy neurites, degenerated neuronal processes (Forno 1996). Although LBs are associated with PD pathology, the toxicity of LBs is still under debate because the presence of these intraneuronal inclusions is found in the surviving cells in the postmortem brains of PD patients (Jellinger 2009). Additionally, LBs are not found in all cases of PD, are reported in cases of Alzheimer's disease, and LBs are even found in healthy aged individuals with no symptoms of Parkinsonism (Jellinger 2009). PD is considered a sporadic movement disorder and although disease etiology is largely unknown, advances from studies of genetics, epidemiology, and neuropathology have contributed to our understanding of the disease.

Etiology - Genetics

Genes linked to familial PD include those inherited in an autosomal dominant pattern including *alpha synuclein* (SYN), *leucine-rich repeat kinase 2* (LRRK2), and *ubiquitin carboxy-terminal hydrolase L1* (UCHL1). Autosomal recessive PD (ARPD) genes include *parkin*, *PTEN-induced kinase 1* (Pink1), and *DJ-1*. Mutations in the *SYN* gene (PARK1/4) cause autosomal dominant Parkinsonism (Polymeropoulos, Lavedan et al. 1997). SYN is expressed ubiquitously in the human brain, and *in vitro* studies have shown that alpha synuclein localizes to synaptic terminals and is important in vesicle

recycling and synaptic function (Irizarry, Kim et al. 1996; Abeliovich, Schmitz et al. 2000; Kahle, Neumann et al. 2000). Mutations in the gene encoding p*arkin* (PARK2) account for more than half of early onset autosomal recessive cases of Parkinsonism (Abbas, Lucking et al. 1999; Lucking, Durr et al. 2000). Parkin is also ubiquitously expressed in the human brain (Kitada, Asakawa et al. 1998), and has been shown to function as an E3 ubiquitin ligase (Imai, Soda et al. 2000; Shimura, Hattori et al. 2000; Zhang, Gao et al. 2000). The contributions of these proteins to PD pathology are discussed below. Once thought to be a sporadic disease, identification of genetic mutations in several families has led to a better understanding of disease etiology. Despite the discovery that PD can be inherited in a Mendelian fashion, the truth remains that genetic mutations account for less than 10% of total PD cases (Mizuno, Hattori et al. 2001; Farrer 2006). The minimal contribution of genetic inheritance to PD has lead to the development of hypotheses in which environmental insults such as oxidative stress and inflammation contribute to the onset and progression of sporadic PD.

Etiology – Infections

In the 1920s an epidemic of encephalitis lethargic (EL) left infected patients with a disease described as Post-encephalitic Parkinsonism (PEP), because infected patients experienced motor symptoms similar to idiopathic PD. EL was characterized by neurologist Constantin von Economo with the peculiar observance that the symptoms of PEP appeared years after the illness was contracted and resolved (Dale, Church et al. 2004). In the 1920s and 30s, PEP accounted for about 50% of all parkinsonism cases (Josephs, Parisi et al. 2002). The cause of EL was unknown until evidence implicated a

mutant strain of the streptococcus bacteria that was also observed to cause basal ganglia dysfunction (Dale, Church et al. 2004). Moreover, EL was long associated with the pandemic of Spanish flu at the time, but identification of the flu virus allowed researchers to later conclude that EL and the Spanish influenza had different causes as postmortem brain samples from EL patients were negative for RNA from the Spanish influenza (Taubenberger, Reid et al. 1997).

Though PEP caused by EL was subsequently linked to bacterial origins, viral encephalitis is also associated with causing symptoms of Parkinsonism. In India, China, and Southeast Asia, patients infected with Japanese encephalitis virus (JEV) for longer than 1 year were also likely develop post-encephalitic parkinsonism (Shoji, Watanabe et al. 1993). Even if patients resolved an acute episode of "summer encephalitis" they were likely to develop persistent neurological symptoms (Dourmashkin 1997). Experimentally, JEV has been used to create a pre-clinical model of post-encephalitic parkinsonism in rats (Ogata, Tashiro et al. 1997) in which JEV induces brain catecholamine (dopamine and norepinephrine) depletion and severe hypokinesia (Hamaue, Ogata et al. 2006). Since the initial reports of PEP by von Economo, other cases of PEP have been reported with the common theme that "idiopathic Parkinsonism itself might be caused by encephalitis, perhaps acquired years earlier" (Rail, Scholtz et al. 1981). Recent work reported that a peripheral infection of avian influenza H5N1 caused neuroinflammation and subsequent loss of DA in the SN (Jang, Boltz et al. 2009). The implications of these studies are that challenges to the immune system may create vulnerability in the central nervous system

that over time, and with the insults of the normal aging process, may lead to neurodegeneration.

Etiology – Mitochondrial toxins

In 1976, a chemical contaminant in homemade heroin gave its users symptoms of Parkinsonism while giving the scientific field a clue into the pathogenesis of Parkinson's disease. The contaminant, 1-methyl-4-phenyl-1,2,3,6-tetrahydropyridine (MPTP), is metabolized to a more toxic form 1-methyl-4-phenylpyridinium (MPP+) which inhibits Complex I of the mitochondrial transport chain and ultimately prevents generation of ATP. Furthermore, chronic treatment of another mitochondrial complex I inhibitor, the pesticide rotenone, increased nigral-specific degeneration of DA neurons in rats with evidence of hypokinesia (Betarbet, Sherer et al. 2000). An epidemiological study conducted in France showed that individuals exposed to the combination of paraquat and maneb, an herbicide and fungicide, within 500 meters of their home had a 75% increased incidence of PD (Costello, Cockburn et al. 2009). An independent study conducted by the American Cancer Society also reported that individuals exposed to pesticides had a 70% increased risk of PD compared to individuals not exposed, and compared to exposure of other toxins such as coal, asbestos, and formaldehyde (Ascherio, Chen et al. 2006). MPTP, rotenone, paraquat and maneb are now used experimentally in animal models to study mitochondrial metabolism and respiration, and inflammation in the pathology of PD.

PD-associated genes and biological functions

Mitochondrial metabolism and respiration can also be linked to the functions of several PD-linked genes. PINK1, DJ-1, and Parkin have been shown to localize to the mitochondrial membrane and provide protection against oxidative stress-induced cellular damage (Canet-Aviles, Wilson et al. 2004; Valente, Abou-Sleiman et al. 2004; Silvestri, Caputo et al. 2005; Narendra, Tanaka et al. 2008; Junn, Jang et al. 2009). In addition to mitochondria associated functions, PD-linked genes also function in protein degradation and oxidation.

Protein aggregation and degradation

The ubiquitin proteasome system (UPS) is a means by which the cell degrades proteins in normal cellular processes such the cell cycle regulation and signal transduction (Hershko and Ciechanover 1998). Importantly in PD, the UPS is critical in removing damaged and misfolded proteins. Treating rats with proteasome inhibitors can lead to behavioral manifestations of Parkinsonism as well as the pathological presence of alpha synuclein-containing LBs and degeneration of the nigrostriatal pathway (McNaught, Perl et al. 2004). Conversely, a study in Drosophila in which a molecular chaperone was overexpressed, either genetically or through pharmacological induction, led to attenuated pathological and motor features generated by overexpression of mutant or wild type *SYN* (Auluck, Chan et al. 2002). Overt inhibition of the UPS can lead to cellular toxicity in general, so the link between UPS dysfunction and PD was strengthened when PD-linked genes were also observed to display abnormalities in protein folding and ubiquination. Alpha synuclein and ubiquitin are present in LBs (Spillantini, Crowther et al. 1998;

Shults 2006). Familial mutations (A53T, A30P) lead to oligomerization and aggregation of mutant *SYN* (Conway, Harper et al. 1998). Similarly, wild type alpha synuclein aggregates in the presence of mitochondrial toxins rotenone and paraquat (Sherer, Betarbet et al. 2002; Sherer, Kim et al. 2003). The *parkin* gene, which encodes a ubiquitin E3 ligase (Imai, Soda et al. 2000; Shimura, Hattori et al. 2000; Zhang, Gao et al. 2000), and UCHL1, a deubiquitinating enzyme (Leroy, Boyer et al. 1998), function in protein degradation further implicating the UPS in disease etiology. Parkin function is discussed in detail below.

Protein oxidation

DJ-1 is ubiquitously and abundantly expressed in the brain (Bandopadhyay, Kingsbury et al. 2004). The familial loss-of-function mutation L166P leads to DJ-1 misfolding and degradation by the proteasome (Bonifati, Rizzu et al. 2003; Miller, Ahmad et al. 2003; Moore, Dawson et al. 2003; Olzmann, Brown et al. 2004). DJ-1 has structural similarity to cysteine proteases, and has been shown to function as an active protease, although no substrates have been identified (Tao and Tong 2003). Overexpression of DJ-1 in cultured cells protects against oxidative stress while acute knockdown of DJ-1 decreases cell viability after oxidative stress (Taira, Saito et al. 2004). DJ-1 may also serve as a direct scavenger for ROS because oxidative stress leads to oxidation of the DJ-1 protein (Mitsumoto and Nakagawa 2001; Canet-Aviles, Wilson et al. 2004; Taira, Saito et al. 2004). Oxidative and nitrosative stress also leads to modifications of other PD-linked genes. Alpha synuclein and parkin are modified by nitrosylation (Giasson, Duda et al. 2000), a modification by nitric oxide, which promotes alpha synuclein aggregation

(Ischiropoulos and Beckman 2003), or results in loss of Parkin E3 ubiquitin activity (Chung, Thomas et al. 2004; Yao, Gu et al. 2004).

Common to these studies is the focus on the normal biological function of PD-associated genes in the context of neuronal viability. Neurons are a logical target of investigation because neuronal death leads to motor impairment in the patients. Nonetheless the PD field is recognizing the role of supporting cells in the brain such as the microglia and astrocytes, and research has begun to look at the role of PD-associated genes in these cell types.

PD-associated genes and microglia function

In a paradigm-shifting study, authors elucidated the role of Nurr1 in microglia and astrocytes (Saijo, Winner et al. 2009). Nurr1 was previously identified as an orphan nuclear hormone receptor important in the development of DA neurons (Zetterstrom, Solomin et al. 1997). Lentiviral knockdown of Nurr1 in microglia and astrocytes led to the increased production and secretion of cytokines and nitric oxide. Nurr1-null animals challenged with an injection of the bacterial endotoxin lipopolysaccharide (LPS) into the substantia nigra (SN) developed degeneration of DA neurons (Saijo, Winner et al. 2009). These studies suggest that Nurr1 not only plays a role in neuronal development but in glial activation and mediation of neuronal health. Additionally, inflammation induced by a single LPS injection into the SN of a mouse model that overexpresses mutant human SYN (A53T), led to significant loss of dopaminergic neurons (Gao, Kotzbauer et al. 2008). In contrast to the above studies in which inflammation was induced directly in the

central nervous system, a model of systemic inflammation also resulted in specific loss of neurons in the SN. Parkin-/- mice given intraperitoneal LPS injections showed increased vulnerability to endotoxin-induced degeneration of dopaminergic neurons in the SN, as well as fine motor impairment (Frank-Cannon 2008). In the studies of LPS injection in the SYN-overexpressing mouse or the Parkin knockout mouse, both independent groups showed no enhanced microglial activation by immunohistochemical staining for microglial surface markers or quantitative PCR for expression of microglial markers. Furthermore, the absence of infiltrating leukocytes suggests the blood brain barrier was not compromised in these models of inflammation, and that the adaptive immune response did not contribute to the loss of TH neurons.

Although these studies demonstrate the importance of the neuroimmune response in the loss of SN dopaminergic neurons, the authors do not directly implicate microglia as the cell type specifically responsible for the neuropathology. However, in a mouse model of amyotrophic lateral sclerosis (ALS), another neurodegenerative disease, microglia dysfunction was directly linked to disease pathology. Selective deletion of the anti-oxidant gene superoxide dismutase 1 (SOD1) in microglia resulted in the death of motor neurons. On the other hand, conditional deletion of SOD1 in neurons only did not produce pathology in mice (Boillee, Yamanaka et al. 2006). These studies directly demonstrate that dysregulation of disease-associated genes in microglia can result to neurodegeneration, because microglia are critical to the health and functioning of DA neurons. Moreover, the study supports the idea that the “neighborhood matters”. After all, glial cell types account for 90 percent of the brain.

Microglia

The brain-resident macrophage

In the 1880s Nissl staining showed that microglia and macrophages are related cell types. In 1919, Pio del Rio-Hortega, who is considered the Father of Microglia and a former student of Santiago Ramon y Cajal, characterized microglia in detail; distinguishing microglia from other glia cell types. Microglia make up 10% of the glial population in the brain (McGeer and McGeer 2008) and are present in high numbers in the midbrain (Lawson, Perry et al. 1990). Microglia, like macrophages, are monocytes derived from bone marrow progenitors. Microglia and macrophages are classified as mononuclear phagocytes (MPs), which contribute to the body's innate immune response against pathogens, tissue damage and infection by migrating to sites of injury and removing cellular debris by phagocytosis (Kreutzberg 1996; Mosley, Benner et al. 2006).

In addition to reacting to invading pathogens, MPs have been shown to be essential for tissue repair by releasing growth factors and trophic factors. Since the identification and description of microglia in the brain, the idea that the brain is immune-privileged has been disproved. Although microglia are weak antigen presenting cells, this allows these immune-competent cells to perform the beneficial functions of phagocytosis and scavenging without actively recruiting leukocytes to brain (Carson, Reilly et al. 1998; Streit 2002). The brain has pruned its requirements for a functioning mononuclear phagocyte as described. This is not uncommon as other tissues such as lung and liver

have evolutionarily dictated the specialized function of the macrophages resident to that specific tissue types (Kumpher, thymic, perivascular, alveoloar, arterial, etc).

Studies report that the parenchymal microglia population in the CNS can be replenished through migration of macrophages from the periphery. These populations of monocytes can be distinguished by levels of $CD45^{hi}$ or $CD45^{low}$ staining; $CD45^{low}$ represents the parenchymal microglia (Dick, Ford et al. 1995; Ford, Goodsall et al. 1995). CD45 is a tyrosine phosphatase present of the cell surface. $CD45^{hi}$ macrophages that migrate into the CNS are stronger antigen presenting cells (APCs), and therefore it is suggested that macrophage recruitment to the brain is indicative of chronic and severe neuroinflammation, because these macrophages are more likely to present antigen and recruit T cells to the brain (Carson, Reilly et al. 1998). In general however, these cell types have similar morphology, cell surface receptor expression and most importantly, immune effector functioning.

Biological function

The main functions of MPs are to respond to cellular injury or pathogen invasion in order to prevent persistent tissue toxicity. To sample the microenvironment and migrate to areas of injury MPs express complement and scavenge receptors as well as cytokine and chemokine receptors to detect chemical gradients created by cytokines and chemokines (Nimmerjahn, Kirchhoff et al. 2005). MPs not only detect but secrete cytokines and chemokines upon stimulation, as well as prostaglandins, matrix metalloproteases (MMPS), cyclooxygenase (COX) enzymes and reactive oxygen and nitrogen species

(Kreutzberg 1996; Mosley, Benner et al. 2006). MPs also express purogenic receptors (P2Y12 and P2Y6) to sense the ATP released from dying cells. MPs migrate towards ATP and excitotoxic stress caused by treatment of kainic acid causes death in neuronal populations while leading to increases in P2Y6 mRNA in rat (Inoue 2002; Inoue 2007). MPs also respond to excitotoxic stress by clearing glutamate in the extracellular space through glutamate transporter 1 (GLT1, aka excitatory amino acid transporter 2 (EEAT2)). Microglia only express EEAT2, while astrocytes express both EEAT1 and EEAT2, and microglia-mediated glutamate uptake is only shown to equate roughly 10% of astrocyte uptake (Nakajima, Tohyama et al. 2001; Persson, Brantefjord et al. 2005). Nonetheless, the presence of GLT1 may serve a divergent function in microglia compared to astrocytes because the presence of tumor necrosis factor (TNF), an inflammatory cytokine, can halt astrocyte-mediated glutamate uptake while TNF increases monocyte-mediated glutamate uptake (Fine, Angel et al. 1996; Rimaniol, Haik et al. 2000; Liao and Chen 2001).

In addition to these pro-inflammatory factors, MPs also release anti-inflammatory cytokines such as IL-4 and IL-10. Exogenous addition of IL-10 reduces the release of pro-inflammatory cytokines and nitric oxide by mixed glial cultures treated with LPS (Molina-Holgado, Grencis et al. 2001; Kremlev and Palmer 2005). Furthermore, levels of circulating IL-10 are elevated in serum from PD patients, which the authors suggest is increased to counteract the increased levels of inflammation (Rentzos, Nikolaou et al. 2009). Microglia also produce trophic factors such as glial derived neurotrophic factor (GDNF) and brain derived neurotrophic factor (BDNF) which are essential in the process

of wound repair and tissue homeostasis (Nakajima and Kohsaka 2004). GDNF and BDNF are produced by microglia in response to neuronal injury (Lai and Todd 2008), and are shown to aid in the sprouting of striatal DA neurons post injury (Batchelor, Liberatore et al. 1999).

Microglial activation

The complex network of chemical reactions produced by microglia in response to injury is one measure of microglial activation. Microglia phenotype and activation of signaling pathways are also means to determine the microglial activation status. Morphologically, resting microglia have small cell bodies and few ramified processes. Upon activation, microglia become hypertrophic as the cell body enlarges and becomes ameboid-like, while the processes retract (Kreutzberg 1996; Mosley, Benner et al. 2006). Activation is also correlated with increased proliferation. Several intracellular signaling pathways are associated with microglia production of pro-inflammatory cytokines, and of particular relevance to the following experiments is activation of the transcription factor nuclear factor κB (NF-κB). NF-κB is inactive in the cytoplasm when bound to an inhibitor of κB (IκB) family member. Stimulation by LPS and TNF can lead to degradation of IκB and release of NF-κB to translocate from the cytoplasm to the nucleus, which induces synthesis of pro-inflammatory cytokines (Karin and Ben-Neriah 2000). Induction of NF-κB is important in inflammatory signaling in microglia and macrophages (Kaltschmidt, Kaltschmidt et al. 1994; Vallabhapurapu and Karin 2009).

Neuroinflammation

Microglia role in Neuroinflammation

In the central nervous system, microglia are the major players in generating and resolving neuroinflammation (Kreutzberg 1996; Mosley, Benner et al. 2006). Inflammation is the process by which the body responds to pathogens, infections and tissue damage to eliminate the harmful agent while healing the tissue. Inflammation can be categorized into acute (short term) and chronic (prolonged) inflammation and is initiated systemically by macrophages and dendritic cells with the release of pro-inflammatory cytokines, interleukins, and prostaglandins. While acute inflammation is necessary for the initial process of tissue repair and wound healing, as discussed above in the example of facial nerve axotomy, chronic inflammation has been associated with diseases such as cancer, heart disease, autoimmune disorders such as psoriasis and rheumatoid arthritis, and neurodegenerative disorders.

Chronic Neuroinflammation

Microglial activation is critical in regulating immune system homeostasis, and studies have shown that inhibition of microglial activation can impede injury repair responses depending on the timing of inhibition. On the other hand, chronic activation of microglia leads to prolonged secretion of cytokines and chemokines that is considered neurotoxic. Taking into consideration the beneficial aspect of microglial activation, it is the distortion of the activation pathway, and possible over-extension of cellular function, that turns the release of microglia-derived biological chemicals into toxic species. Another distortion of

microglial activation is premature biological aging, or senescence, in which microglial activation is dampened and the lack of supporting function may contribute to neuronal death (Streit 2006). Aberrant microglial activation is observed in models of PD including MPTP, rotenone, paraquat/maneb, and LPS (Liu and Hong 2003; Bartels and Leenders 2007). Furthermore, genetic or pharmacological inhibition of microglia mitigates toxin-induced death.

Neuroinflammation in PD

The hypothesis that microglial activation contributes to neuronal viability has been explored in other neurodegenerative diseases. Microglial activation was first described in Alzheimer disease (AD) patients over 20 years ago, and is also observed in postmortem brain tissue of PD patients (McGeer, Itagaki et al. 1988; Yamada, McGeer et al. 1992; Croisier, Moran et al. 2005). It is unclear, however, whether microglial activation is a result of the neuronal degeneration or a contributor to the onset of the disease (McGeer, Itagaki et al. 1988; Banati, Daniel et al. 1998; Hunot, Dugas et al. 1999; Cassarino, Halvorsen et al. 2000; Pavese, Gerhard et al. 2006; Whitton 2007). Though the debate continues, the evidence for activation of microglia in PD patients is abundant and robust in imaging, pathological, genetic, and epidemiological studies. *In vivo* positron emission tomography (PET) imaging studies of idiopathic PD patients show increased microglial activation in the pons and basal ganglia, brain regions most affected by PD, compared to healthy, age-matched controls (Gerhard, Pavese et al. 2006). In a follow up study, the same PK11195 ligand which binds benzodiazepine receptors on microglia was increased in PD patients as binding of a ligand to dopamine transporter was decreased (Ouchi,

Yoshikawa et al. 2005). The authors of this study concluded that the degree of microglial activation was inversely correlated with DA neuron viability. Therefore, microglia may become and remain activated early in the disease process, possibly contributing to disease progression (for review see (Tansey, McCoy et al. 2007; Whitton 2007).

In addition to the presence of activated microglia, elevated levels of pro-inflammatory mediators are detected in the cerebral spinal fluid (CSF) and serum of PD patients (Mogi, Harada et al. 1994; Blum-Degen, Muller et al. 1995; Mogi, Harada et al. 1996; Nagatsu and Sawada 2005; McGeer and McGeer 2008). The increased levels of cytokines could result from aging, exposure to environmental toxins or genetic susceptibility. For example, a population-based study revealed that individuals with polymorphisms in the genes encoding *TNF* and *IL1b* had increased expression of these cytokines, and a two-fold increased susceptibility of developing PD (Wahner, Sinsheimer et al. 2007). In support of the pathological studies of microglial activation and inflammation in PD etiology, epidemiological studies have shown that individuals on chronic regimens of non-steroidal anti-inflammatory drugs (NSAIDs) have up to a 45% lower risk of PD (Chen, Zhang et al. 2003; Chen, Jacobs et al. 2005; Samii, Etminan et al. 2009).Taken together, these findings strongly implicate neuroinflammation as a major factor in PD.

Parkin

Historical perspective

In 1998, deletions in the *parkin* gene were identified in Japanese families with autosomal recessive juvenile Parkinson's disease (ARPD) (Hattori, Kitada et al. 1998; Kitada, Asakawa et al. 1998). Point mutations, exon deletions and truncations, and duplications in the *parkin* gene are responsible for more than half of ARPD cases (Lucking, Durr et al. 2000). The average onset for a patient with *parkin* mutations is 32-38 +/- 12 years old (Abbas, Lucking et al. 1999; Lucking, Durr et al. 2000), while the average age for onset in patients without *parkin* mutations is 42 +/- 11 years old. Analysis of postmortem brains of PD patients with *parkin* mutations revealed the absence of LBs (Shimura, Hattori et al. 1999; Hayashi, Wakabayashi et al. 2000; Shimura, Hattori et al. 2000; Yamamura, Hattori et al. 2000). However, isolated cases report *parkin* loss-of-function mutations with LBs (Farrer, Chan et al. 2001; Pramstaller, Schlossmacher et al. 2005).

Parkin structure and function

Parkin is a 465 amino acid protein with a molecular mass of 52 kDa. Parkin is highly expressed in heart, testis, brain and skeletal muscle (Kitada, Asakawa et al. 1998). At the protein level, parkin is 85-95% conserved between the human, rat and mouse (D'Agata, Zhao et al. 2000; Gu, Abbas et al. 2000; Kitada, Asakawa et al. 2000). At the amino terminus is the Ubiquitin-like (UBL) domain and at the carboxyl terminus two RING (Really Interesting New Gene) domains flank an IBR (Inbetween Ring) domain (Morett and Bork 1999). Proteins containing RING domains are identified as E3 ligases, targeting

proteins for degradation by the ubiquitin proteasome system (Hershko and Ciechanover 1998). Parkin was identified to have E3 ubiquitin ligase activity, and *parkin* mutations in patients resulted in the loss of E3 activity (Imai, Soda et al. 2000; Shimura, Hattori et al. 2000; Zhang, Gao et al. 2000).

Post-translational modification

Parkin is capable of self-ubiquitination and signaling its own degradation (Imai, Soda et al. 2000; Shimura, Hattori et al. 2000; Zhang, Gao et al. 2000). Phosphorylated Parkin is increased in the caudate of postmortem PD patients, but not in the cortex or in control tissue (Rubio de la Torre, Luzon-Toro et al. 2009). Parkin is phosphorylated by casein kinase 1 at residues S101, S127, S378 (Yamamoto, Friedlein et al. 2005), and by cyclin-dependent kinase (cdk) 5 at S131 (Avraham, Rott et al. 2007). Although phosphorylation by individual kinases did not affect E3 activity or solubility, compound phosphorylation by both casein kinase 1 and cdk5 led to increased aggregation of Parkin into inclusions (Rubio de la Torre, Luzon-Toro et al. 2009).

Parkin is also modified by oxidative stress, which is relevant considering that dopamine production and metabolism are sources of oxidation in the ventral midbrain and dopamine-producing neurons are the main neuronal resident of the SN. Dopamine is shown to modify Parkin causing its inactivation and loss of E3 ligase activity (LaVoie, Ostaszewski et al. 2005). In fact, dopamine-modified Parkin was only observed in the SN of human brains and not other regions suggesting that dopaminergic death may contribute to parkin loss of function. Another source of oxidative stress, nitric oxide (NO), can lead

to s-nitrosylation of Parkin *in vitro*, which disrupts Parkin E3 ligase activity (Chung, Thomas et al. 2004). The cysteine which is targeted for modification by nitric oxide is suggested to be located in the RING1-IBR-RING2 domains (Yao, Gu et al. 2004). S-nitrosylated Parkin was also detected in MPTP treated mice, rotenone treated rats, and in the postmortem brain tissue of patients with PD and diffuse Lewy body disease (DLBD) (Chung, Thomas et al. 2004; Yao, Gu et al. 2004). Nitrosative stress is a sign of pathology in PD (Ischiropoulos and Beckman 2003; Jenner 2003).

Putative substrates

A prevailing hypothesis is that Parkin mutations lead to the accumulation of its substrates that result in cellular toxicity. Parkin substrates have a multitude of functions including vesicle trafficking, cell cycle, endoplasmic reticulum stress, and microtubule organization. The identification of glycosylated alpha synuclein was an initial finding that linked idiopathic and familial PD (Shimura, Schlossmacher et al. 2001). Other synaptic vesicle related substrates include GTPase, CDC-rel1 (Zhang, Gao et al. 2000), membrane trafficking proteins synaptotagmin IX (Huynh, Scoles et al. 2003), and alpha synuclein interacting protein synphilin1 (Chung, Zhang et al. 2001). The identification of Pael-R led to the theory that Parkin is involved in ER stress because Pael-R is a G-protein coupled endoplasmic reticulum (ER)-associated receptor that signals the unfolded protein response (UPR) (Imai, Soda et al. 2000; Imai, Soda et al. 2001). Microtubule-associated protein tau is aggregated in neurodegenerative diseases such as Frontotemporal Dementia and in a rat model of tau-overexpression induced degeneration, viral expression of Parkin was able to rescue loss of TH neurons in the SN possibly through targeting tau for

degradation (Klein, Dayton et al. 2006). The identification of putative Parkin substrates has been critical to the understanding of Parkin interactions *in vitro;* nevertheless, an important caveat of these studies is that these interactions are derived from overexpression studies. The *in vivo* significance is still questionable because accumulation of these substrates has yet to be verified in the brains of PD patients. In *parkin*$^{-/-}$ mice, the steady state levels of several identified substrates (such as CDC-rel1 and synphilin1) were not changed in the mouse brain (Goldberg, Fleming et al. 2003).

Parkin and mitochondria

Although the *parkin*$^{-/-}$ mice did not exhibit the neurodegenerative pathology of human patients, the striatal neurons exhibited decreased excitability and altered vesicle release (Goldberg, Fleming et al. 2003; Itier, Ibanez et al. 2003). Two-dimensional gel proteomics and mass spectrometry performed using *parkin*$^{-/-}$ mouse brains identified several dysregulated proteins, the majority of which were mitochondrial proteins involved in regulating respiration (Palacino, Sagi et al. 2004). Moreover, loss of parkin leads to dysregulated mitochondrial morphology in Drosophila melanogaster, and weakened flight muscles, a sign a motor degeneration (Greene, Whitworth et al. 2003). Parkin localizes to the outer mitochondrial membrane under conditions of mitochondrial-dependent cell death and prevents mitochondrial swelling (Darios, Corti et al. 2003). Parkin functions downstream PTEN-induced kinase 1 (PINK1), rescuing mitochondrial dysfunction caused by inactivation of PINK1 in Drosophila (Clark, Dodson et al. 2006; Park, Lee et al. 2006; Yang, Gehrke et al. 2006). Parkin deficiency is also observed to have aberrant effects on mitochondrial functioning in human cells. Human fibroblasts

from *parkin*-/- patients displayed decreased Complex I activity and ATP production, with no changes in morphology. Changes in mitochondrial morphology were only observed when the parkin deficient fibroblasts were challenged with the rotenone, leading the authors to conclude that Parkin plays a role in mitochondria dynamics under conditions of cellular stress (Mortiboys, Thomas et al. 2008). Finally, Parkin is selectively recruited to damaged mitochondria to also facilitate mitochondrial clearance through an autophagy-dependent pathway (Narendra, Tanaka et al. 2008). Overall, Parkin activity is observed to be essential in mitochondria respiration, dynamics, and turnover; all of which are critical in maintaining cellular viability.

Parkin and neuroinflammation

The protective role that Parkin plays in closely guarding mitochondrial respiration and dynamics was studied in neuronal cell types. In fact, parkin expression was initially reported exclusively in the processes and cell bodies of neurons (Huynh, Scoles et al. 2000), but recent work has shown Parkin is not only expressed in non-neuronal cell types, but that Parkin is also functionally important in microglia, astrocytes and endothelial cells. Parkin subcellular localization is cell type dependent with predominant ER-associated localization in neurons and nuclear and Golgi-localization in astrocytes (Ledesma, Galvan et al. 2002). Parkin is abundantly expressed in microglia, and *parkin*-null mice have increased number of microglia by immunocytochemical analysis (Casarejos, Menendez et al. 2006). Additionally, parkin loss of function in microglia resulted in enhanced toxicity to dopaminergic neurons after rotenone treatment (Casarejos, Menendez et al. 2006). This finding showed a novel function for Parkin in

microglia, but the authors did not identify the chemical mediators nor identify signaling pathways that mediated microglia-derived toxicity.

Finally, the authors that generated the *parkin*$^{-/-}$ mouse postulated that the *parkin*$^{-/-}$ mice needed an additional stimulus to signal degeneration of nigral DA neurons (Goldberg, Fleming et al. 2003). A study from our lab reported inflammation was a means to induce neurodegeneration in the *parkin*$^{-/-}$ mice. Systemic injections of LPS caused increased loss of DA neurons in the SN of *parkin*$^{-/-}$ mice compared to LPS-injected wild type mice (Frank-Cannon 2008). Moreover, *parkin*$^{-/-}$ mice displayed fine locomotor deficits.

Objectives of the Dissertation research

Parkin mutations account for the majority of ARPD, and the literature reveals the important role of parkin in mitochondria functioning. With the importance of microglia and the micro-environment in the onset and progression of PD, it is important to explore the role of PD-linked genes in microglia. In light of the studies that demonstrate *parkin*$^{-/-}$ animals are susceptible to inflammation-induced neurodegeneration, and loss of parkin leads to increased cellular toxicity, we hypothesize that Parkin functions in signaling pathways essential in microglia activities. We postulate that if Parkin is essential in the activities of MPs like microglia and macrophages, then it follows that Parkin levels may also be affected by inflammatory stimuli. We propose in the following studies to investigate the extent that inflammation affects expression of Parkin and how,

conversely, loss of Parkin function may disrupt pathways that program a microglia to become acutely or chronically activated.

In addition, we explore a model of inflammation in PD that mimics pathways of inflammatory initiation (intranasal TNF administration) in the *DJ-1*$^{-/-}$ mouse. Intranasal delivery of soluble TNF may represent a more physiological model, because olfactory bulb pathology is observed in PD (Hawkes, Shephard et al. 1997). Finally, with the emphasis on the contribution of microglia to neuroinflammation, we examine therapeutic relevance of a synthetic triterpenoid, 2-cyano-3,12-dioxooleana-1,9,-dien-28-oic acid (CDDO), in rescuing DA neuron toxicity. We observe that microglia are the primary target, and that even direct inhibition of inflammatory pathways in the neurons themselves is not sufficient to protect against death from microglia-derived toxic factors.

CHAPTER TWO

Parkin Expression is Negatively Regulated by Inflammatory Signaling and Loss of Parkin Results in Chronic Activation of Microglia

The contents of this chapter were written up for publication in a manuscript by the same title.

Introduction

Mutations in the *parkin* gene (PARK2) are the leading cause of early-onset, autosomal recessive Parkinson's disease (PD) (Abbas, Lucking et al. 1999; Lucking, Durr et al. 2000). Parkin was initially reported to regulate neuronal development (Wang, Suzuki et al. 2001), and recent studies demonstrate that Parkin also functions in protection of mitochondrial respiration (Palacino, Sagi et al. 2004) and in regulating mitochondrial morphology (Deng, Dodson et al. 2008; Poole, Thomas et al. 2008; Park, Lee et al. 2009). Parkin may play a role in limiting apoptosis during cellular oxidative stress or excitotoxicity.

We recently demonstrated that Parkin-deficient mice are more susceptible to systemic lipopolysaccharide (LPS)-induced death of dopaminergic (DA) neurons in the substantia nigra, the hallmark of PD (Frank-Cannon 2008). A myriad of studies implicate neuroinflammation as a contributing factor in PD pathogenesis (Wersinger and Sidhu 2002; McGeer and McGeer 2004; Hirsch, Hunot et al. 2005; Lee, Tran et al. 2009). Neuroinflammation is largely characterized by activation of microglia, monocyte-derived

brain resident macrophages (Whitton 2007). Microglia are central players in innate immune responses in the brain. In cases of acute brain injury, microglial effector functions are essential for tissue repair (Colton 2009). However, chronic activation of microglia may compromise neuronal survival, and promote infiltration of peripheral immune cells which could hasten further neuronal destruction (Rezai-Zadeh, Gate et al. 2009). Thus, microglia are a logical target to explore the relationship between Parkin, neuroinflammation and DA neuron death.

To date, studies aimed at identifying the cellular function of Parkin have focused on neuronal populations. Here, we evaluate the regulation of Parkin in microglia and macrophages by inflammatory signaling and its role in microglial activation. Our findings demonstrate that Parkin expression is regulated by LPS and TNF in an NF-κB-dependent manner and suggest that in addition to its role in neuronal responses to oxidative stress, Parkin may be an important regulator of microglial activation status.

Results

LPS and TNF induce downregulation of Parkin expression in microglia. Our previous data demonstrate that *parkin*-deficient mice are more susceptible to inflammation-induced death of DA neurons in the substantia nigra (Frank-Cannon 2008). However, whether inflammation directly modulates Parkin levels is unknown. Therefore, to investigate the extent to which Parkin expression is regulated by inflammatory stimulation, we examined Parkin mRNA and protein levels in BV2 murine microglia,

primary microglia and primary peritoneal macrophages. Based on reports that Parkin protection against rotenone, glutamate and kainate correlated with increased Parkin mRNA and protein levels, we predicted that inflammatory stimuli would also increase Parkin expression. Surprisingly, we found that treating primary microglia, BV2 microglia, and macrophages with the bacterial endotoxin lipopolysaccharide (LPS) or the inflammatory cytokine tumor necrosis factor (TNF) for 4 hours resulted in dose-dependent decreases in Parkin mRNA as measured by quantitative PCR **(Figure 2.1a,b,c)**. Immunoblot analysis revealed a corresponding decrease in Parkin protein levels in LPS-treated primary microglia, BV2 microglia, and primary macrophages **(Figure 2.1a,b,c)**. Addition of cyclohexamide did not affect the rate of LPS-induced Parkin degradation (data not shown); suggesting that downregulation of Parkin is regulated primarily at the transcriptional level.

MyD88 and NF-κB activation are necessary for Parkin downregulation by LPS. LPS signals by binding to the toll like receptor 4 (TLR4) and MD-2 co-receptor complex to propagate inflammatory signaling via recruitment of MyD88, a receptor-associated adapter protein for TLR4 and interleukin 1 receptor (IL1R)(Janssens and Beyaert 2002). To examine whether Parkin downregulation is specific to the LPS pathway, we used *MyD88*$^{-/-}$ mice which display abnormal inflammatory signaling and lack LPS-induced cytokine production (Kawai, Adachi et al. 1999). Immunoblot analyses of isolated macrophages from wild type and *MyD88*$^{-/-}$ mice revealed that treatment with LPS, for 24 or 48 hours, induced Parkin downregulation in wild type macrophages, but not in *MyD88*$^{-/-}$ macrophages **(Figure 2.1c)**.

Given that LPS and TNF stimulation leads to downstream activation of transcription factor NF-κB in microglia and macrophages (Karin and Ben-Neriah 2000), we used several different techniques to determine whether Parkin levels are regulated by NF-κB. In the cytoplasm NF-κB is bound to IκB; phosphorylation of IκB by IκB kinase (IKK) and subsequent degradation of IκB releases NF-κB allowing it to translocate to the nucleus and activate transcription of target genes (Ghosh, May et al. 1998). To inhibit NF-κB activation in BV2 cells, we expressed a form of IκB that lacks the N-terminal domain (IκBΔN), and therefore cannot be phosphorylated by IKK. Electroporation of IκBΔN in BV2 cells did not inhibit transcription of the downstream target gene TNF in response to LPS (**Figure 2.2a**). Importantly though, blocking NF-κB activation prevented downregulation of Parkin mRNA (**Figure 2.2a**). As a pharmacological means to test the requirement of the NF-κB pathway in mediating the LPS-induced downregulation of Parkin, we stimulated BV2 cells with the protease inhibitor *N*-α-tosyl-*L*-lysine chloromethyl ketone (TLCK), which has been shown to block NF-κB activation by suppressing IκB degradation in RAW 264.7 macrophages (Jeong, Kim et al. 1997). We observed upregulation of Parkin mRNA levels when stimulated with TLCK without LPS, but TLCK did not rescue the LPS-induced downregulation of Parkin levels (**Figure 2.2b**). Additionally, we treated BV2s with CDDO-Imidazole, a synthetic triterpenoid which has been reported to block activation of NF-κB (Ahmad, Raina et al. 2006; Thimmulappa, Scollick et al. 2006; Yore, Liby et al. 2006). Pre-stimulating BV2 microglia with CDDO-Im before LPS treatment also did not prevent LPS-induced downregulation of Parkin (data not shown). However, stimulating BV2 microglia with

CDDO-Im alone, without LPS, resulted in a dose-dependent increase in Parkin mRNA levels. As expected, this anti-inflammatory compound decreased levels of the inflammatory cytokine TNF (**Figure 2.2c**). Overall, these data derived from genetic and pharmacological techniques, suggest that Parkin expression levels are negatively regulated by NF-κB activation in microglia.

Identification of a functional NF-κB binding site in the mouse Parkin gene. Based on sequence alignment of NF-κB binding sites found in established NF-κB target genes, the following consensus sequence has been reported: 5'-GGGRNNYYCC-3' where R is A or G and Y is C or T (Hiscott, Kwon et al. 2001). Sequence analysis of the mouse *parkin* gene, including 3.2 kb upstream of the transcriptional start site, revealed the presence of 3 sequences that closely resemble this consensus sequence (**Figure 2.3a**). To identify a functional NF-κB binding site in the *parkin* gene, we generated a series of reporter plasmids in which different regions of the mouse *parkin* gene promoter were cloned upstream of a luciferase coding sequence in the promoterless pGL4 vector. We electroporated these plasmids into BV2 microglia cells along with a plasmid that constitutively expresses Renilla luciferase as an internal control. The electroporated cells were subsequently treated with saline, 10 ng/ml TNF, or 1 μg/ml LPS for 18 hours after which firefly and Renilla luciferase activity were measured. As shown in **Figure 2.3b**, luciferase activities were decreased 3.7-fold and 1.3-fold by TNF and LPS treatments, respectively. These reporter assay experiments reveal that the promoter of the mouse *parkin* gene, which contains putative NF-κB binding sites, is repressed by TNF. Together

with our biochemical data, these results strongly suggest that Parkin expression is regulated at the transcriptional level by inflammatory stimuli, such as TNF and LPS.

TNF regulates steady-state levels of Parkin but is not required for its LPS-induced downregulation. Given that TNF is a well-known effector of LPS action and an inflammatory cytokine that elicits classic activation responses in a number of immune cell types through NF-κB-dependent signaling, we investigated the extent to which TNF regulates steady-state Parkin expression by measuring Parkin levels in macrophages from *TNF*$^{-/-}$ mice. In unstimulated *TNF*$^{-/-}$ macrophages, we observed greater than two-fold increases in Parkin protein and mRNA levels compared to unstimulated wild type macrophages (**Figure 2.4a,b**). Interestingly, even in the absence of TNF, LPS treatment caused a dose-dependent downregulation of Parkin mRNA; indicating that while TNF stimulation can decrease Parkin levels, TNF signaling is not required to regulate Parkin expression in response to LPS. Additionally, we measured Parkin levels in macrophages from *TNFR1*$^{-/-}$ and *TNFR2*$^{-/-}$ mice, and did not observe increased basal levels of Parkin mRNA, suggesting that signaling through either TNF receptor is sufficient to regulate steady-state Parkin levels (**Figure 2.4b,c**). Moreover, LPS-induced downregulation of Parkin remained intact in *TNFR1*$^{-/-}$ and *TNFR2*$^{-/-}$ mouse macrophages.

parkin$^{-/-}$ *mice display dysregulated inflammatory gene expression and serum cytokine levels.* Inflammatory signaling downregulates Parkin levels, therefore, we predicted that *parkin*-deficiency would result in chronic inflammatory activation in *parkin*$^{-/-}$ mice. In **Figure 2.5a**, we evaluated inflammatory cytokine and chemokine expression in the

brains of adult *parkin*$^{-/-}$ mice compared to wild type mice. We performed PCR array analysis on the midbrains from animals given intraperitoneal injections of saline or LPS for 6 months as described previously (Frank-Cannon 2008) (**Figure 2.5a**). Analysis of the 90 genes on the array revealed that 14.4% of the inflammatory genes were basally upregulated in *parkin*$^{-/-}$ midbrains compared to wild type midbrains, while 7.7% were downregulated. It is worth noting that saline-treated *parkin*$^{-/-}$ mice displayed an inflammatory gene profile comparable to that of wild type mice chronically treated with LPS. Additionally, analysis of cytokine levels in the serum of unstimulated adult *parkin*$^{-/-}$ mice showed significantly increased interleukin-1β (IL-1β) and chemokine KC production compared to wild type mice, with no significant change in IL-10 levels (**Figure 2.5b**). Other cytokines in the assay (IL-12p70, IL-10, IL-6 and TNF) were not robustly detected in the serum. These *in vivo* data suggest that *parkin* deficiency results in dysregulated inflammatory responses.

parkin$^{-/-}$ *microglia display upregulated cell surface activation markers.* The dysregulated cytokine levels we observed in the *parkin*$^{-/-}$ mice may not have been produced by microglia or macrophages because the midbrain and serum samples were comprised of numerous cell types. To determine whether the microglia specifically contributed to the increased expression of cytokines and chemokines in the midbrains of these mice, we performed immunocytochemical to examine expression of cell surface markers that may indicate microglial activation such as CD45 and Iba1. Analysis revealed that unstimulated *parkin*$^{-/-}$ microglia displayed increased immunoreactivity for activation marker CD45 compared to wild type microglia (**Figure 2.6b**). Microglia were also

stained for expression of Iba1 (ionized calcium binding adaptor molecule 1), which is also upregulated in activated microglia (Ito, Imai et al. 1998). We also detected clear morphological differences in *parkin*$^{-/-}$ macrophages treated with LPS compared to wild type. Specifically, *parkin*$^{-/-}$ macrophages treated with LPS displayed characteristics of activated macrophages such as punctuate nuclei and increased number of extended processes (**Figure 2.6c**). These data show the increased expression of activation markers in *parkin*-deficient microglia, which suggest that Parkin may play an important role in limiting or attenuating microglial activation in response to LPS.

Macrophages from parkin$^{-/-}$ *mice exhibit increased caspase activation in vitro*. Stimulation of cells with TNF or LPS leads to activation of caspases and cellular apoptosis unless the opposing anti-apoptotic NF-κB signaling cascade is activated soon thereafter to counteract it (Karin and Gallagher 2009). To investigate the extent to which loss of Parkin influenced the LPS or TNF signaling outcome in microglia or macrophages, we measured whole-cell caspase activity (specifically caspases 2, 3, 6, 7, 8, and 9) in resting or stimulated macrophages. Compared to wild type macrophages, resting *parkin*$^{-/-}$ macrophages exhibited significantly higher levels of caspase activity (**Figure 2.7**); TNF and LPS treatment did not lead to significant or sustained caspase activity in either cell type. Pre-treatment with the TNF-inhibitor Etanercept significantly reduced caspase activation in the *parkin*$^{-/-}$ macrophages, suggesting that the elevated caspase activation is mediated by TNF activation.

Discussion

The pathological hallmark of PD is the death of DA neurons in the substantia nigra. Therefore, most of the research into the mechanism by which familial mutations in single genes give rise to heritable forms of PD has focused on the function of said gene products in neurons. However, evidence has emerged implicating the role of microglia dysfunction in DA neuron death and PD. Studies have recently shown that Nurr1, a transcription factor involved in the development and maintenance of DA neurons (Zetterstrom, Solomin et al. 1997), also regulates cytokine expression in microglia and astrocytes such that reduced Nurr1 expression in brain exacerbated neuroinflammation that led to death of DA neurons in LPS-treated mice (Saijo, Winner et al. 2009). Therefore it is important to consider how the microenvironment affects the health and survival of neurons, and not just the neurons themselves.

While other studies report oxidative stress increases Parkin expression in SH-SY5Y dopaminergic neuron-like cells (Henn, Bouman et al. 2007), our data show that inflammatory stimuli such as LPS can reduce Parkin levels in microglia, a cell type that responds to external factors that have the potential to either resolve or exacerbate inflammation in the central nervous system. This is a significant finding because changes in Parkin levels are affected by stimuli that activate microglia, and the loss of Parkin consequently increases inflammation. Additionally, inflammatory regulation of Parkin occurs in primary macrophages, the microglia counterpart in the peripheral immune system. These monocyte-derived cells that can cross the blood brain barrier to replenish

populations of microglia that die, or in response to chemotactic factors that may be overproduced in disease states (Ransohoff and Perry 2009). It is possible that Parkin levels are specifically regulated by different stimuli. Parkin function is important in mitochondrial respiration, and oxidative stress may require Parkin to quickly mobilize to the mitochondria. Oxidative stress can lead to nitrosylation of Parkin, causing disruption of E3 ubiquitin ligase activity (Chung, Thomas et al. 2004). Parkin is also known to auto-ubiquitinate (Imai, Soda et al. 2000; Shimura, Hattori et al. 2000; Zhang, Gao et al. 2000); therefore oxidative stress may prevent Parkin auto-ubiquitination and readily make Parkin available to be recruited to the mitochondria. Conversely, inflammation may regulate Parkin levels specifically at the transcriptional level, and most likely through the NF-κB pathway.

Microglia and macrophages activate the NF-κB signaling pathway in response to LPS and TNF treatment. Expression of cytokines and chemokines as well as immune cell proliferation and function depends on the activation of NF-κB (Ghosh, May et al. 1998; Karin and Ben-Neriah 2000). Although NF-κB activates the expression of many target genes, it has also been reported to repress gene transcription, including inhibition of the rat androgen receptor (Supakar, Jung et al. 1995). Moreover, the *Drosophila melanogaster* homolog of NF-κB/Rel (*dorsal)*, positively regulates some genes while negatively regulating others during embryonic development (Jiang, Cai et al. 1993). *dorsal* is reported to act as a repressor when it associates with a neighboring co-repressor. Utilizing the mouse *parkin* promoter to drive luciferase activity, our studies indicate that the decrease in Parkin expression is in part mediated by NF-κB activation. Luciferase

activity was detectable, though not robust, because the BV2 microglia are a difficult cell type to transfect. We are currently repeating these studies in HEK293 cells, which are responsive to TNF and are also a common cell line to study signaling. Additionally, we are currently conducting studies to determine which of the 3 putative NF-κB binding sites is regulated in the *parkin* promoter by performing luciferase activity assays using vectors in which each site is individually expressed. We are also performing chromatin immunoprecipitation (ChIP) assays to determine whether NF-κB physically interacts with the *parkin* promoter in BV2 microglia.

Our hypothesis that Parkin levels may influence the extent of microglial activation is supported by our studies in primary macrophages from *TNF*$^{-/-}$ mice. We found increased basal levels of Parkin in macrophages isolated from *TNF*$^{-/-}$ mice, which have been reported to have impaired microglial activation when challenged with oxidative stress (Ferger, Leng et al. 2004; Zhao, Ling et al. 2007). However, the ability of LPS to downregulate Parkin levels in *TNF*$^{-/-}$ macrophages indicates that LPS-induced downregulation of Parkin through the NF-κB pathway does not require endogenous TNF production, which is not an unexpected finding given that NF-κB activation by LPS can also occur through TNF-independent pathways. Nevertheless, in wild type cells LPS treatment leads to the production of TNF which may in turn function in an autocrine manner by binding to TNFR1 and/or TNFR2 receptors. Functionally, we show that the TNF signal that limits Parkin levels in microglia and macrophages can be transduced through either TNF receptor as we did not observe basal elevation of Parkin mRNA levels in macrophages from *TNFR1*(*tnfsf1a*)$^{-/-}$ or *TNFR2*(*tnfsf1b*)$^{-/-}$ mice.

The biological significance of NF-κB-mediated downregulation of Parkin levels is not yet clear; however, our observations that *parkin*$^{-/-}$ mice display increased inflammatory gene expression and overproduce cytokines, detected in the serum, suggest that an important function of Parkin may be to curtail the extent of microglial activation. On the other hand, the absence of Parkin or low levels of Parkin may prevent resolution of an inflammatory response and lead to sustained microglial activation. We observe increased CD45 expression in unstimulated *parkin*$^{-/-}$ microglia, which may be indicative of chronic activation. Our studies confirm data that report increased microglial proliferation and activation in *parkin*$^{-/-}$ mice compared to wild type (Casarejos, Menendez et al. 2006). Functionally, chronic microglial activation has been known to trigger cell death (Tansey 2008). Microglia quickly proliferate in response to acute injury, but have also been demonstrated to undergo apoptosis once the wound healing is completed; as a form of population control (Streit and Xue 2009). Either as a function of chronic activation or population control, we also observe increased caspase activation, a measure of apoptosis, in *parkin*$^{-/-}$ microglia.

Of interest is the fact that *parkin*$^{-/-}$ mice do not show signs of neurodegeneration, in the absence of additional environmental insults, despite the observation that they display basally increased inflammation. One explanation may be that *parkin*$^{-/-}$ mice upregulate glutathione synthase (GSH) as a compensatory mechanism to handle increased oxidative stress burden (Solano, Menendez et al. 2006). Additionally, microglia from *parkin*$^{-/-}$ mice also upregulate mRNA levels of Regulator of G protein signaling 10 (RGS10)

(unpublished observation), a protein found to be protective in a chronic model of LPS-induced nigral degeneration (Lee, McCoy et al. 2008). Therefore, developmental compensation in *parkin*$^{-/-}$ mice may overcome the effects of increased microglial activation that we observe under resting conditions, and it is not until microglia become chronically activated by repeated systemic LPS administration, for example, that nigral DA neuron death ensues (Frank-Cannon 2008). Taken together, our findings indicate that Parkin functions to negatively regulate inflammatory responses in microglia.

The implication of our findings is that in humans that do not have a genetic *parkin* mutation, chronic inflammation arising from environmental toxins, infections, arthritis, diabetes, obesity and/or the normal aging process may downregulate Parkin levels to effectively mimic *parkin* loss of function mutations. Consequently, we show that loss of Parkin results in the enhanced expression and production of pro-inflammatory cytokines and chemokines as present in the midbrain and serum. In time, chronic activation of microglia may exceed the compensatory mechanisms employed by the microglia to survive, and lead to a toxic microenvironment for surrounding cells. Overproduction of inflammatory mediators may chronically expose a healthy DA neuron to pro-inflammatory cytokines and chemokines, and promote neuronal death (**Figure 2.8**). Focusing on the function of PD-linked genes in both neurons and glia will lead to a more complete understanding of processes that contribute to neurodegeneration and the development of PD.

Figures

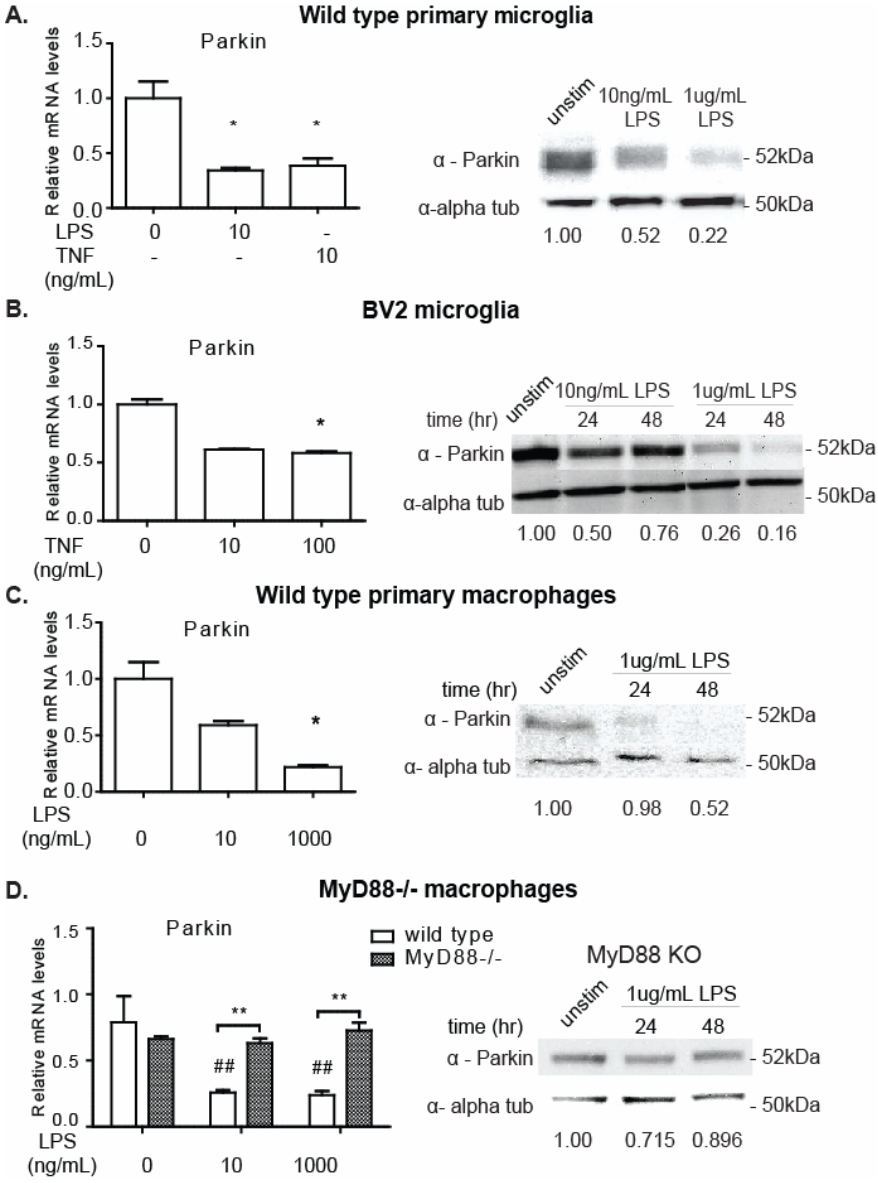

Figure 2.1. *LPS and TNF stimulation downregulate expression of Parkin mRNA and protein in primary microglia and macrophages. A,* Parkin mRNA levels in primary microglia treated with LPS or TNF as indicated above for 24 hrs, and protein levels treated with LPS for 48 hrs. One way ANOVA followed by Tukey'post hoc test, * p<

0.05 compared to unstimulated sample. *B,* Parkin mRNA levels in BV2 murine microglia cell line treated with TNF for 4 hrs, and protein levels treated with LPS for 24 and 48 hrs. *C,* Parkin mRNA levels in primary peritoneal macrophages after LPS stimulation for 4 hrs, and protein levels after LPS treatment for 24 and 48 hrs. *A,B,C,* One way ANOVA followed by Tukey's post hoc test, * $p<0.05$ compared to unstimulated sample. *D,* Parkin mRNA levels in primary macrophages isolated from adult wild type or MyD88$^{-/-}$ mice and treated with LPS for 4 hrs, and protein levels after LPS treatment for 24 and 48 hrs. Two way ANOVA followed by Bonferroni's post hoc test, ## $p<0.01$ compared to unstimulated sample, ** $p<0.01$ compared to wild type. For Western blots optical densitometry was performed to quantify Parkin protein levels relative to α-tubulin protein levels.

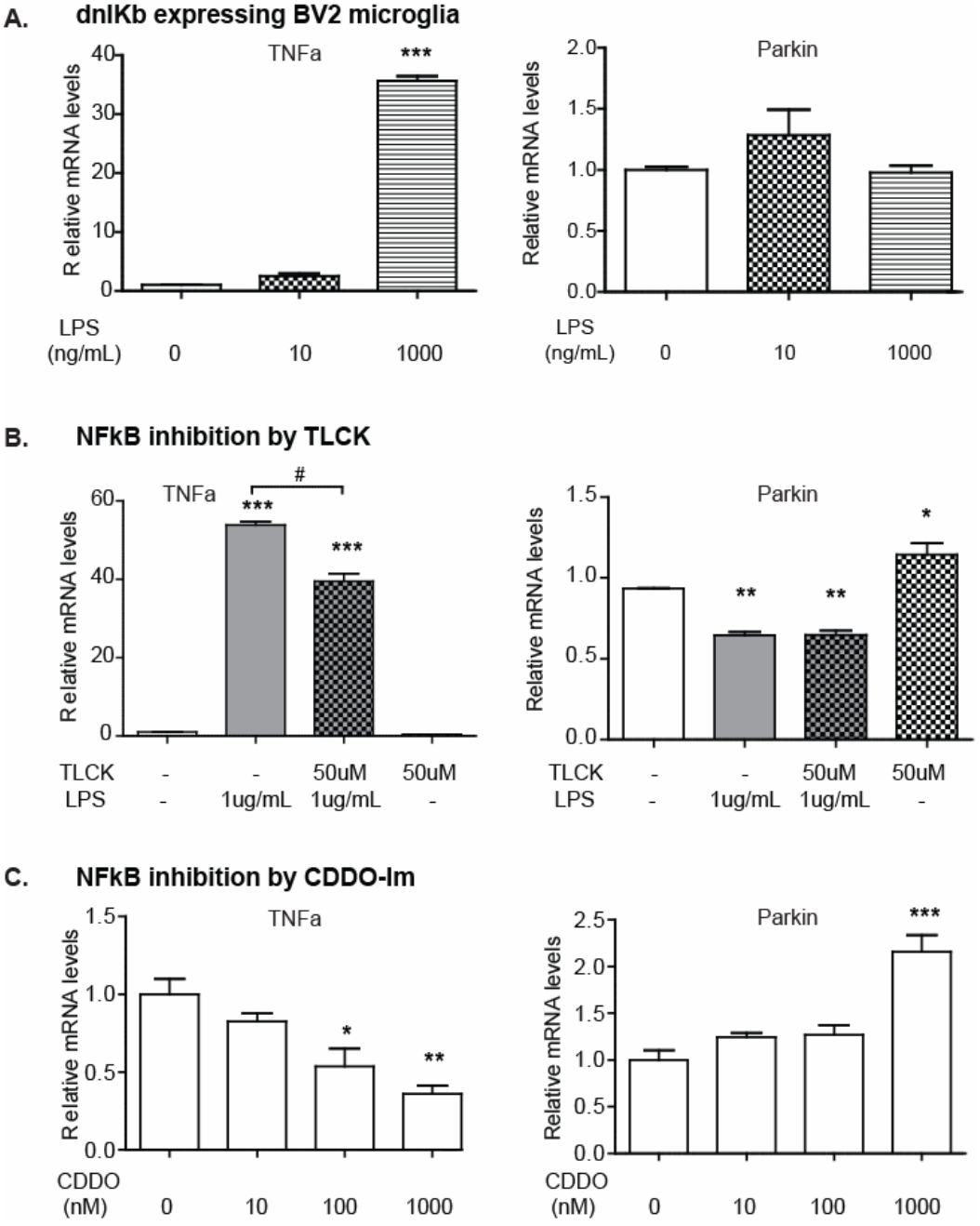

Figure 2.2. *Inflammation-induced Parkin downregulation involves NF-κB activation. A,* TNF and Parkin mRNA in BV2 cells electroporated with dnIκBΔN and stimulated with LPS for 4 hours. *B,* TNF and Parkin mRNA expression in BV2 cells after an overnight

exposure to NF-κB inhibitor TLCK, followed by LPS treatment for 4 hours. *C,* TNF and Parkin mRNA expression in unstimulated BV2 cells after exposure to anti-inflammatory compound, CDDO-Im for 4 hours. ANOVA followed by Tukey's post hoc test,* $p< 0.05$, ** $p< 0.01$, and *** $p< 0.001$ compared to vehicle treatment; and # $p<0.05$.

A. Sequence of the *parkin* promoter

GAGATGGTGTGACAAGGGGAATGAGAAGACAGTCTGGGAGATATCATGGACTCTAGCCAGATTCT
AATGAAGAGAGTGATCACAACAGCAGAGGTGATGTCACTTCAAGATCTCGCTCGAAATCCACTGT
CACCTGTGAGCTAAGAACACAGGGTGCAAAATCCTTACACAGAGTATGGAGGCCTTATCAAGAAC
CTACAACCATTTCACAGAGTCCAGAACTCTTCACAGAACCTAGATTCAAAACCTTGCCCAGAGTTC
TTTCATAGGCCCCAAGCTCTCTTCAGCTGTCTACACAGTGGCTTCCATTTCCACCATTTCTTTCTGG
GGCATCCACATGCTGCCTTTGAGTTTTATGCAAAGGACTCTGCGGAGGGAGTGAGCATTTGTTCAG
TCTTTTGGAGCAGAATAGTCTATACACTCATGGGAATCTTGAGATTCCAATCAAGCAAGTTCTCCG
CTTTACTCCCTCTGTTCCAGGAGGGCTGTGAAAGGCACAAAACTGCCGTAGTCTGCAGGTCACTGA
CCAGGGTCTGAGCAGGAAAACACCTAGGGAAAAACACCTAGGGGAAACTGTTTTTGGTTTTGTTT
GTTTTTTTTTTTGTTGTTGTTGTTTTGTTTTGTTTTGTCTTTTTTCTAACTACTGCTCTATACTATAAA
TTTATGCTCTGTGATAAATGGAAGAAAATATATGCCATGCACTGGAGGGCAGGTGAGGGGCAAGC
TGCTTCAGAGACATTTCACTGGCCATTAAGGGTTTGGAGTAATATTCTTTCTTCTCTCTCTGCCCCT
GGTCTTGT

B. Luciferase activity driven by the *parkin* promoter

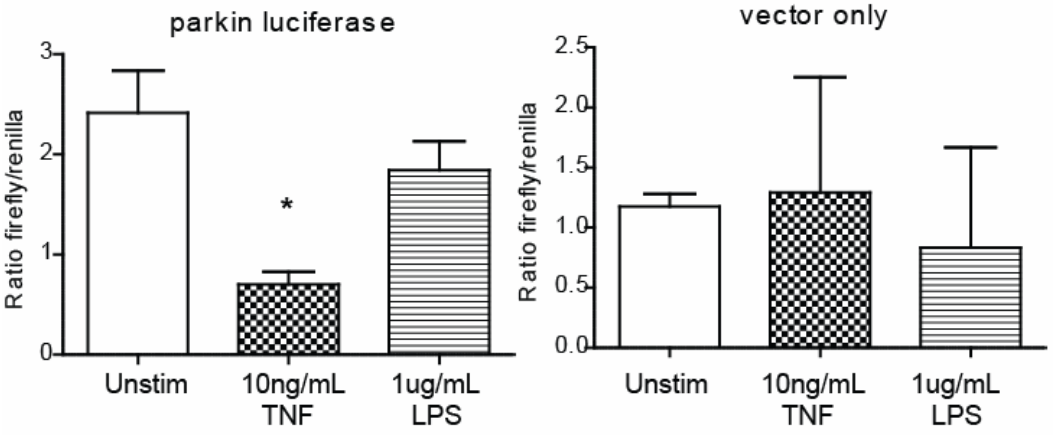

Figure 2.3. *The mouse parkin promoter contains several putative NF-κB binding sites and is repressed by TNF. A,* Sequence of the mouse *parkin* promoter containing 800 nucleotides upstream of the transcriptional start site. Putative NF-κB binding sites are highlighted in yellow. *B,* BV2 cells were electroporated with 1µg Parkin_pGL4 plasmid, containing all 3 putative binding sites, and 0.4 µg Renilla plasmid. Fold induction of firefly luciferase activity was measured after an overnight treatment of 10ng/mL TNF or 1µg/mL LPS. Firefly luciferase activity was normalized to internal control Renilla luciferase activity. ANOVA followed by Tukey's post hoc test,* $p < 0.05$.

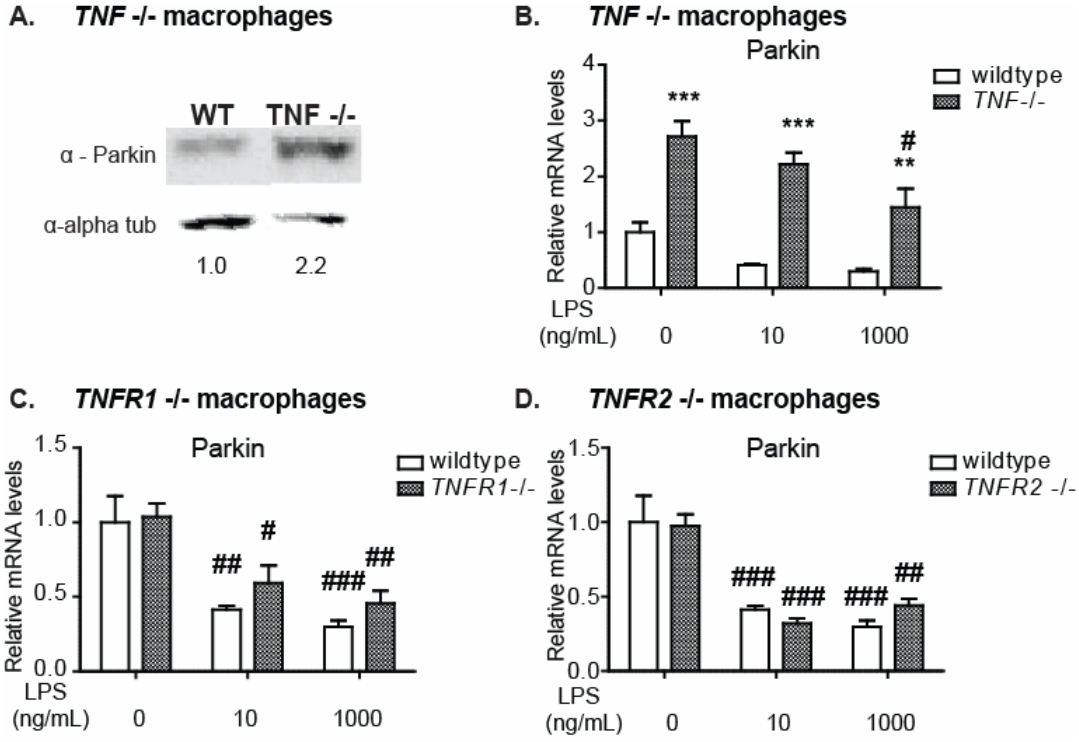

Figure 2.4. *TNF negatively regulates Parkin steady-state levels but does not contribute to LPS-induced downregulation of Parkin. A,* Parkin protein levels in untreated macrophages. For Western blot optical densitometry was performed to quantify Parkin protein levels relative to α-tubulin protein levels. *B-D,* Parkin mRNA levels in macrophages isolated from *TNF*$^{-/-}$, *TNFR1*$^{-/-}$, and *TNFR2*$^{-/-}$ mice, respectively, treated with LPS for 4 hours. ANOVA followed by Bonferroni's post hoc test, ** $p<0.01$ and *** $p<0.001$ compared to wild type unstimulated sample and $^{\#}$ $p<0.05$, $^{\#\#}$ $p< 0.01$, $^{\#\#\#}$ $p<0.001$ compared to the unstimulated sample for the respective genotype.

A.

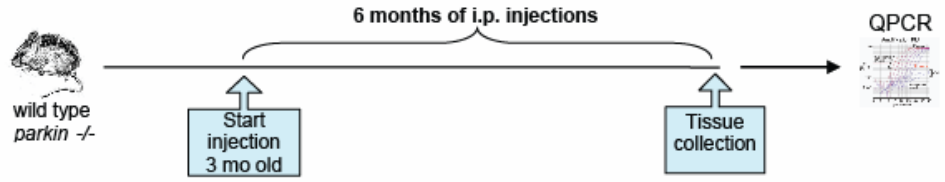

B.

	WT LPS_WT SAL	PK LPS_PK SAL	PK SAL_WT SAL	PK LPS_WT LPS
Symbol	Fold Up- or Down-Regulation	Fold Up- or Down-Regulation	Fold Up- or Down-Regulation	Fold Up- or Down-Regulation
	WT LPS/WT SAL	PK LPS/PK SAL	PK SAL/WT SAL	PK LPS/WT LPS
Il2rb	20.36	1.29	8.68	-1.81
Il10	5.64	-2.31	5.29	-2.46
Il8rb	4.23	-1.01	3.00	-1.42
Ccr6	3.09	1.51	3.80	1.85
Cd40lg	2.81	-1.33	2.79	-1.34
Il20	2.47	1.05	2.97	1.26
Cxcl13	2.09	3.97	-2.32	-1.22
Il2rg	2.08	1.63	1.22	-1.05
Tnfrsf1b	1.87	1.02	-1.21	-2.22
Cxcr3	1.85	-1.13	2.08	-1.01
Il11	1.82	-2.69	2.63	-1.86
Il16	1.74	-9.64	12.28	-1.36
Xcr1	1.42	-5.33	5.17	-1.47
Ccl3	1.31	-1.30	-1.50	-2.57
Blr1	1.26	1.93	-4.96	-3.23
Il1b	1.19	-1.21	-1.44	-2.09
Ifng	1.18	3.36	-4.84	-1.70
Bcl6	1.12	-1.89	2.10	-1.01
Tollip	-1.02	-1.17	1.01	-1.13
Ccr5	-1.03	1.30	-1.30	1.03
Cxcl5	-1.07	-1.32	-1.62	-2.00
Ccl4	-1.18	-1.04	-11.64	-10.23
Il3	-1.37	-4.89	2.66	-1.34
Cxcl15	-1.37	-3.94	2.15	-1.34
Il1f6	-1.37	-2.72	1.48	-1.34
Il13	-2.08	3.52	-3.64	2.01
Ccl11	-2.14	1.07	-2.48	-1.08
Ccl1	-2.80	-3.93	-1.42	-1.99
Il5ra	-2.88	1.18	-1.66	2.05
Ccr4	-3.57	-1.46	-3.27	-1.34
Cxcl11	-6.87	-1.20	1.58	9.04

C.

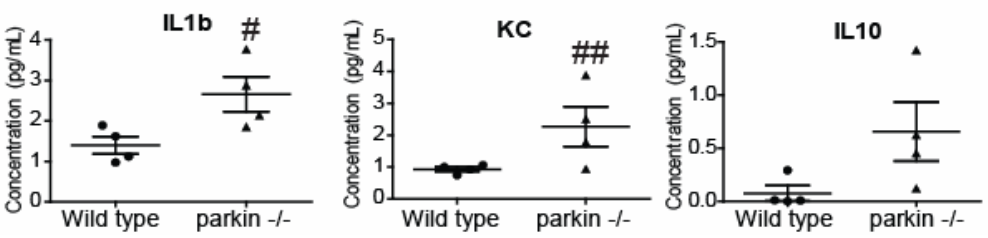

Figure 2.5. *Midbrains and serum from parkin$^{-/-}$ mice display increased inflammation. A,* Dosing paradigm of adult wild type and *parkin$^{-/-}$* mice given twice weekly intraperitoneal injections of LPS or saline for 6 months. *B,* Profile of inflammatory gene expression in the midbrain. PCR array data represent fold up- or down-regulation compared to wild type saline injected, and are representative of two independent PCR arrays. Values that are increased greater than two-fold relative to wild type are highlighted pink and down-regulation is highlighted blue. *C,* Cytokine and chemokine levels in the serum of unstimulated 8 month wild type and *parkin$^{-/-}$* mice. Multi-analyte ELISA (MSD) was performed on n=4 animals per genotype. Analysis was performed by one-tailed Student's t-test and # $p< 0.05$ and ## $p< 0.01$.

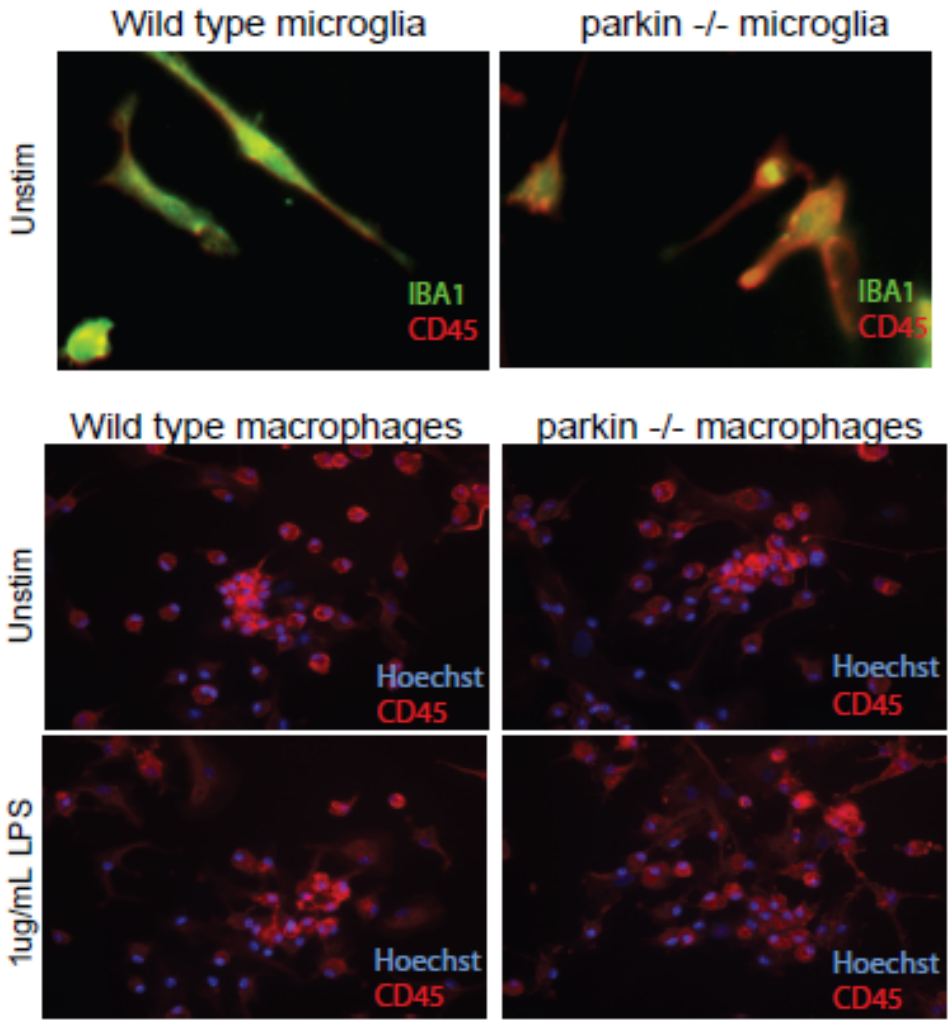

Figure 2.6. *Isolated microglia from parkin$^{-/-}$ mice upregulate markers of activation. A,* CD45 (red) and Iba1 (green) immunoreactivity in unstimulated wild type and *parkin$^{-/-}$* microglia. Microglia were fixed 1 day after isolation from mixed glial cultures. *B,* CD45 expression in macrophages from wild type and *parkin$^{-/-}$* mice treated with LPS for 48 hours. Activation was assayed using immunoreactivity for CD45 (red) and Hoechst 33258 as the nuclear marker (blue).

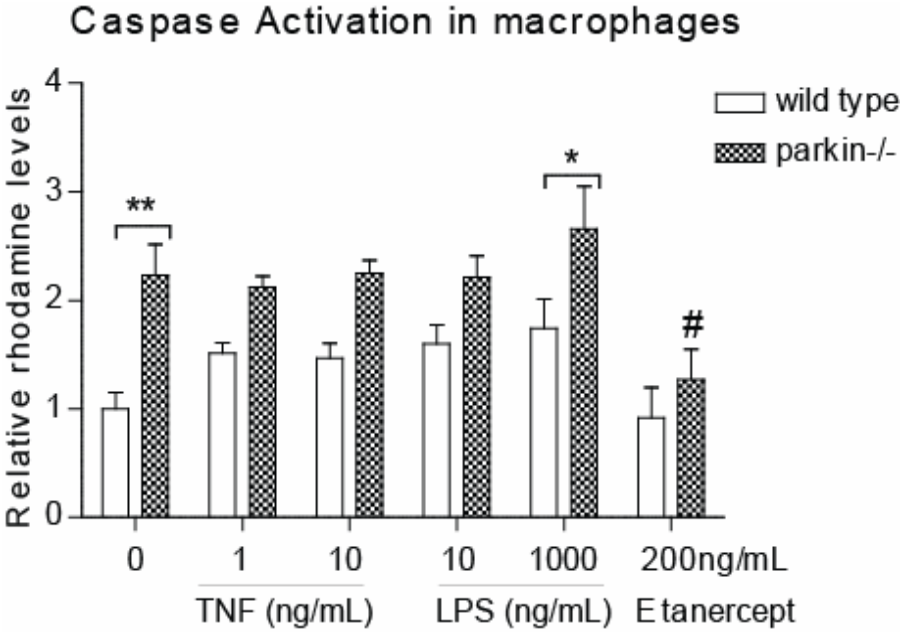

Figure 2.7. *Macrophages from parkin$^{-/-}$ mice exhibit increased caspase activation in vitro.* Whole-cell caspase activity was measured in macrophages treated with saline, TNF, LPS, or the TNF inhibitor etanercept for 1 hour. Cells were then incubated with caspase substrate for 1 hour. Data are representative of quadruplicate wells. ANOVA followed by Bonferroni's post hoc test, * $p<0.05$ and ** $p< 0.01$ compared to wild type; # $p<0.05$ compared to vehicle treated *parkin*$^{-/-}$ macrophages.

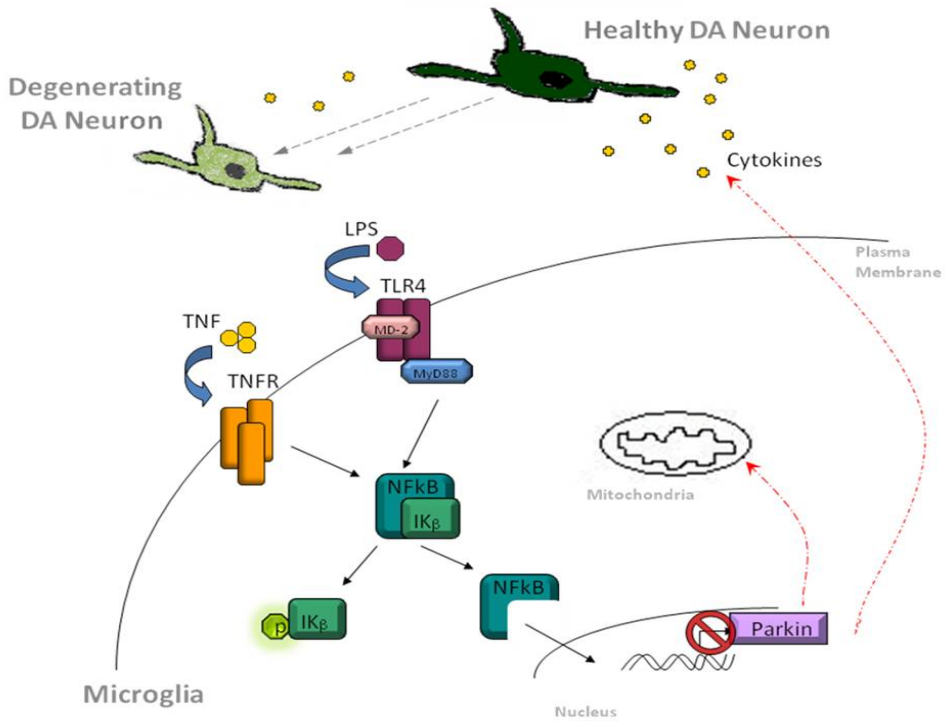

Figure 2.8. *Model of LPS-induced and NF-κB-dependent Parkin downregulation.* LPS and TNF stimulate microglia and macrophages by binding TLR4 and TNFR1/2 respectively, to propagate intracellular signaling through adapter proteins including MyD88 and transcription factor NF-κB. Activation of microglia and macrophages downregulates Parkin mRNA, while the inhibition LPS signaling at the receptor level or by blocking NF-κB prevents downregulation of Parkin. *parkin*$^{-/-}$ macrophages have increased caspase activity, which may counteract the increased proliferation or indicate mitochondrial stress, because Parkin has been implicated in protecting mitochondrial respiration. *parkin*$^{-/-}$ microglia and macrophages display activation even in the absence of stimulation, and the elevated inflammatory profile of the *parkin*$^{-/-}$ microglia correlates with increased production of cytokines, thereby creating a toxic microenvironment for DA neurons.

CHAPTER THREE

Parkin-deficiency alters microglia and macrophage effector functions

Introduction

In the central nervous system (CNS), microglia are brain-resident macrophages that perform immune functions that are essential in maintaining health and homeostasis in the brain. To support normal neuronal functioning microglia scavenge and phagocytose cellular debris as well as secrete trophic factors (Whitton 2007; McGeer and McGeer 2008). Microglia actively survey the microenvironment of the brain by extending processes and localizing to sites of neuronal injury (Nimmerjahn, Kirchhoff et al. 2005). During acute injury, microglia also release cytokines and chemokines, among other biological factors, to induce proliferation as well as mobilize additional microglia to the site of injury (McGeer and McGeer 2008; Streit and Xue 2009). In fact, activation of microglia following acute injury enhances sprouting by dopaminergic neurons (Batchelor, Liberatore et al. 1999). Microglia are dynamic contributors to the viability and maintenance of neurons in the CNS.

However, it has been shown that chronic microglial activation can lead to prolonged release of chemokines and cytokines, such as tumor necrosis factor (TNF) and interleukins, which lead to cellular toxicity (McGeer and McGeer 2008). Pharmacological inhibition of soluble TNF production can significantly rescue

neurodegeneration in rodents treated with the oxidative neurotoxin 6-hydroxydopamine (6-OHDA) or bacterial inflammogen lipopolysaccharide (LPS) (McCoy, Martinez et al. 2006). A follow-up study used lentiviral delivery of a dominant negative TNF (dnTNF) to rescue 6-OHDA induced neurodegeneration. Lentiviral dnTNF largely transduced microglia, and not DA neurons nor astrocytes, blocking microglial activation as evidenced by reduced NF-κB nuclear translocation compared to lentiviral transduction of GFP (McCoy, Ruhn et al. 2008). In addition to TNF toxicity, microglial production of nitric oxide (NO) has also been identified as a chemical species toxic to DA neurons. In an *in vitro* co-culture experiment, macrophages stimulated with LPS produced NO that led to the nitrosylation and accumulation of alpha-synuclein in the neurons in the culture (Shavali, Combs et al. 2006). Neurons do not express the receptor for LPS and are unresponsive to LPS, therefore it was cytotoxic species derived from the microglia that consequently caused oxidative stress in the DA neurons leading to neuronal death.

Previously, we demonstrated that Parkin levels are regulated by LPS and TNF, and that *parkin*-deficiency can increase cytokine levels detected in the serum of *parkin*$^{-/-}$ mice. Moreover, published studies show that rotenone-treated *parkin*$^{-/-}$ microglia are more toxic to neurons (Casarejos, Menendez et al. 2006). These data suggest that Parkin is necessary to regulate microglial activation, but the cytotoxic species produced by *parkin*$^{-/-}$ microglia have not yet been identified. In the following studies we investigated the specific properties of microglial activation such as release of cytokines, chemokines, NO and the effect of these biological chemicals on DA neuron survival. We also examined macrophage chemotaxis, or the ability to migrate, in response to inflammatory stimuli.

Results

Isolated parkin$^{-/-}$ microglia secrete less cytokines

parkin$^{-/-}$ microglia treated with rotenone are reported to be more toxic to dopaminergic neuronal cultures (Casarejos, Menendez et al. 2006). However these studies did not determine which microglial-derived factors mediated neuronal cytotoxicity. As a measure of microglial activation and cytotoxicity, we collected the conditioned media (CM) from isolated *parkin*$^{-/-}$ and wild type microglia and measured cytokine secretion after stimulation with LPS over a time course. Unexpectedly we observed a robust reduction in all cytokines secreted by the *parkin*$^{-/-}$ microglia treated with 1ug/mL LPS, compared to similarly treated wild type microglia **(Figure 3.1)**. Next we compared cytokine levels in LPS-stimulated macrophages from wild type and *parkin*$^{-/-}$ mice (**Figure 3.2**). We treated the macrophages for 24 hrs, since it is the time point in which we detected the largest differences between LPS-treated wild type and *parkin*$^{-/-}$ microglia (**Figure 3.1**). Interestingly, only interleukin 1 beta (IL-1b) was increased in unstimulated *parkin*$^{-/-}$ macrophages. The multiplexed ELISA only measured seven cytokines and chemokines; it is possible that *parkin*-deficiency may increase production of a specific cytokine that we did not measure which confers toxicity to MN9D dopaminergic cells. Therefore, we tested the cytotoxicity of conditioned media (CM) from microglia and macrophages towards MN9D cells. The viability of MN9D cells was significantly reduced by LPS-treated microglia and macrophage CM, but *parkin*-deficiency did not enhance this

neuronal toxicity (**Figure 3.3**). We concluded that loss of Parkin does not potentiate LPS-induced production of cytokines and chemokines.

Parkin aberrantly affects cytokine production in BV2 microglia.

Since it is possible that the isolated *parkin*$^{-/-}$ microglia may have made developmental compensations, which masked enhanced cytokine production and/or cytotoxicity toward MN9D cells, we next measured MN9D survival after stimulation with CM from BV2 microglia in which we acutely reduced Parkin expression by siRNA. Parkin levels were reduced greater than 70% as determined by Western blot (data not shown). MN9D cell survival was significantly decreased when incubated in CM from BV2s stimulated with LPS for 24 hrs. Similar to the result in primary microglia, Parkin knockdown failed to enhance LPS-induced cytotoxicity **(Figure 3.4)**. We then wanted to see the effect of Parkin overexpression (OE) on LPS-induced cytokine production in BV2s. We generated a stable cell line of BV2s that overexpressed Parkin ten-fold, as determined by mRNA levels (data not shown). Parkin OE in BV2s only increased TNF production when cells were stimulated with 10ng/mL LPS for 24 hrs. At a higher concentration of LPS, we observed increased production of TNF as well as interleukin 6 (IL-6), interferon gamma (IFNg), IL-12p70, IL-10, and chemokine KC (**Figure 3.5)**. Interestingly, IL-1b was the only cytokine that had reduced levels with Parkin OE. We observed decreased cytokine production in *parkin*-deficient microglia and increased cytokine production in Parkin OE BV2s. These data are complimentary in terms of a genetic approach, but were functionally contradictory to what we predicted.

Mixed glia cultures

Our observation that *parkin*-deficiency in microglia diminished secretion of cytokines led us to hypothesize that the isolation of pure microglia generated a phenotype that was not physiologically relevant. In the milieu of the brain, microglia function in a network with neurons and other cell types including astrocytes, oligodendrocytes, and endothelial cells. Therefore, we measured cytokine release in wild type and *parkin*$^{-/-}$ mixed glia cultures of microglia and astrocytes. The preparation of these cultures is identical to the preparation of isolated microglia cultures, except we did not dissociate the microglia from the astrocyte bed. We observed increased levels of IFNg, IL-12p70, IL-1b, and IL-10 between 4 and 12 hrs after treatment with 1ug/mL LPS **(Figure 3.6)**. However, cytokine levels from *parkin*$^{-/-}$ mixed glia cultures equaled wild type production after about 24 hrs, suggesting either that the cytokines were degraded by this time point, or that the aberrant response of *parkin*$^{-/-}$ mixed glia was not robust. The transiently increased cytokine production in *parkin*$^{-/-}$ mixed glia did not correspond with increased toxicity in MN9D cells upon transfer of mixed glia CM at either 4 hrs or 24 hrs after LPS stimulation (**Figure 3.7**).

Parkin overexpression increases NF-κB activation in BV2 microglia.

Parkin was demonstrated to regulate NF-κB signaling by ubiquitinating IκB, which targets IκB for degradation by the proteasome and frees NF-κB to translocate to the nucleus and activate gene transcription (Henn, Bouman et al. 2007; Sha, Chin et al. 2010). Microglial production of cytokines and chemokines is regulated by NF-κB activation. Due to the fact that we observe decreased cytokine production in *parkin*$^{-/-}$

microglia and increased levels in Parkin OE BV2s, we next examined NF-κB activation in microglia predicting that increased Parkin levels would result in increased induction of NF-κB. We transduced BV2 cells with a lentivirus encoding GFP that is driven by the NF-κB promoter. We serum-deprived the BV2 microglia to decrease the level of basal activation, and then measured NF-κB activity in the presence of serum. As predicted, measurement of GFP fluorescence in a plate reader assay indicated that BV2s overexpressing Parkin significantly activated NF-κB more than Parental BV2s (**Figure 3.8**). This experiment confirms other studies that NF-κB induction is positively regulated by Parkin, although a question remains of why this pattern of regulation in isolated *parkin*$^{-/-}$ microglia and macrophages does not hold up in mixed glia production of cytokines.

Nitric oxide levels are comparable in parkin$^{-/-}$ *and wild type microglia and mixed glia cultures.*

As mentioned above, microglia and macrophage-derived nitric oxide (NO) is toxic to neuronal cells (Dawson, Dawson et al. 1992; Shavali, Combs et al. 2006). Therefore, we investigated the level of NO release in isolated microglia as well as mixed glia cultures from *parkin*$^{-/-}$ and wild type mice. *parkin*$^{-/-}$ microglia treated with LPS for 1,2 or 6 days showed a trend for reduced levels of NO compared to wild type microglia (**Figure 3.9**), a similar observation as reduced cytokine production in these cultures. Additionally, mixed glia from *parkin*$^{-/-}$ mice displayed comparable increases in NO levels as wild type mixed glia. These data suggest that Parkin does not regulate NO synthesis or release.

Macrophage migration may be susceptible to age

The ability of mononuclear phagocytes (MPs) to migrate towards damaged tissue is essential to neuronal viability. Given that cytokine and chemokine production as well as NO release were mildly dysregulated, we measured an additional microglia effector function, chemotaxis. Macrophages were isolated from *parkin*$^{-/-}$ and wild type mice and seeded in a cell culture insert in serum free media. To visualize chemotaxis beyond a filter that selectively allows detection of the rhodamine wavelength, we labeled the macrophages with Mitotracker Red. Other studies have shown that gross mitochondrial differences are not detected between wild type and *parkin*$^{-/-}$ cells labeled with Mitotracker Red. Chemotaxis towards serum-containing media had no genotype dependent effect in macrophages isolated from 5 month old mice. However, *parkin*$^{-/-}$ macrophages from 20 month old mice had enhanced migration compared to macrophages from age-matched wild type mice (**Figure 3.10**). Chemotaxis of macrophages towards TNF-treated or mechanically injured MN9D cells was not significantly different between wild type and *parkin*$^{-/-}$ macrophages of either age (data not shown). This observation suggests that peripheral macrophages may more readily migrate to the CNS to populate lost or dying microglia populations in the brain. Additionally, the chemotaxis could be a response to increased age-related inflammation.

Discussion

parkin-deficient mice are more vulnerable to inflammation-induced loss of DA neurons in the SN, but it is unclear whether the loss of Parkin in the neurons or the glia is more detrimental. We observed increased expression of inflammatory markers in the serum and midbrain of *parkin*$^{-/-}$ mice compared to that of wild type mice. In addition, it has been reported that microglia from *parkin*$^{-/-}$ mice are more toxic to neurons in a co-culture when stimulated with rotenone (Casarejos, Menendez et al. 2006). However, in these studies it is unknown whether loss of *parkin* specifically increased the generation of cytokines, chemokines, and nitric oxide or other cytotoxic mediators. Here, we show that isolated microglia from *parkin*$^{-/-}$ mice release reduced levels of TNF, IL-6, IL-10, IL-12p70, KC and IFN-g. BV2 microglia with acutely reduced Parkin levels also released less cytokines compared to parental BV2 cells suggesting that the aberrant response of *parkin*$^{-/-}$ microglia is not from developmental compensation.

On the other hand, mixed glia cultures from *parkin*-null mice which contain microglia and astrocytes produce increased cytokines, suggesting that interaction between microglia and astrocytes is essential for proper regulation of cytokine production and release by microglia. Mixed glia cultures may strongly influence the responses of microglia because astrocytes release granulocyte and macrophage colony stimulating factor (GM-CSF), macrophage colony stimulating factor (M-CSF) and ICAM1 that bind receptors on the microglia to signal activation (McGeer and McGeer 2008). Therefore, the release of chemical mediators by astrocytes also serves to prune microglial responses to

inflammation. To extend these studies and investigate the contribution of astrocyte-derived factors on the activation of isolated microglia, we hypothesize that isolated *parkin*$^{-/-}$ microglia cultured with the GM-CSF, M-CSF or ICAM1 will increase production of cytokines, as similarly evidenced in the mixed glia cultures. If the astrocyte-derived factors are not sufficient to induce elevated cytokine production in the absence of astrocyte co-culturing, we would conclude that microglia inflammatory responses are mediated in some form by physical contact with astrocytes. Additionally, the loss of Parkin in astrocytes has not been explored in the contribution to neuronal health.

The phenotype of *parkin*$^{-/-}$ microglia and macrophages may be influenced not only by co-culturing with astrocytes, but also by a possible phenotype switching from classical to alternative activation in the absence of astrocytes. Classic activation of microglia is termed M1 and is described as increased levels of pro-inflammatory cytokine and NO production (i.e. supporting tumoricide). On the other hand, alternatively activated microglia display the M2 characteristics of decreased cytokine secretion, and decreased production of NO. In studies using cancer cell lines, an M2 phenotype is associated with tumorigenesis and is induced by chronic activation of macrophages. We observe the decreased levels of cytokines as well as significantly lower iNOS levels in the *parkin*$^{-/-}$ microglia and macrophages (data not shown) consistent with the M2 phenotype. To more thoroughly explore whether the isolated microglia and macrophages are alternatively activated, we will measure YM1, arginase1, and FIZZ1 levels, which are reported to increase in alternatively activated or M2 macrophages.

Of interest is the increased and sustained production of IL-1b by *parkin*$^{-/-}$ microglia and macrophages compared to the other cytokines measured in the multiplexed ELISA. IL-1b is cleaved from pro-IL-1b by activation of caspase 1. Parkin may function in caspase 1 activation directly or through interaction with a complex of proteins that recruits and activates caspase 1, known as the "inflammasome" (Bryant and Fitzgerald 2009). Exploring the role Parkin in these interactions would be of interest in future studies.

Migration of mononuclear phagocytes (MPs) such as microglia and macrophages to a site of tissue injury is another effector function performed by MPs. Our examination of macrophages from *parkin*$^{-/-}$ mice showed increased chemotaxis in macrophages isolated from 20 month old mice compared to wild type mice. However, no genotype-dependent difference was observed with macrophages from 5 month old mice. Increased inflammation is correlated with age, so the loss of Parkin in aged mice may potentiate inflammation and increase chemotaxis. MPs localize to areas of injury by migrating towards chemical gradients and stop at site of damage to promote tissue repair. The significance of increased chemotaxis of aged *parkin*$^{-/-}$ macrophages is that in concert with the increased activation status, the *parkin*$^{-/-}$ macrophages may not correctly recognize sites of injury, or are unable to inactivate to provide support at the injury site. We did not explore the variable of age in cytokine secretion although in one preparation of macrophages from 18 month old *parkin*$^{-/-}$ mice (macrophages were generally harvested from adult mice 6 to 12 months), we observed significantly increased cytokine

production and increased toxicity to MN9D cells (data not shown). These data would suggest multiple effector functions in *parkin*$^{-/-}$ microglia which be exacerbated with age.

Studying cytokine secretion in isolated microglia versus microglia in the presence of astrocytes has led to a better understanding of cellular responses resulting from *in vitro* cell culture. Another explanation for our observation that *parkin*$^{-/-}$ microglia are not more toxic to MN9D dopaminergic neurons when treated with LPS, may the explicit use of LPS in our studies. In the studies that reported the enhanced toxicity of *parkin*$^{-/-}$ microglia, the mitochondrial toxin rotenone was used to stimulate the microglia. Treatment with an inflammogen that directly activates the microglia may require Parkin in a different capacity compared to treatment with rotenone, which impairs mitochondrial respiration and generates oxidative stress. Parkin upregulation in response to oxidative stress (Henn, Bouman et al. 2007) and the immediate recruitment of Parkin to the mitochondria to deal with respiratory injury may also suggest a time-dependent effect of Parkin loss in cellular toxicity induced either by oxidative stress or receptor-mediated activation of inflammation. Toxicity from oxidative stress may be more immediate in the absence of Parkin, whereas cellular toxicity induced by inflammatory responses may take longer to manifest in the absence of Parkin; such as in a chronic inflammatory study, which we recently investigated.

In previous studies we observed that Parkin regulates microglia phenotype and activation status. From these studies we conclude that age at the time of cell isolation and conditions of cell culture, such as co-culturing with astrocytes, may be essential in the cytotoxic

phenotype of *parkin*$^{-/-}$ microglia and macrophages. The induction of either oxidative stress or inflammation may also play an important role in the capacity at which Parkin serves a protective role in the cell. The role Parkin in NF-κB signaling needs to be further explored to determine whether Parkin regulation of NF-κB signaling is dependent on cell type. We learned that cytokine release may not be overtly dysregulated in isolated *parkin*$^{-/-}$ microglia and macrophages, but the specific regulation of IL-1b is unique and may prove to be physiologically relevant. Finally, age may affect the toxic phenotype of *parkin*$^{-/-}$ microglia which is significant because age contributes to increased levels of inflammation in the body and ultimately in the risk of developing PD.

Figures

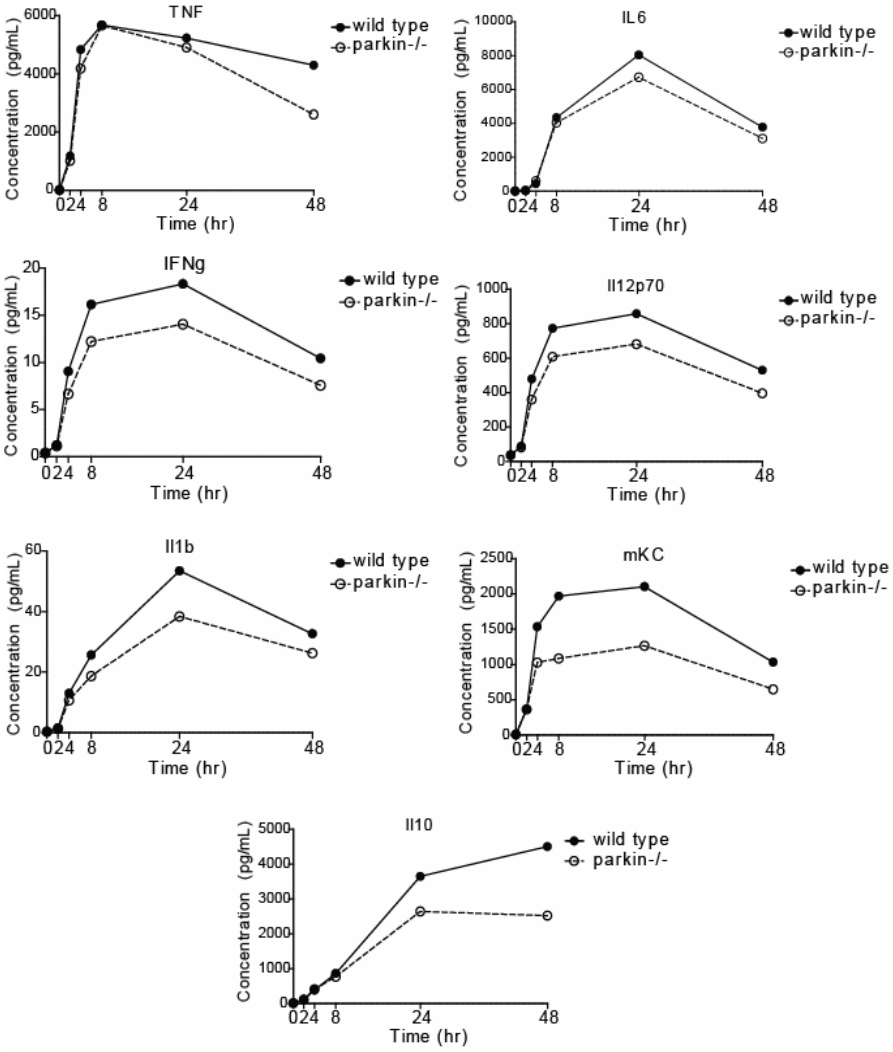

Figure 3.1 *parkin*$^{-/-}$ *microglia secrete diminished levels of cytokines compared to wild type microglia after LPS stimulation.* Microglia isolated from postnatal wild type and *parkin*$^{-/-}$ mice (n=3-6) were treated with 1ug/mL LPS, and supernatants collected at the time points indicated. Multi-analyte ELISA was performed to measure cytokine and chemokine levels from pooled samples (one sample is 3 separate wells of a tissue culture plate). Data are representative of 3 independent dissections and treatments.

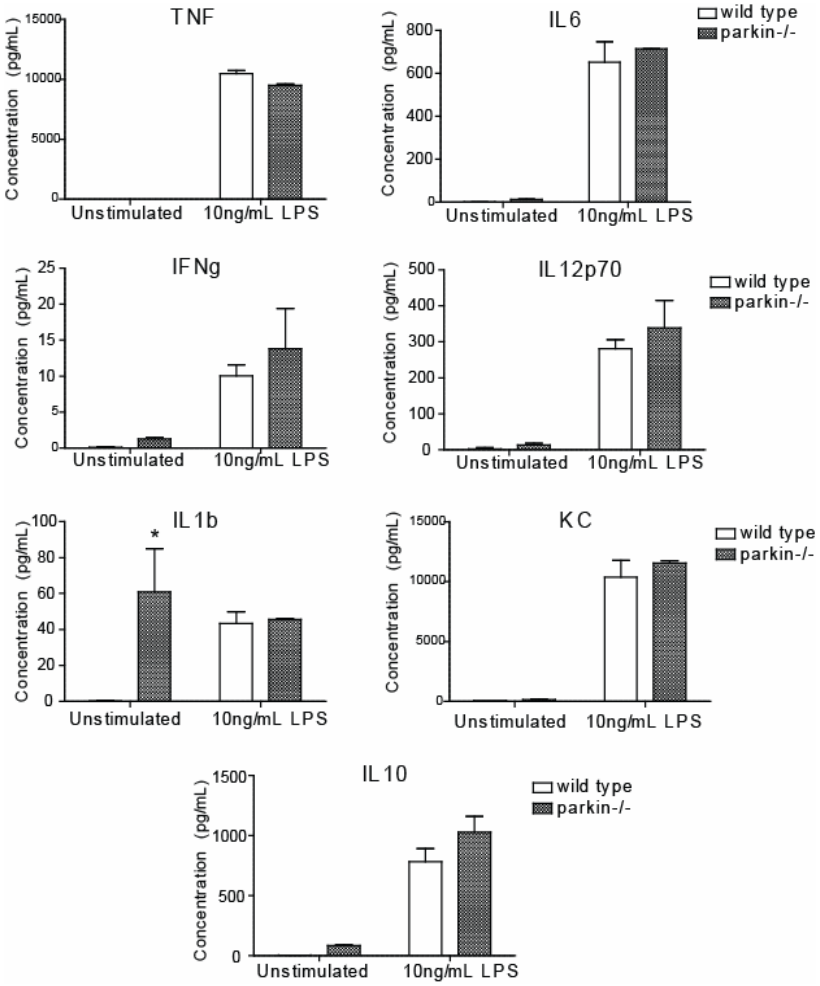

Figure 3.2 *parkin*$^{-/-}$ *primary macrophages secrete similar levels of cytokines in response to LPS as wild type macrophages.* *parkin*$^{-/-}$ and wild type macrophages isolated from 10 month old mice were treated with 10ng/mL LPS for 24 hrs. LPS-induced cytokine and chemokine release does not differ between genotypes as measured by multi-analyte ELISA. IL-1b was the only cytokine increased in unstimulated *parkin*$^{-/-}$ macrophages. Values represent mean cytokine release $\pm$ SEM. Two way ANOVA and Bonferroni's post hoc, * $p<0.05$ represents significance relative to wild type. Data are representative of 3 independent dissections and treatments.

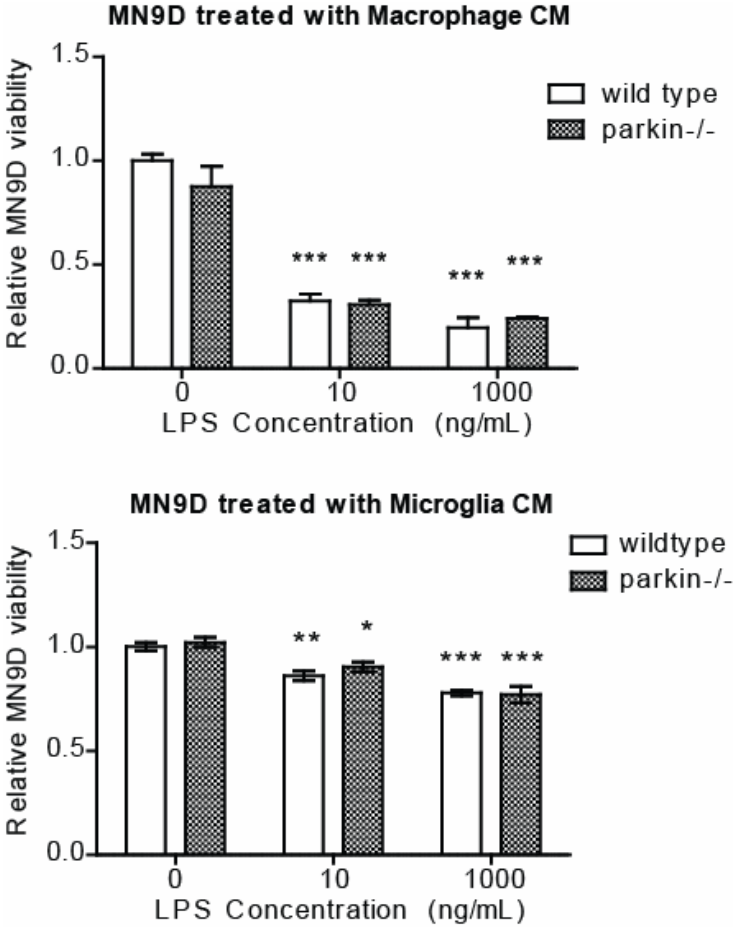

Figure 3.3. *parkin*$^{-/-}$ *primary microglia and macrophage conditioned media (CM) is not more toxic to MN9D dopaminergic neurons.* Supernatant was collected from *parkin*$^{-/-}$ and wild type microglia and macrophages treated with LPS for 24 hrs and transferred to a culture of MN9D cells. LPS-induced effect on MN9D cell viability was significant as measured by MTS assay, but no genotype effect was observed. Two way ANOVA and Bonferroni's post hoc, * $p<0.05$, ** $p<0.01$and *** $p<0.001$ represents significance relative to untreated sample. Data are representative of 3 independent experiments.

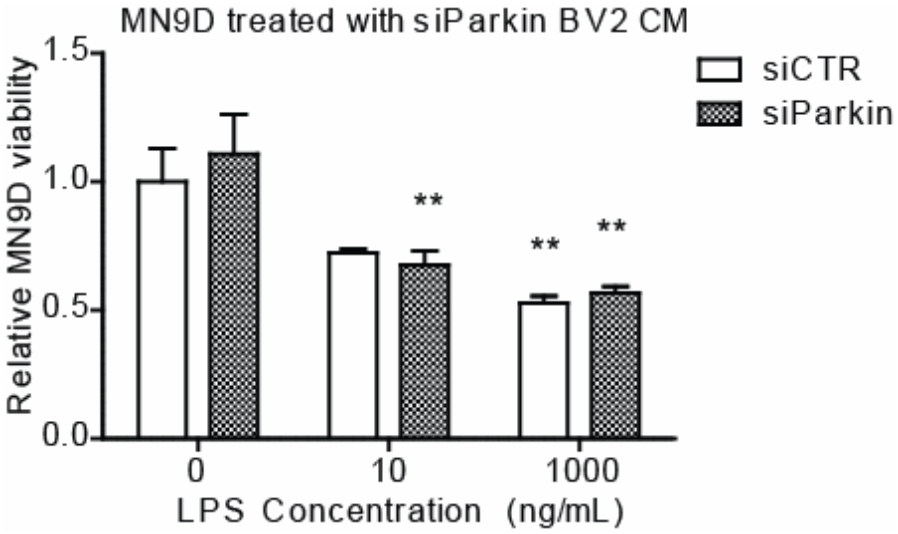

Figure 3.4. *siRNA-mediated knockdown of Parkin (siParkin) in BV2 cells does not increase LPS-induced toxicity compared to siControl (siCTR).* siParkin BV2 microglia were treated with LPS for 24 hrs, CM was collected and transferred to a culture of MN9D cells. LPS-induced effect on MN9D viability does not differ between siCTR and siParkin as measured by MTS assay. Two way ANOVA and Bonferroni's post hoc, ** $p<0.01$ represents significance relative to untreated sample. This graph represents data from one cell culture study.

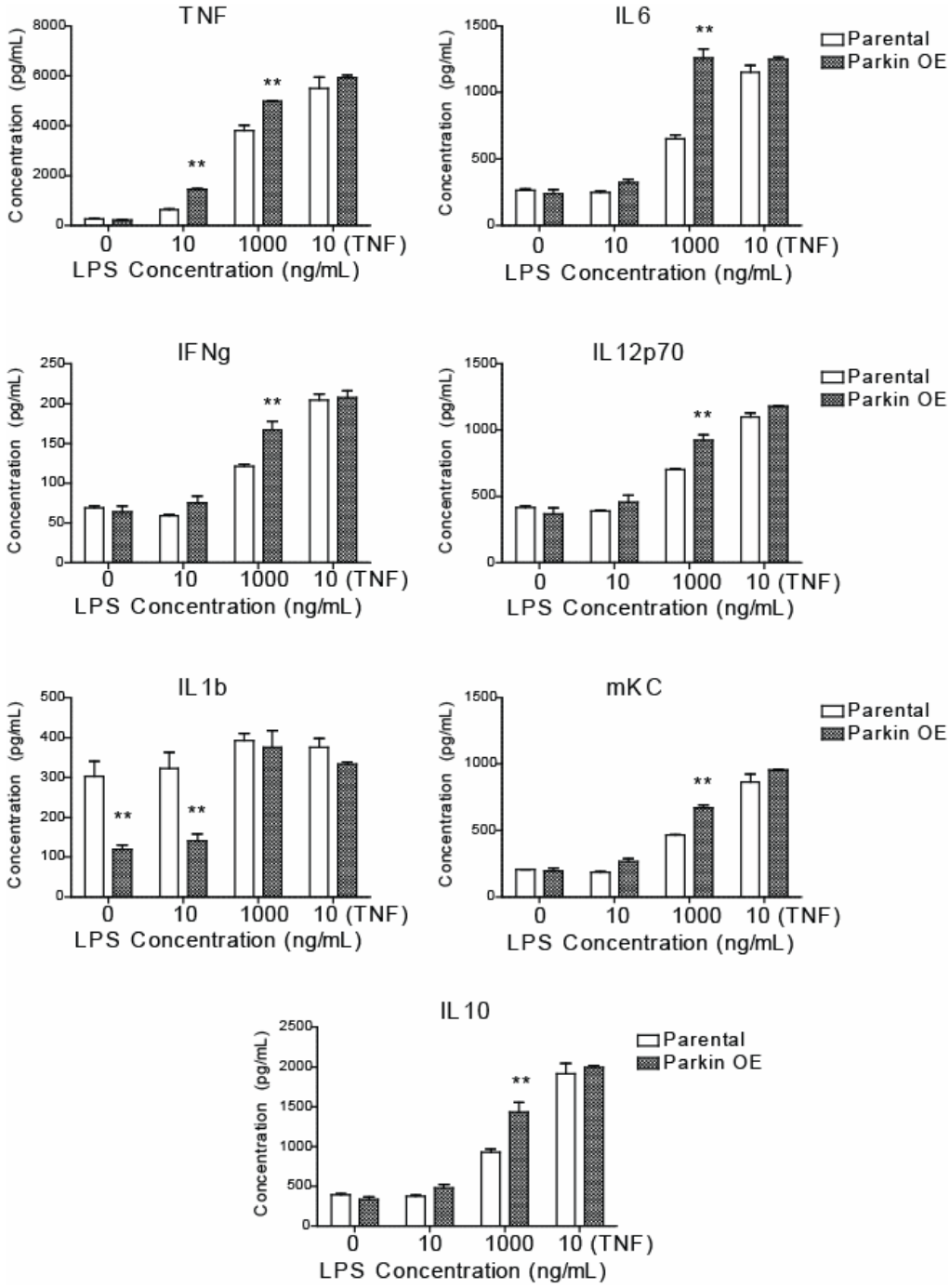

Figure 3.5. *BV2 cells overexpressing Parkin (Parkin OE) secrete elevated levels of cytokines in response to LPS.* Parkin OE BV2 microglia release more cytokines in

response to a 24 hr treatment of 1ug/mL LPS; only TNF levels were enhanced with the 10ng/mL (low) LPS dose. Parkin overexpression did not affect cytokine levels after TNF treatment. IL-1b was the only cytokine decreased in unstimulated Parkin OE BV2 cells and when treated with the lower LPS dose. Multi-analyte ELISA was performed to measure cytokine and chemokine levels. Values represent mean cytokine release $\pm$ SEM. Two way ANOVA and Bonferroni's post hoc, ** $p<0.01$ represents significance relative to Parental BV2s for each treatment. This graph represents data from one cell culture study.

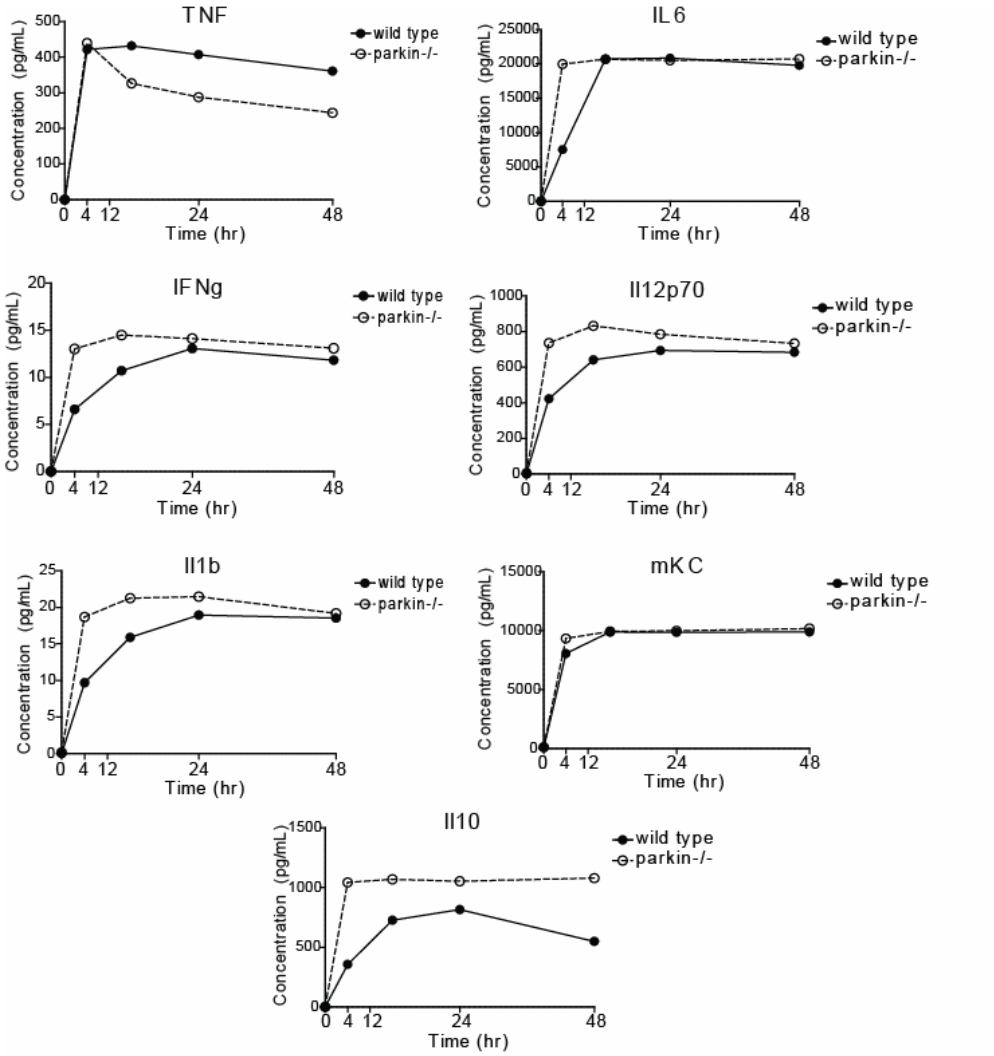

Figure 3.6. *LPS stimulation enhances cytokine secretion in parkin$^{-/-}$ mixed glia cultures compared to wild type cultures.* Mixed glia (microglia and astrocyte) cultures isolated from post natal wild type and *parkin$^{-/-}$* mice (n=3-6) were treated with 1ug/mL LPS, and supernatants collected at the time points indicated. Multi-analyte ELISA was performed to measure cytokine and chemokine levels from pooled samples (one sample is 3 separate wells of a tissue culture plate). Data are representative of 3 independent dissections and treatments.

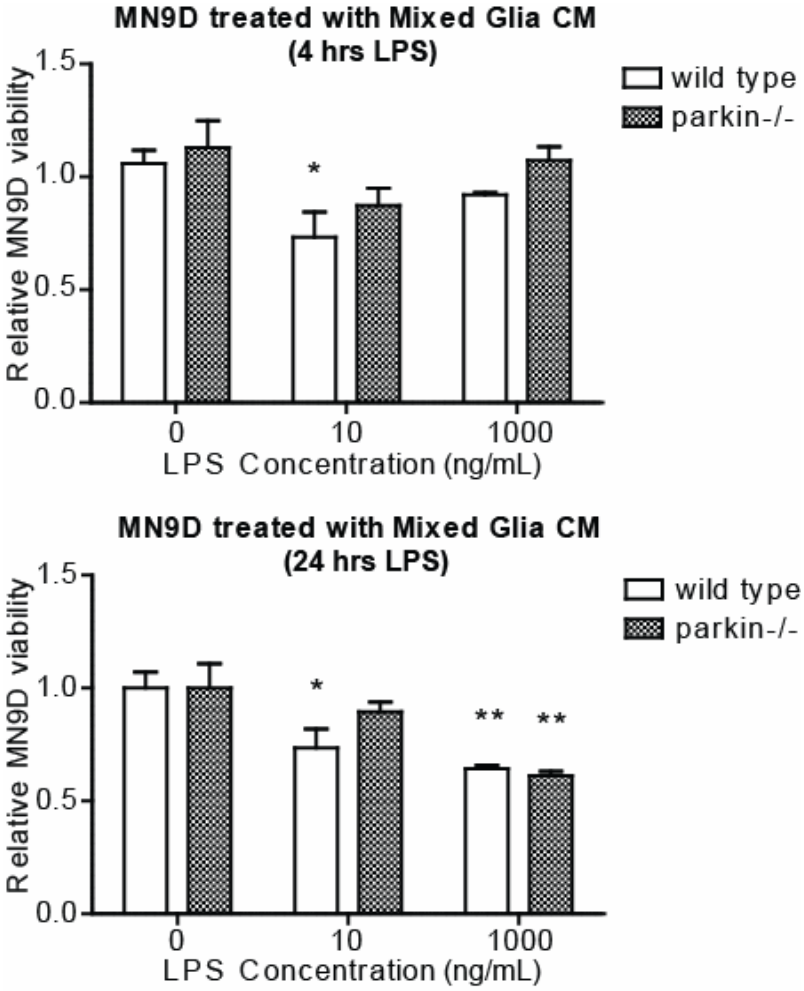

Figure 3.7. *CM from parkin$^{-/-}$ primary mixed glia are not more toxic to MN9D cells.* Supernatants was collected from *parkin$^{-/-}$* and wild type mixed glia treated with 1ug/mL LPS for 4 and 24 hrs, and transferred to MN9D cells. LPS-induced effect on MN9D viability does not differ between genotypes as measured by MTS assay. Two way ANOVA and Bonferroni's post hoc, * $p<0.05$ and ** $p<0.01$ represents significance relative to wild type. This graph represents data from one cell culture study.

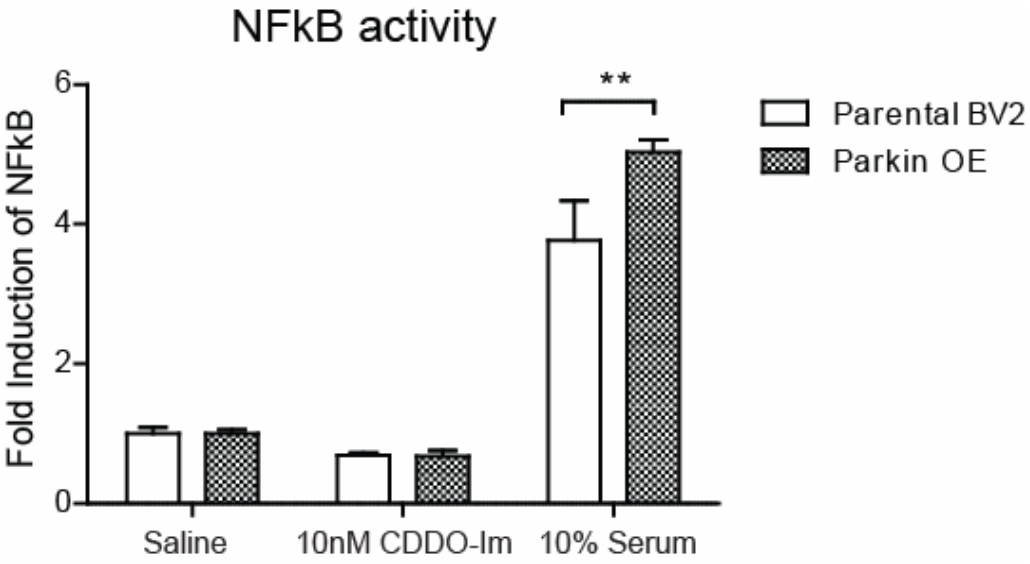

Figure 3.8. *BV2 cells overexpressing Parkin (Parkin OE) show increased NF-κB activity.* Induction of NF-κB was measured in BV2 cells infected with a lentiviral vector in which the NF-κB promoter drove GFP expression. BV2 cells were serum-deprived prior to the start of the assay. GFP fluorescence was then measured in the presence of serum. Parkin OE BV2 cells had increased NF-κB induction compared to Parental BV2 cells. Fluorescence was measured in a plate reader assay. Two way ANOVA and Bonferroni's post hoc, ** $p<0.01$ represents significance relative to Parental BV2 cells. These data are representative of 3 independent studies.

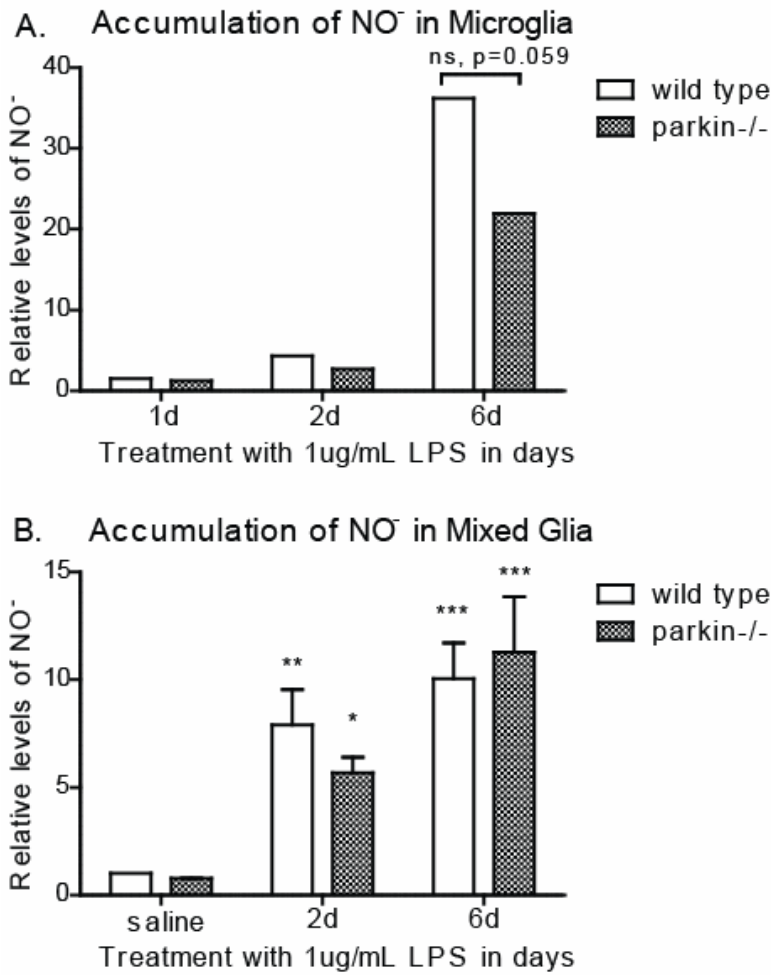

Figure 3.9. *Nitric oxide release does not differ between parkin$^{-/-}$ and wild type microglia or mixed glia cultures. A*, Primary microglia were treated with 1ug/mL LPS for 1, 2, or 6 days, and media was collected to measure nitrate levels by the Greiss reaction. *B*, Primary mixed glia cultures were treated with LPS similar to microglia. Nitrate levels in the media did not differ between genotypes. Two way ANOVA and Bonferroni's post hoc, * $p<0.05$, ** $p<0.01$ and *** $p<0.001$ represent significance relative to saline treated. No genotype effect was observed. These data are representative of two independent dissections and treatments each.

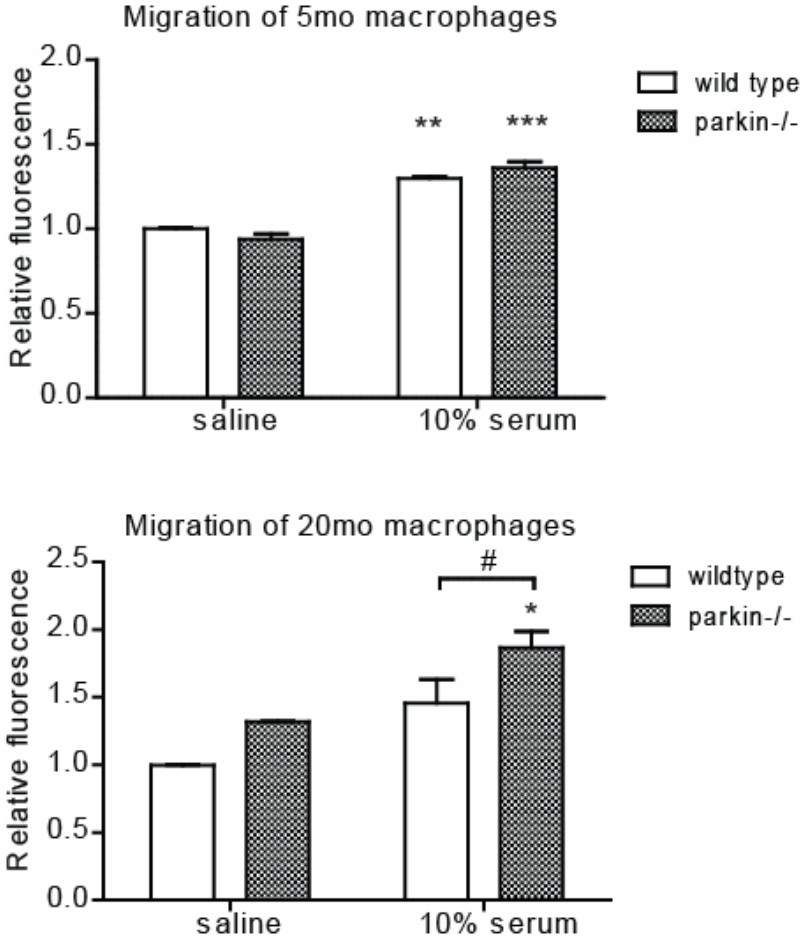

Figure 3.10. *Migration displays age-dependent effect in parkin$^{-/-}$ and wild type macrophages.* Primary macrophages were isolated from 5 mo or 12 mo mice and seeded in a cell culture insert in serum free media. Macrophages were labeled with Mitotracker Red (for visualization of chemotaxis), and migration across the insert towards serum-containing media was measured by a fluorescent plate reader. Two way ANOVA and Bonferroni's post hoc, * $p<0.05$, ** $p<0.01$ and ** $p<0.001$ represent significance relative to saline treated. # $p<0.05$ significance relative to wild type. These graphs represent data from one dissection and cell culture study each.

CHAPTER FOUR

The synthetic triterpenoid CDDO-methyl ester modulates microglial activities, inhibits TNF production, and provides dopaminergic neuroprotection

The contents of this chapter were written up for publication in a manuscript by the same title.

Introduction

Targeting inflammation as a therapeutic for Parkinson's disease has proved largely unsuccessful in clinical trials perhaps because of the inhibition of the beneficial aspects of inflammation as well as the detrimental ones. Therefore understanding the biology of microglia, the cell type responsible for inflammation in the CNS, and cellular pathways responsible for activation and cytotoxicity has been a key endeavor. Plant-derived triterpenoids, including oleanolic acid and ursolic acid, have been used extensively in Asian countries for their anti-inflammatory and anti-tumor properties (Liu 1995). In an attempt to increase the potency of these natural products, over 300 synthetic derivatives of oleanolic acid were generated and tested for their ability to inhibit NO production in activated macrophages (Honda, Rounds et al. 1998; Honda, Rounds et al. 1999; Honda, Rounds et al. 2000). Some of the most potent of these, including 2-cyano-3,12dioxooleana-1,9-dien-28-oic acid (CDDO; RTA 401) and its methyl ester (CDDO-Me; RTA 402), exhibit greater than 2 × 105-fold increased potency compared to the parental compound. CDDO-Me is presently in Phase I/II clinical trials for the treatment of solid tumors. In light of their potent bioactivity, this new class of compounds has

therapeutic potential in the treatment and prevention of acute and chronic inflammatory syndromes.

Although identification of the molecular targets of triterpenoids is just underway, a number of recent studies have identified key mechanisms that mediate the potent effects of triterpenoids. One of these mechanisms involves decreasing the levels of reactive oxygen species (ROS) through activation of Nrf2-dependent transcription (Dinkova-Kostova, Liby et al. 2005; Thimmulappa, Scollick et al. 2006). In addition, the triterpenoids directly inhibit NF-κB signaling (Ahmad, Raina et al. 2006; Yore, Liby et al. 2006), a key pathway that regulates the production of a number of inflammatory mediators and their signaling cascades (e.g. TNF, IL-1ß, IFN., TLR) (Kulms 2006). Increased levels of antioxidant enzymes produced by Nrf2 reduce the cellular levels of ROS, thereby further attenuating NF-κB signaling and the transcription of pro-inflammatory genes such as iNOS and TNF (Asehnoune, Strassheim et al. 2004; Dinkova-Kostova, Liby et al. 2005; Thimmulappa, Fuchs et al. 2007).

The role of neuroinflammation in neurodegenerative disease has been under intense investigation in recent years and there is now overwhelming evidence that inflammation-induced oxidative stress compromises neuronal survival and may contribute to the progression of neurodegenerative diseases including Parkinson's (PD) and Alzheimer's disease (AD) (reviewed in (Liu and Hong 2003; Hald and Lotharius 2005; Hirsch, Hunot et al. 2005; Wersinger and Sidhu 2006; Block, Zecca et al. 2007; Tansey, McCoy et al. 2007; Whitton 2007)). We reasoned that if CDDO-Me were able to suppress microglial

activities that contribute to neurotoxicity while promoting those that support neuronal survival, it may be capable of exerting neuroprotective effects. Therefore, the overall purpose of these studies was to investigate the cellular basis for the anti-inflammatory properties of CDDO-Me; specifically, to identify microglial activities modulated by CDDO-Me in vitro and the extent to which this modulation protects against inflammatory stimuli.

Results

CDDO-Me inhibits proliferation and activation of microglia.

Neuroinflammatory processes are associated with a number of neurodegenerative conditions and have been implicated in the underlying progressive loss of neurons (McGeer and McGeer 2004; Griffin 2006; Wyss-Coray 2006; McGeer and McGeer 2007; Tansey, McCoy et al. 2007; Whitton 2007). Therefore, inflammatory factors and mechanisms that contribute to neurotoxicity and compromise neuronal survival need to be elucidated and specifically targeted without interfering with the neuroprotective effects of glial activities (Liu and Hong 2003). Synthetic triterpenoids have potent anti-proliferative and differentiating effects on tumor cells and anti-inflammatory activities on activated macrophages. Therefore, we hypothesized that CDDO-Me may be able to promote neuronal survival by suppressing neurotoxic microglial activities without compromising overall microglial cell viability. In pilot experiments, we established the concentration range of CDDO-Me beyond which anti-proliferative and toxic effects could be detected in a murine BV2 microglial cell line. We found that CDDO-Me

concentrations at or above 100 nM inhibited the proliferative response to bacterial lipopolysaccharide (LPS) as measured by Alamar blue reduction and that concentrations greater than 500 nM were toxic (data not shown). Based on these results, we chose to use concentrations of CDDO-Me at or below 100 nM for our studies.

We first investigated the ability of CDDO-Me to inhibit activation of microglia in response to specific inflammatory stimuli. Treatment of rat primary mesencephalon neuron/glia cultures with CDDO-Me alone did not elicit microglial activation; but CDDO-Me pre-treatment resulted in attenuated LPS-, TNF- or fibrillar Aβ-induced increase in microglial activation, as measured by the number of F4/80-immunoreactive microglia (**Figure 4.1**). These findings suggested that differential modulation of microglial activities might be possible at concentrations of CDDO-Me below 100 nM without cytotoxic effects to the cells.

CDDO-Me suppresses transcription of inflammatory mediators in microglia and macrophages.

A number of microglial-derived mediators have been reported to mediate neuronal death in experimental models of neurodegeneration (reviewed in (Tansey, McCoy et al. 2007)), raising the possibility that anti-inflammatory therapies may be an effective means of delaying or attenuating neuron death. Therefore, we investigated the ability of CDDO-Me to regulate expression of inflammation- and oxidative stress-related genes in primary microglia, macrophages, and the BV2 microglia cell line. We performed real-time quantitative polymerase chain reaction (QPCR) to measure mRNA levels for a number of

inflammation-related genes. LPS-induced production of TNF mRNA was significantly reduced in all cell types while IL-1β mRNA was significantly reduced in primary microglia and macrophages but not BV2 cells (**Figure 4.2**). CDDO-Me also significantly attenuated the LPS-induced mRNA expression of MIP-1α and iNOS. Multiplexed immunoassay analysis of BV2 microglia-conditioned medium (CM) confirmed that CDDO-Me attenuated LPS-induced production of factors such as IL-12, IL-6, and TNF all of which are known to promote autocrine signaling in microglia (**Figure 4.3**). Given that both IL-6 and TNF can compromise DA neuron survival, these findings raised the possibility that CDDO-Me may be able to protect neuronal populations that display increased vulnerability to inflammation-induced oxidative stress and apoptotic death, in particular dopaminergic neurons (De Pablos, Herrera et al. 2005; Tansey, McCoy et al. 2007), by limiting the production of these neurotoxic factors by chronically activated microglia without compromising other microglial functions. It should be noted, however, that not all chemokines and cytokines typically associated with pro-inflammatory responses were depressed by exposure to CDDO-Me. For instance, CDDO-Me increased production of CXCL1 (also known as keratinocyte-derived chemokine (KC)), a potent chemoattractant to neutrophils (Frink, Hsieh et al. 2007) (**Figure 4.3**). Curiously, while CDDO-Me reduced (not significantly) LPS-induced IL-1β mRNA in the BV2 microglia cell line (**Figure 4.2**), it potentiated secretion of this cytokine by BV2 cells (**Figure 4.3**). The reason for this effect is unclear but these findings raise the interesting possibility that synthetic triterpenoids may be able to differentially regulate inflammatory responses by altering transcription of specific subsets of genes and perhaps by modulation of post-transcriptional signaling cascades that influence secretion of specific inflammatory

factors. Future research into this area will provide much needed insight into other mechanisms of action for synthetic triterpenoids. To complement these findings and survey a larger number of inflammation-related genes, we performed oligonucleotide gene arrays in BV2 microglia treated with saline or LPS in the presence of CDDO-Me or its vehicle (DMSO). In resting microglia, CDDO-Me upregulated the receptor for a classic anti-inflammatory cytokine IL-10 while inhibiting basal expression of 12 inflammation-related genes, including TNF, iNOS2, IL-18, MCP1 (CCL2), Mip1α (CCL3), and Mip1β (CCL4) (**Figure 4.4a**). These results indicate CDDO-Me coordinately attenuates gene expression of pro-inflammatory genes and enhances genes known to be part of anti-inflammatory responses. As expected, stimulation of BV2s with LPS-triggered upregulation of the gene for the pro-inflammatory cytokine TNF as well as genes for the chemokines Mip1β (CCL4) and Mip1γ (CCL9) while downregulating IL-15, IL-18, IL-2, and IL-8 (**Figure 4.4b**). Consistent with the well-known fact that the normal cellular response to an inflammatory stimulus is to activate anti-inflammatory response loops to return the cell to a pre-activation status, we also detected increased IL-10 receptor expression in response to LPS. In support of its anti-inflammatory properties, CDDO-Me attenuated LPS-induced increases in pro-inflammatory gene expression including TNF and MCP1 (CCL2) (**Figure 4.4c**); these results are similar to those reported for CDDO-Im in LPS-stimulated peripheral neutrophils (Thimmulappa, Scollick et al. 2006). In agreement with real-time QPCR results, treatment with CDDO-Me blocked the LPS-induced increases in iNOS, MIP1α, and CCL2. Moreover, CDDO-Me was able to reverse the LPS-induced downregulation of IL-15 and IL-2 genes (**Figure 4.4c**). Lastly, the oligonucleotide arrays indicated that expression of receptors for the

anti-inflammatory cytokines IL-10 and IL-13 as well as complement component (required for destroying bacterial pathogens) were also upregulated by CDDO-Me exposure (**Figure 4.4b, c**), suggesting CDDO-Me may be an effective anti-infective.

CDDO-Me attenuates microglial-mediated neuronal oxidative stress.

Oxidative stress, which is defined as the cellular condition when production of reactive oxygen and nitrogen species (ROS/RNS) exceeds the capacity of antioxidant defenses, is a trigger for glial activation and is a feature of most neurological and neurodegenerative conditions. Therefore, the use of antioxidants has been intensely investigated in models of neurodegeneration for their direct neuroprotective effects and for their ability to protect by suppressing the glial-mediated inflammatory response (Wang, Wen et al. 2006; Reynolds, Laurie et al. 2007). We investigated the ability of CDDO-Me to inhibit intracellular accumulation of ROS using the cell permeant dye DCFDA in mixed neuron-glia cultures from rat basal forebrain. Inflammation-induced intracellular ROS accumulation was evident primarily in cells with morphological characteristics consistent with that of neurons and to a lesser extent in the surrounding glial cells after treatment with LPS + fibrillar Aβ42 (**Figure 4.5a, b**). Co-addition of CDDO-Me to these cultures inhibited the intracellular ROS accumulation induced by LPS + fibrillar Aβ42. The accumulation of ROS in neuronal cells was confirmed by treatment of the dopaminergic cell line MN9D with conditioned media from LPS and CDDO-Me treated BV2 microglial cells. Pretreatment of BV2s with 10 nM CDDO-Me before LPS exposure attenuated the ability of the conditioned media (CM) from BV2 microglia cultures to induce ROS accumulation in terminally differentiated MN9D cultures (**Figure 4.5c**).

Pretreatment of differentiated MN9Ds with CDDO-Me did not attenuate intracellular ROS accumulation resulting from direct TNF treatment (**Figure 4.5d**). Taken together, these findings suggest that the mechanism by which CDDO-Me protects neuronal cells may be primarily through changes in microglial-derived mediators and not through direct anti-oxidant effects on neuronal cells.

CDDO-Me protects the dopaminergic MN9D cell line from inflammation-induced death. Pro-inflammatory cytokines, in particular TNF, exert potent toxic effects on dopaminergic neurons and have been implicated in neurodegenerative disease pathogenesis (Mrak and Griffin 2005; Mrak and Griffin 2007; Tansey, McCoy et al. 2007; Whitton 2007). To investigate the ability of CDDO-Me to protect dopaminergic neuron-like cells from inflammation-induced death, we performed in vitro target-effector cell survival assays. Survival of differentiated MN9D dopaminergic cells was measured after direct incubation with soluble TNF or in undifferentiated cultures after incubation with CM from LPS-treated BV2 microglia cells. We found that 10 nM CDDO-Me abolished MN9D cell death induced by exposure to CM from LPS-stimulated BV2 microglia (**Figure 4.6a**), but ineffectively attenuated cell death induced by the direct addition of TNF to MN9D cells (**Figure 4.6b**). These findings were consistent with a mechanism by which the neuroprotective effects of CDDO-Me in these assays are mediated by its ability to inhibit microglial-derived TNF production (**Figure 4.3**) or by interfering with the intracellular site of action of other neurotoxic cytokines elicited by LPS rather than by direct inhibition of TNF-dependent death signaling by CDDO-Me.

To test this idea directly, we added the TNF decoy receptor etanercept to bind and deplete soluble TNF from CM of BV2 microglia stimulated with LPS alone or in combination with CDDO-Me prior to CM transfer to MN9D dopaminergic cells. In support of this model, we found that etanercept attenuated MN9D cell death equivalent to that obtained with CDDO-Me treatment alone and together the two were not additive (**Figure 4.6a**).

CDDO-Me enhancement of microglial phagocytic activity is stimulus-specific.

Our findings that CDDO-Me attenuates production of some but not all inflammatory mediators raised the interesting possibility that other microglial activities could be modulated differentially by CDDO-Me. To investigate the ability of CDDO-Me to regulate phagocytic responses of BV2 microglia, we stimulated the cells with different inflammatory agents and analyzed their ability to phagocytose fluorescently labeled E. coli particles. We found that CDDO-Me had minimal effect on basal phagocytic activity of BV2 microglia or phagocytosis induced by LPS, but was able to enhance phagocytosis induced by TNF or fibrillar Aβ1–42 peptide (**Figure 4.7**). These findings suggest stimulus-specific modulation of microglial phagocytosis by CDDO-Me and warrant further investigation in models of amyloid deposition.

Discussion

Chronic neurodegenerative diseases are often associated with neuroinflammatory processes that may not only occur in response to neuron loss but may also contribute to it (McGeer and McGeer 2004; Griffin 2006; Wyss-Coray 2006; McGeer and McGeer 2007;

Tansey, McCoy et al. 2007; Whitton 2007). Because certain inflammatory responses in the brain are required for clearing cellular debris, limiting tissue damage, and contributing to wound repair, it is critical that inflammatory factors and mechanisms that contribute to neurotoxicity and compromise neuronal survival be identified and selectively targeted without interfering with the neuroprotective effects of glial activities (Liu and Hong 2003). Our previous studies established a critical role for TNF as a mediator oxidative neurotoxin and endotoxin-induced dopaminergic neuron death in models of PD (McCoy, Martinez et al. 2006). The ability of CDDO-Me to inhibit new synthesis of TNF in microglia and to effectively reduce soluble TNF production by activated cells offers one possible mechanism by which the anti-inflammatory properties of CDDO-Me affords protection to dopaminergic cells. In addition to its anti-inflammatory properties, CDDO-Me may be able to boost or strengthen the immune system through upregulation of IL-2 signaling. IL-2 has been shown to be critical for survival, proliferation and differentiation of T-cells into effector cells and to confer a survival advantage to CD4+ T-cells to facilitate development of a memory population (Dooms, Kahn et al. 2004; Isomaki, Clark et al. 2005). In chronic inflammatory syndromes characterized by persistent elevation of pro-inflammatory cytokines, localized IL-2 depletion at sites of inflammation has been shown to be the most profound effect of long term exposure to TNF (Clarke and Branton 2002); our data suggests that therapeutic use of CDDO-Me may be able to reverse this phenomenon.

The observed antioxidant effects of CDDO-Me are not surprising given that synthetic triterpenoids have been shown to activate Nrf2, the key transcription factor that globally

regulates the phase II detoxification pathway. Regardless of whether the primary antioxidant effect of CDDO-Me is mediated via direct action on neuronal populations or by suppression of glial-derived extracellular ROS production to reduce oxidative stress in neurons, the mechanisms by which synthetic triterpenoids exert antioxidant effects merit further investigation in animal models of neurodegeneration where oxidative stress is believed to be the primary mediator of neuron death. In support of this idea, it was recently reported that feeding pharmacological inducers of the phase II detoxification pathway to Drosophila parkin mutants or flies overexpressing α-synuclein suppressed the neuronal loss in both models of Parkinson's disease (Trinh, Moore et al. 2008).

In summary, our findings indicate that in response to specific inflammatory triggers, CDDO-Me is able to differentially regulate microglial activities without compromising either microglial survival or the ability of microglia to perform basic functions (i.e. phagocytosis). Moreover, the ability of CDDO-Me to limit production and secretion of neurotoxic pro-inflammatory cytokines and to attenuate intracellular ROS accumulation strongly suggest that chronic administration of brain-permeant synthetic triterpenoids will confer neuroprotection *in vivo*. Several other anti-inflammatory agents have been reported to have neuroprotective properties in in vitro and in vivo models of Parkinson's disease. Specifically, the tetracycline derivative minocycline, which inhibits TNF synthesis, potently attenuates DA neuron loss resulting from nigral LPS treatment of rats (Tomas-Camardiel, Rite et al. 2004). Similarly, thalidomide (a non-selective immune modulating drug that reduces TNF expression through degradation of TNF mRNA) has been demonstrated to partially attenuate dopamine depletion in an MPTP mouse model of

PD (Ferger, Leng et al. 2004). Naloxone, an opioid receptor antagonist, protected rat DA neurons against inflammatory damage through inhibition of microglial activation and superoxide generation (Liu, Du et al. 2000); and the kappa-opioid receptor agonist dynorphin A (1–17) attenuated inflammation-mediated degeneration of DA neurons in rat midbrain neuron-glia cultures (Liu, Qin et al. 2001). In addition, dextromethorphan (DM), an ingredient widely used in antitussive remedies, has been shown to reduce the inflammation-mediated degeneration of DA neurons through inhibition of microglial activation (Liu, Qin et al. 2003). Therefore, the neuroprotective properties of CDDO-Me and related compounds merit further investigation in pre-clinical animal models of PD.

Lastly, it may be of interest to determine the extent to which the CDDO-Me-induced enhancement of microglial phagocytic activity observed in our in vitro studies can be achieved in vivo with brain-permeant synthetic triterpenoids. This issue may be of particular therapeutic relevance in the treatment of AD because pro-inflammatory cytokines, including TNF, have been shown to preferentially attenuate phagocytic activity of microglia induced by fibrillar Aβ amyloid peptides (but not by IgG antibody activation of Fc Receptor) through an E prostanoid receptor- dependent mechanism (Koenigsknecht-Talboo and Landreth 2005). On the basis of our results, we speculate that synthetic triterpenoids will be able to promote fibrillar amyloid clearance by potentiating the phagocytic activity of microglia at plaque sites characterized by inflammation where TNF is locally elevated. If synthetic triterpenoids can promote plaque clearance, their use as an adjunct therapy to reduce amyloid burden in patients with AD may be beneficial.

Figures

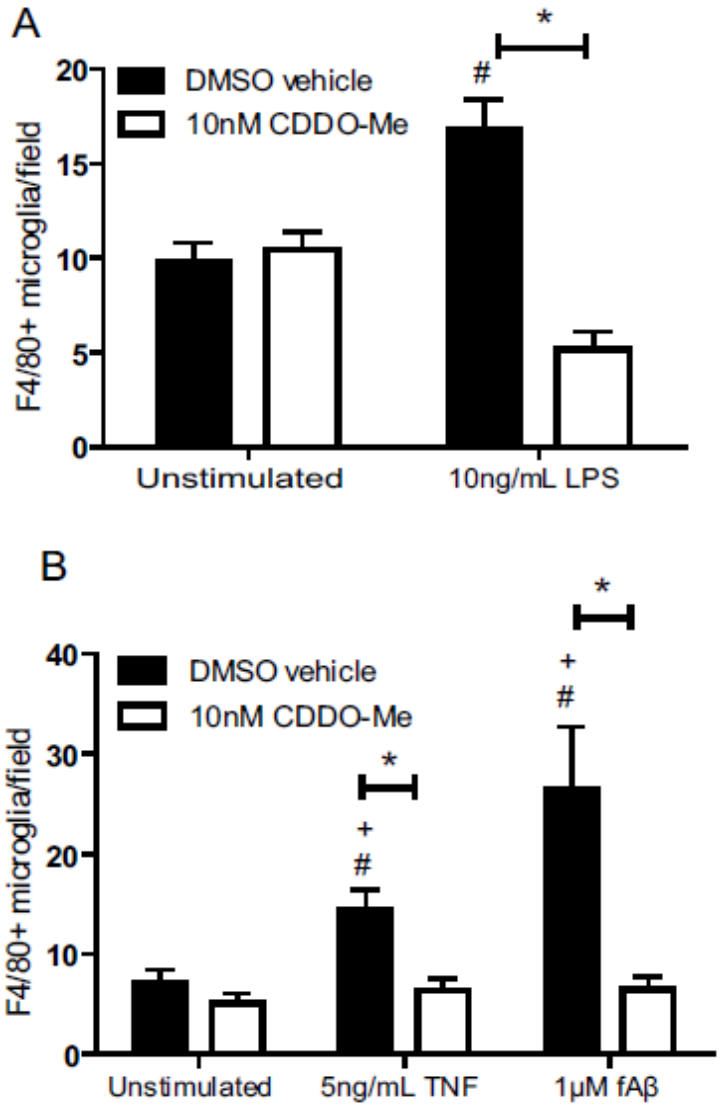

Figure 4.1. CDDO-Me attenuates LPS-, TNF-, and fibrillar Aβ42-induced primary microglial activation. Rat embryonic ventral mesencephalon primary cultures were treated at day 5 *in vitro* with indicated compounds (LPS 10 ng/mL, TNF 5 ng/mL, fAβ 1 μM, CDDO-Me 10 nM). Cells were fixed at 2 days post-treatment and stained with an

antibody against activation marker F4/80 to quantify number of activated microglia. Each condition was done in triplicate; 20 random sites were visited per well; results are expressed as mean number of F4/80-positive microglia per field $\pm$ S.E.M.. Values were analyzed by two-way ANOVA followed by Tukey post hoc test, * denotes CDDO-Me is significantly different from its DMSO vehicle for a given treatment; # denotes significant difference from the DMSO vehicle in unstimulated cells; + denotes significant difference from CDDO-Me in stimulated cells; all symbols at $p < 0.05$.

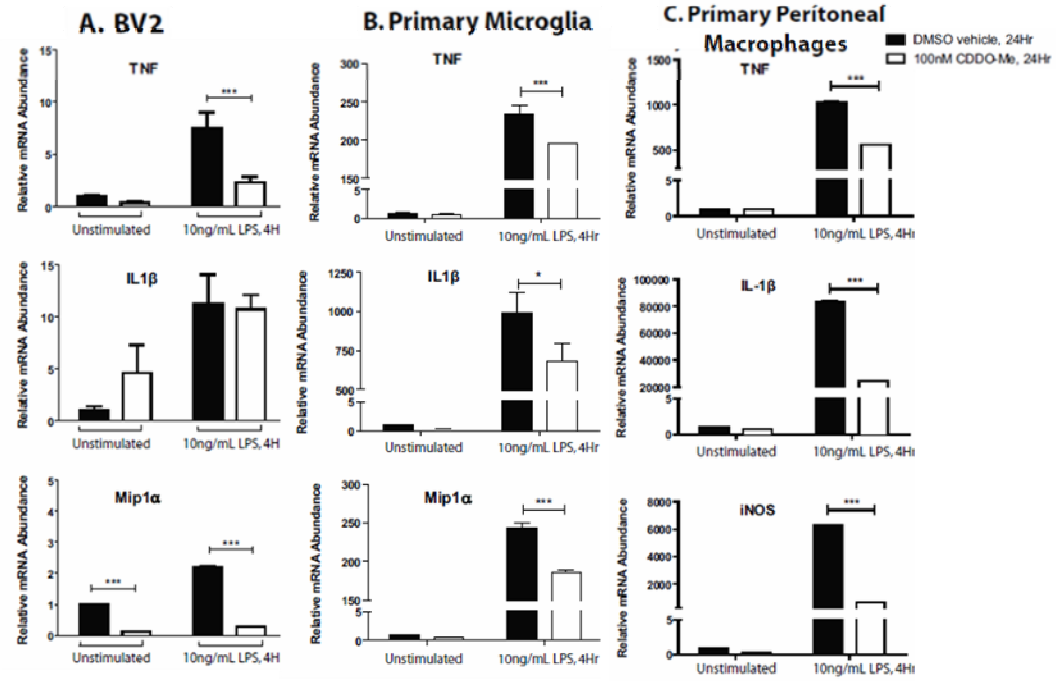

Figure 4.2. CDDO-Me downregulates expression of mRNAs for pro-inflammatory genes. *A*, BV2 microglia maintained in growth-medium supplemented with 5% heat-inactivated FBS were pre-treated with 10 nM CDDO-Me for 17 hr before a 4-hr stimulation as indicated. *B*, Microglia from post-natal day 2 (P2) wild-type mice growing in medium supplemented with 10 % heat-inactivated FBS were pre-treated with 100 nM CDDO-Me for 24 hr before a 4hr stimulation as indicated. *C*, Peripheral macrophages from adult wild-type mice growing in medium supplemented with 10 % heat-inactivated FBS were pre-treated with 100 nM CDDO-Me for 24 hr before a 4-hr stimulation as indicated. Values represent mean $\pm$ S.E.M. and are expressed relative to vehicle-treated, vehicle-stimulated conditions. Values were analyzed by two-way ANOVA followed by Bonferroni's post hoc. * denotes significance at $p < 0.05$, *** denotes significance at $p < 0.001$.

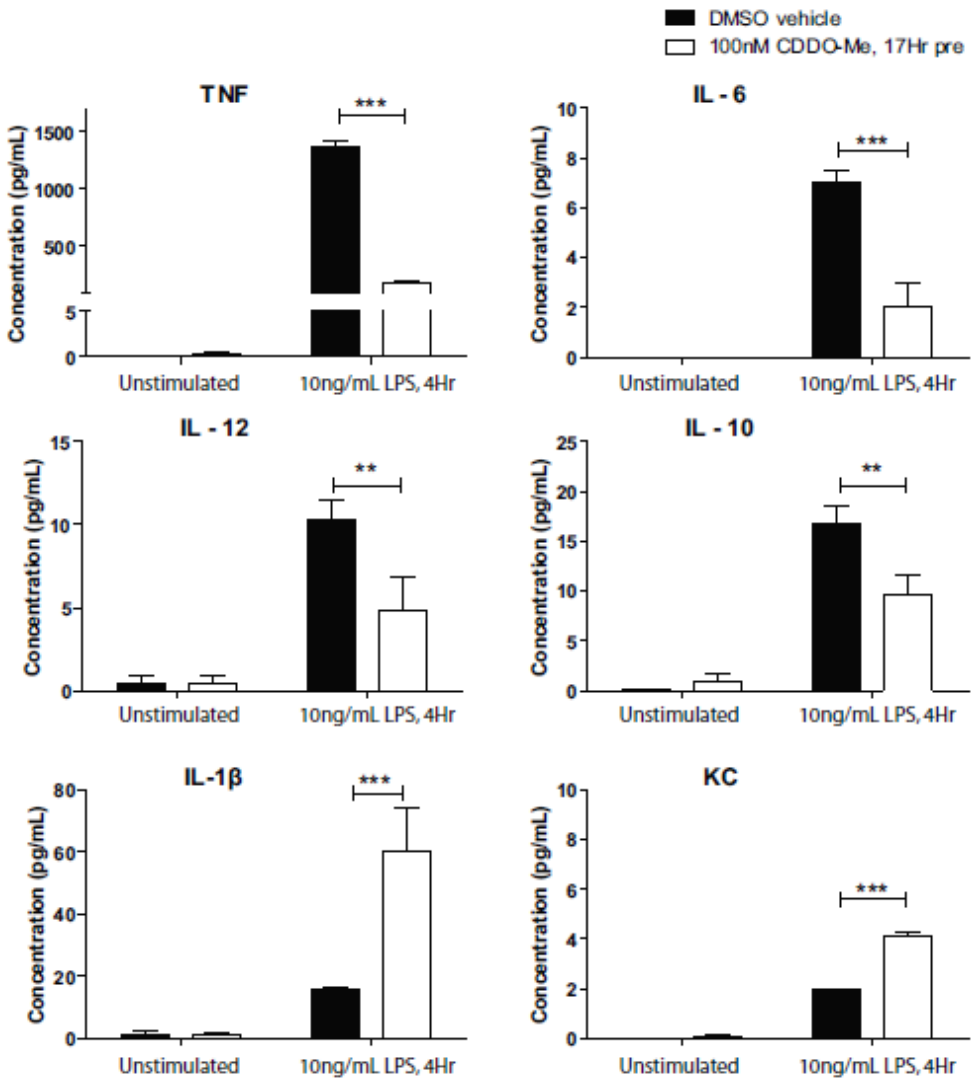

Figure 4.3. CDDO-Me suppresses production of cytokines with known neurotoxic effects on dopaminergic cultures. BV2 microglia growing in medium supplemented with 5 % heat-inactivated FBS were pre-treated with 100 nM CDDO-Me or DMSO vehicle for 17 hrs before a 4-hr stimulation with LPS (10 ng/mL). Inflammatory cytokine and chemokine production were measured from CM using a 7-plex inflammatory cytokine

profile immunoassay from Meso-Scale Discovery on an MSD 2400 plate reader. Values represent mean cytokine production $\pm$ SEM. Values were analyzed by two way ANOVA followed by Bonferroni's post hoc. ** denotes significance at $p < 0.01$, *** denotes significance at $p < 0.001$.

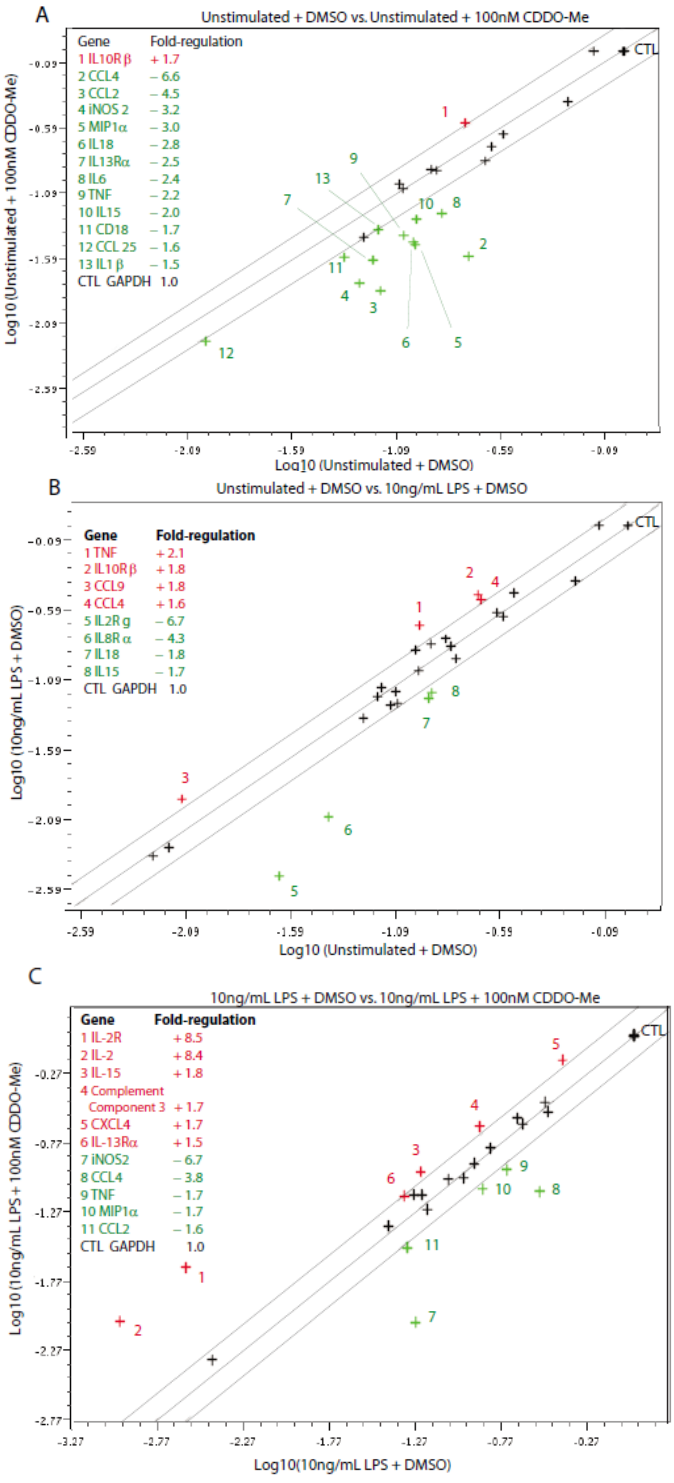
A
Unstimulated + DMSO vs. Unstimulated + 100nM CDDO-Me
Gene Fold-regulation
1 IL10Rβ + 1.7
2 CCL4 – 6.6
3 CCL2 – 4.5
4 iNOS 2 – 3.2
5 MIP1α – 3.0
6 IL18 – 2.8
7 IL13Rα – 2.5
8 IL6 – 2.4
9 TNF – 2.2
10 IL15 – 2.0
11 CD18 – 1.7
12 CCL 25 – 1.6
13 IL1β – 1.5
CTL GAPDH 1.0
Log10 (Unstimulated + 100nM CDDO-Me)
Log10 (Unstimulated + DMSO)
B
Unstimulated + DMSO vs. 10ng/mL LPS + DMSO
Gene Fold-regulation
1 TNF + 2.1
2 IL10Rβ + 1.8
3 CCL9 + 1.8
4 CCL4 + 1.6
5 IL2Rg – 6.7
6 IL8Rα – 4.3
7 IL18 – 1.8
8 IL15 – 1.7
CTL GAPDH 1.0
Log10 (10ng/mL LPS + DMSO)
Log10 (Unstimulated + DMSO)
C
10ng/mL LPS + DMSO vs. 10ng/mL LPS + 100nM CDDO-Me
Gene Fold-regulation
1 IL-2R + 8.5
2 IL-2 + 8.4
3 IL-15 + 1.8
4 Complement Component 3 + 1.7
5 CXCL4 + 1.7
6 IL-13Rα + 1.5
7 iNOS2 – 6.7
8 CCL4 – 3.8
9 TNF – 1.7
10 MIP1α – 1.7
11 CCL2 – 1.6
CTL GAPDH 1.0
Log10 (10ng/mL LPS + 100nM CDDO-Me)
Log10(10ng/mL LPS + DMSO)

Figure 4.4. CDDO-Me suppresses basal and inflammation-induced gene expression. BV2 microglia cultures growing in medium supplemented with 5 % heat-inactivated FBS were pre-incubated with 100nM CDDO-Me for 17 hrs before a 4-hr stimulation with 10ng/mL LPS in serum-free medium. *A*, Scatterplot of baseline inflammatory gene expression in unstimulated BV2 cells in the presence of DMSO vehicle (0.1 %) versus unstimulated cells in the presence of 100 nM CDDO-Me. *B*, unstimulated cells in the presence of DMSO vehicle versus cells stimulated with LPS (10 ng/mL) in the presence of DMSO vehicle, or (C) cells stimulated with LPS in presence of DMSO vehicle versus cells stimulated with LPS in the presence of 10 nM CDDO-Me plus. Data analyses were performed using the Scatter Plot data analysis tool in the SuperArray GEArray Analysis Suite online at (See Methods). The boundary is 1.5-fold regulation in either direction. Genes shown with a red plus (+) sign were up-regulated and genes shown with a green minus (-) sign were down-regulated in the treatment condition, which is plotted on the Y-axis relative to the control condition plotted on the X-axis. Seven housekeeping genes (including GAPDH shown in black) were used for normalization.

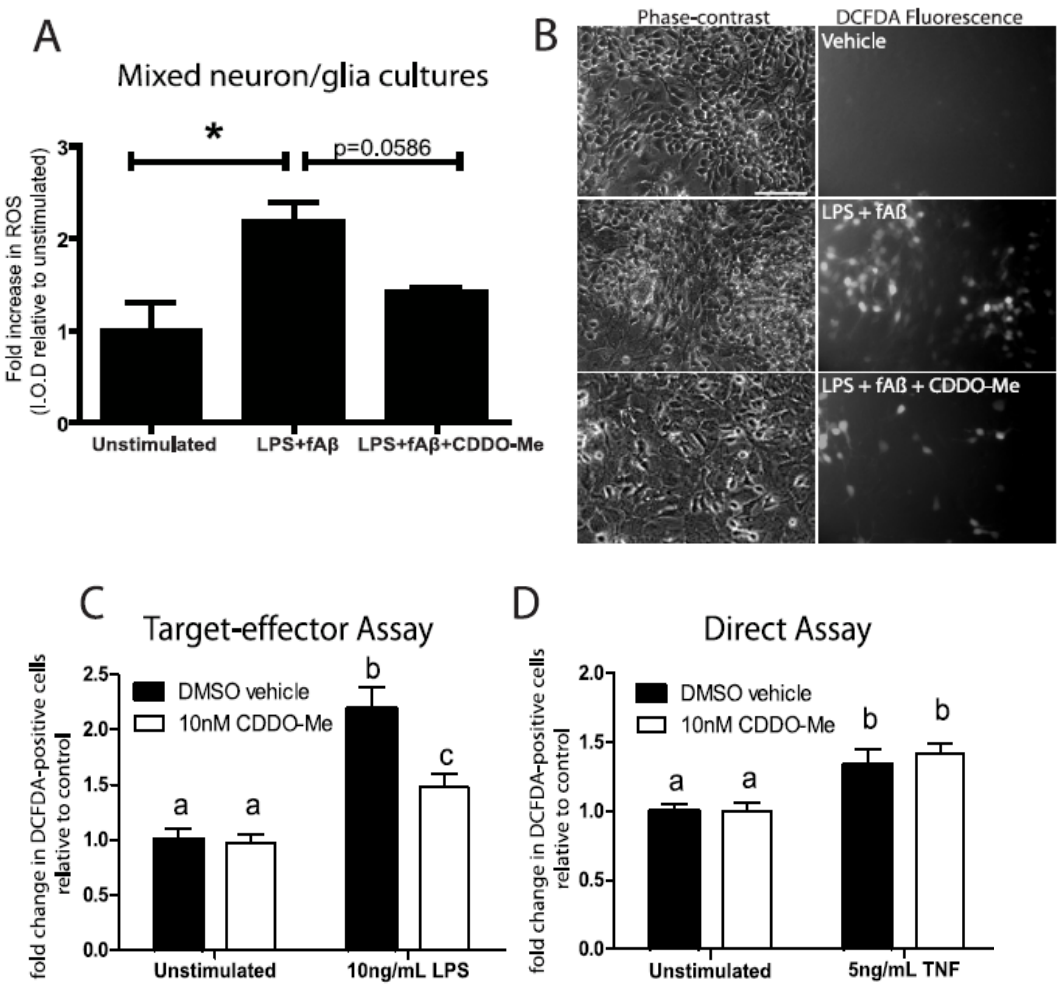

Figure 4.5. CDDO-Me inhibits intracellular ROS accumulation induced by LPS and fibrillar Aβ42 in neuronal cultures from rat basal forebrain and in dopaminergic cells. A, Fold-change in intracellular ROS. Integrated optical density was measured from digital images of treated cultures. Results are expressed as the mean ± S.E.M. of each condition relative to vehicle treatment. Values were analyzed by one-tailed Student's t-test, * denotes significance at $p < 0.005$. *B,* Images of treated E14 rat basal forebrain cholinergic

mixed neuron-glia cultures in medium containing 2.5 % heat-inactivated FBS loaded with the fluorescent indicator DCFDA. Intracellular ROS accumulation is evident after 24-hour treatment with 10 ng/mL LPS + 1 μM fAβ-42, but co-treatment with 100 nM CDDO-Me attenuated neuronal ROS accumulation. Scale bar = 50 μm. *C,* Target-effector survival assays of MN9D dopaminergic cells 48 hrs after transfer of conditioned medium (CM) from saline- or LPS-treated (24 hrs) BV2 microglia pre-incubated with CDDO-Me (10 nM) or vehicle (DMSO). Viability was measured by MTS reduction during the last 4 hrs of a 2-day culture. Values shown represent group means ± S.E.M of triplicate treatments and are representative of two independent experiments. Groups denoted by different letters are significantly different at $p < 0.05$. *D*, Direct survival assays of MN9D dopaminergic cells treated with TNF (5 ng/mL) after pre-incubation with CDDO-Me (10 nM) or vehicle (DMSO). Viability was measured by MTS reduction during the last 4 hrs of a 2-day culture. Groups denoted by different letters are significantly different at $p < 0.05$.

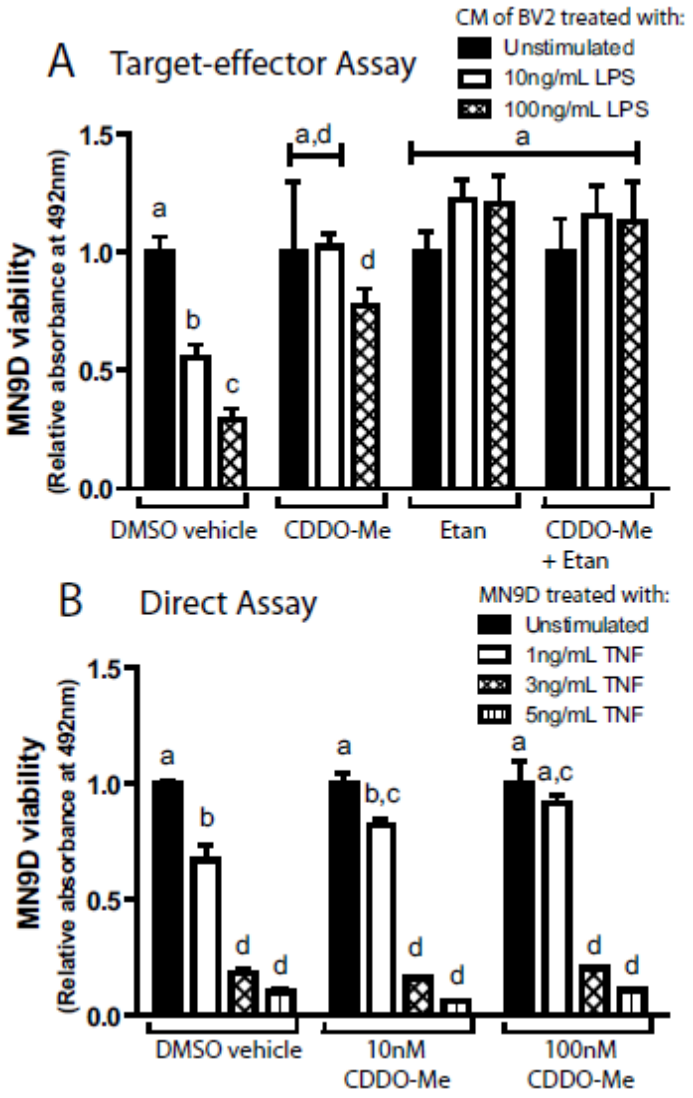

Figure 4.6. CDDO-Me rescues dopaminergic MN9D cells by attenuating LPS-induced TNF production rather than by direct inhibition of TNF-induced death. A, MN9D cells were incubated with conditioned medium (CM) from BV2 microglia cultures stimulated with 0, 10 or 100 ng/mL LPS alone or with the same concentrations of LPS plus 10 nM CDDO-Me; 200 ng/mL etanercept; or both CDDO-Me and etanercept. Survival of MN9D cells was evaluated after 2 days of incubation in the CM using an MTS viability

assay (See Methodology). *B,* Differentiated MN9D dopaminergic cells were treated with 0, 1, 3, or 5 ng/mL TNF alone or with the same concentrations of TNF plus 10 nM or 100 nM CDDO-Me. Survival was evaluated after 3 days using an MTS viability assay. Results are expressed as mean $\pm$ SEM. Values were analyzed by one-way ANOVA followed by Tukey's post hoc, groups denoted by different letters are significantly different from each other at $p < 0.05$.

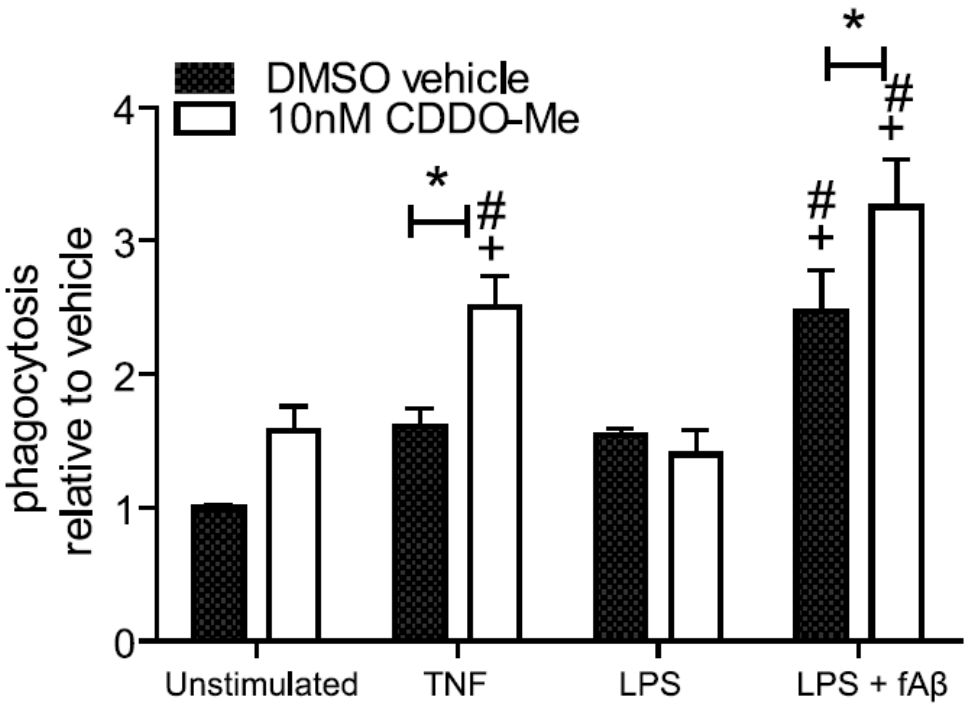

Figure 4.7. CDDO-Me enhances phagocytotic activity of BV2 microglia induced by TNF or LPS + fibrillar Aβ 1-42 peptide. BV2 microglia were plated, switched to serum-free media 24 hours later, and stimulated overnight as indicated (LPS, 10 ng/mL; TNF, 10 ng/mL; fAβ42, 1 μM; and CDDO-Me, 10 nM.). Fluorescently-labeled *E. coli* particles were added to the cultures for 2 hours following stimulation and phagocytosis of particles was measured by fluorescence emission at 520 nm. Values represent mean phagocytic activity relative to baseline (vehicle-stimulated control) $\pm$ SEM. Values were analyzed by two-way ANOVA followed by Tukey's post hoc test, * denotes CDDO-Me is significantly different from its DMSO vehicle for a given treatment; # denotes significant difference from the DMSO vehicle in unstimulated cells; + denotes significant difference from CDDO-Me in stimulated cells; all symbols at $p < 0.05$.

CHAPTER FIVE

DJ-1-null mice do not display increased vulnerability to inflammation-related nigral degeneration

The contents of this chapter were written up for publication in a manuscript by the same title.

Introduction

Over the last decade, a great wealth of new information has emerged to suggest that inflammation-derived oxidative stress and cytokine-dependent neurotoxicity are likely to contribute to nigrostriatal pathway degeneration (Wersinger and Sidhu 2002; McGeer, Schwab et al. 2003; Mrak and Griffin 2005; Zhang, Dawson et al. 2006; Tansey, McCoy et al. 2007), the pathological hallmark of Parkinson's Disease (PD) in humans. Post-mortem analyses of brains from PD patients confirmed the presence of inflammatory mediators in the area of substantia nigra (SN) where maximal destruction of vulnerable melanin-containing dopamine (DA)-producing neurons occurs in PD patients (McGeer, Itagaki et al. 1988; Banati, Daniel et al. 1998; Hunot, Dugas et al. 1999; Cassarino, Halvorsen et al. 2000; Pavese, Gerhard et al. 2006; Whitton 2007). Signs of inflammation included activated microglia and accumulation of cytokines (including TNF, IL-1β, IL-6, and IFNγ) which exert neurotoxic effects on DA neurons; and SN dopaminergic neurons may be uniquely vulnerable to neuroinflammatory insults that enhance oxidative stress (Tansey, McCoy et al. 2007). The higher sensitivity of nigral DA neurons to injury induced by neuroinflammatory mediators may be secondary to reduction of endogenous

anti-oxidant capacity (i.e. glutathione depletion). Pharmacologically, chronic infusion of various anti-inflammatory compounds (including COX-2-selective NSAIDs or soluble TNF-selective inhibitors) rescues nigral DA neurons from progressive degeneration and death (Sanchez-Pernaute, Ferree et al. 2004; McCoy, Martinez et al. 2006; McCoy, Ruhn et al. 2008). These findings raise the interesting possibility that environmental triggers initiate cytokine-driven neuroinflammation and contribute to the development of PD in humans.

Monogenic forms of PD have been linked to loss-of-function mutations in a number of genes, giving rise to autosomal recessive parkinsonism (Farrer 2006), including mutations in *parkin*, which encodes an E3 ligase, and in *DJ-1*, which encodes a putative redox sensor that associates with chaperones (Li, Niki et al. 2005) and translocates to mitochondria during conditions of oxidative stress (Bonifati, Rizzu et al. 2003; Bonifati, Oostra et al. 2004; Canet-Aviles, Wilson et al. 2004; Goldberg, Pisani et al. 2005; Zhang, Goodlett et al. 2005; Zhang, Shimoji et al. 2005). In addition to a proposed role for DJ-1 as a redox sensor (Shen and Cookson 2004), DJ-1 may also have important functions as an RNA binding protein chaperone during the unfolded protein response (UPR) to minimize protein misfolding and aggregate formation (van der Brug, Blackinton et al. 2008). Although *DJ-1*-null mice have been reported to be hypersensitive to the neurotoxin MPTP (Kim, Smith et al. 2005) and display abnormalities in dopaminergic function when exposed to the herbicide paraquat (Yang, Chen et al. 2007), these mice do not develop nigrostriatal degeneration (Goldberg, Pisani et al. 2005; Yamaguchi and Shen 2007). Interestingly, recent *in vitro* studies implicated a role for DJ-1 in astrocytes

as an important regulator of nitric oxide production, raising the possibility that exposure to chronic inflammatory stress may induce nigral degeneration in these mice. Therefore, the purpose of our study was to investigate the extent to which loss of DJ-1 increases the vulnerability for inflammation-induced nigrostriatal degeneration *in vivo*. To this end, we investigated the extent to which repeated intraperitoneal injections of low-dose lipopolysaccharide (LPS) or intranasal soluble Tumor Necrosis Factor (TNF) induced locomotor deficits, neuroinflammation, enhanced oxidative stress, or nigral DA neuron loss in *DJ-1*-null or age-matched wild type mice.

Results

DJ-1-null mice exposed to prolonged, serial low-dose systemic LPS do not develop locomotor deficits.

To test the hypothesis that DJ-1 regulates vulnerability to inflammation-related nigral degeneration, we exposed wild type and *DJ-1*-null mice to various systemic LPS regimens (**Figure 5.1**). A number of behavioral tasks were measured at the time-points indicated to investigate the extent to which the prolonged, serial low-dose systemic LPS regimens induced locomotor alterations; subsequently various cohorts were sacrificed as indicated for immunohistological analysis or determination of gene expression of microdissected brain tissue. To assess fine-motor performance, mice were subjected to the narrow beam-walk test. Our results indicate that *DJ-1*-null mice chronically injected with LPS did not display significantly slower average time-to-cross compared to saline-treated *DJ-1*-null mice or either group of WT mice (**Figure 5.2a**). To assess gross

locomotion, we measured rotarod performance. No differences were noted on rotarod performance (Figure 5.2B; $p = 0.19$) or open-field testing (data not shown). Thus, in the present study, prolonged, serial i.p. injections of LPS or saline did not cause gross motor abnormalities.

Chronic low-dose systemic LPS does not promote loss of nigral DA neurons in DJ-1-null mice.

We performed endpoint immunohistological by staining midbrain sections with the DA neuron marker tyrosine hydroxylase (TH) and the pan-neuronal marker NeuN, to measure DA neuron number and total neuron number by unbiased stereological analyses (**Figure 5.3**). Compared to similarly dosed wild type mice, *DJ-1*-null mice that received 3 months of repeated low-dose systemic LPS did not exhibit significant reductions in TH positive or NeuN positive neurons in the SNpc. Similarly, 3 months of repeated low-dose systemic LPS followed by a 3-month lag period or 6 months of repeated low-dose systemic LPS did not significantly reduce the number of TH positive or NeuN positive SNpc neurons in *DJ-1*-null mice or wild type mice (**Figure 5.3a**). Levels of TH and NeuN positive neurons were also unchanged in the ventral tegmental area (VTA) (**Figure 5.3b**).

To investigate whether repeated low-dose systemic LPS affected dopaminergic terminals at the striatum, we labeled striatal sections for TH. No decreases in striatal TH fiber immunoreactivity were detectable in brain sections from *DJ-1*-null mice treated with low-dose systemic LPS for 3 or 6 months or for 3 months followed by a 3-month lag

period (**Figure 5.4b**), densitometric analysis of multiple sections indicated the only significant change occurred in *DJ-1*-null exposed to 3-month LPS which displayed an increase in striatal TH-fiber density (**Figure 5.4a**). To extend and confirm these findings, we measured the tissue levels of DA and its metabolites in microdissected striatum by HPLC and electrochemical detection. In agreement with the immunohistological results, repeated low-dose i.p. LPS injections caused a detectable increase in striatal DA content in *DJ-1*-null mice exposed to the 3-month regimen; no changes in DA turnover were observed in any treatment group of either genotype (**Figure 5.4c**).

DJ-1$^{-/-}$ and wild type mice display similar neuroinflammatory responses in midbrain in response to low-dose systemic LPS administration.

To investigate the possibility that the lack of nigral neuron loss in LPS-treated *DJ-1*-null mice may have been attributed to an attenuated neuroinflammatory response, we used QPCR to measure the relative mRNA expression of TNF and CD45 in midbrain and cortex in the mice from the 6-month treatment groups. We found that the *DJ-1*-null mice displayed increased TNF mRNA in response to the LPS challenge in both midbrain and cortex but an attenuated LPS-induced expression of CD45 compared to the wild type mice in midbrain. Together, these data suggest that the repeated low-dose LPS injections triggered similar midbrain neuroinflammatory responses in WT and *DJ-1*-null mice. Based on previous work in which we found that Parkin function may influence neuroinflammatory responses and vulnerability to inflammation-induced nigral degeneration (Frank-Cannon et al., 2008); we measured the levels of Parkin expression in

both genotypes. We found no differences in the levels of Parkin expression between genotypes (**Figure 5.5a,b**).

DJ-1-null mice do not display basal upregulation of anti-oxidant genes in midbrain or in response to low-dose systemic LPS administration.

We next investigated whether the lack of nigral cell loss in *DJ-1*-null mice following repeated, serial systemic low-dose LPS administration might have been attributed to upregulation of anti-oxidant responses as a consequence of DJ-1 loss. We used QPCR to measure the expression of key anti-oxidant genes implicated in protection of DA neurons in the midbrain of WT or *DJ-1*-null mice that received 3- or 6-month low-dose systemic LPS administration. Based on the current literature, we elected to analyze the transcription factor NF-E2 related factor (Nrf2), which binds to the anti-oxidant response element (ARE) to induce expression of antioxidant and phase 2 detoxification enzymes, NAD(P)H:quinone oxidoreductase (NQO1), heme-oxygenase-1 (HO-1), inducible nitric oxide synthase (iNOS), superoxide dismutase-1 (SOD1), and superoxide dismutase-2 (SOD2). We found no significant upregulation of anti-oxidant genes in either genotype or in response to LPS treatment (**Figure 5.6**).

Intranasal soluble TNF delivery does not promote nigral DA neuron loss in WT or DJ-1-null mice

Because the repeated i.p. LPS injections failed to trigger nigral DA neuron loss in *DJ-1*-null mice, we tested an additional inflammatory regimen designed to trigger neuroinflammation directly in the olfactory bulb. We delivered rhodamine-labeled human

TNF (rh-TNF) intranasally to confirm uptake and transport by nasal epithelia (NE). Immunofluorescence analyses of cryosectioned rostral and caudal tissues revealed detectable uptake and transport of rh-TNF in rostral sections of NE during the early time points. As expected, the distribution of rh-TNF decreased in rostral sections and increased in caudal sections as a function of time (**Figure 5.7**). Because TNF can induce cachexia, we investigated the extent to which intranasal TNF (inTNF) administration decreased food and water intake. Murine soluble TNF was administered intranasally twice weekly at one of two doses (T1= 0.5ng) and (T2= 5ng) for 1 week (Paradigm 1, P1) or for 2 weeks (Paradigm 2, P2) in WT or *DJ-1*-null mice. Food consumption was monitored for 4-5 weeks just prior to and during the inTNF dosing. Results revealed no adverse systemic effects (i.e., loss of appetite or other cachexic effects) after repeated systemic inTNF dosing (data not shown). Upon confirmation that inTNF uptake and transport did not elicit cachexic effects, we investigated the extent to which inTNF dosing triggered an inflammatory response in the midbrain. We administered three inTNF doses of 0.5 or 5ng TNF followed by a 3 week wait then measured inflammatory gene expression by QPCR. We found that *DJ-1*-null mice displayed increased expression of TNF, CD45 and Cox-1 compared to WT mice, but inTNF exposure did not significantly potentiate these responses (data not shown).

Next we investigated whether the enhanced neuroinflammatory gene expression in *DJ-1*-null mice resulted in detectable nigral DA neuron loss. Building on the intranasal dosing paradigm, we subjected older (10-mo old) *DJ-1*-null mice and age-matched WT mice to an experimental regimen of inTNF administration that included several boost doses and a

two-month lag time such that mice were on average 13 mos old at the time of sacrifice (**Figure 5.8a**). Stereological analyses to determine the extent to which the experimental paradigm induced nigral DA neuron loss revealed no inTNF-induced nigral DA neuron loss in mice of either genotype (**Figure 5.8b**). Consistent with immunohistological findings, measurements of striatal DA, DA metabolites and DA turnover (**Figure 5.8c**) as well as 5-HT (data not shown) by HPLC and electrochemical detection showed no effects on DA or 5-HT metabolism.

Discussion

Although, *DJ-1*-null mice do not display loss of nigral DA neurons they display deficits in dopaminergic function (Goldberg, Pisani et al. 2005) which are further accentuated when exposed to paraquat (Yang, Chen et al. 2007) and MPTP (Kim, Smith et al. 2005), suggesting a protective role for DJ-1 in mitochondrial function and/or against oxidative stress. In support of this molecular model, DJ-1 has been shown to translocate to mitochondria (Zhang, Shimoji et al. 2005) in response to oxidative stress when key cysteine residues become acidified (Canet-Aviles, Wilson et al. 2004) and to interact with multifunctional regulators of transcription and RNA metabolism in the nucleus (Xu, Zhong et al. 2005). More recently, DJ-1 (but not pathogenic mutants linked to familial parkinsonism) was shown to associate with a number of different RNA targets in cells in an oxidation-dependent fashion, including mitochondrial genes, genes involved in glutathione metabolism, and PTEN/PI3K pathway components (van der Brug, Blackinton et al. 2008) which are consistent with studies implicating DJ-1 in malignancies through

suppression of PTEN-induced apoptosis and these interactions have been confirmed in human brain (Blackinton, Kumaran et al. 2009).

In the last 10 years, a role for DJ-1 in regulation of inflammation-induced oxidative stress has been implicated by *in vitro* observations that i.p. LPS can robustly increase DJ-1 expression in peritoneal macrophages in response to NADPH oxidase-derived ROS (Mitsumoto and Nakagawa 2001), and that *DJ-1*-null astrocytes overproduced nitric oxide when stimulated with LPS (Waak, Weber et al. 2009). However, we report here the unexpected finding that *DJ-1*-null mice do not display increased vulnerability to inflammation-induced nigral degeneration when exposed to repeated i.p. LPS injections or direct intranasal delivery of soluble TNF. We speculate that compensatory gene expression in mitochondrial enzymes in *DJ-1*-null mice (Pham, Giesert et al. 2009) may be one possible explanation for their apparent resistance to inflammation-induced loss of nigral DA neurons *in vivo*. Alternatively, it is possible that a longer lag-time between the delivery of the inflammatory stimuli and the endpoint of the study (greater than 3 months) might be required to uncover increased vulnerability to inflammation-induced degeneration.

Previous work from our group demonstrated that the same serial regimen of low-dose i.p. LPS injections used in these studies triggered a modest neuroinflammatory response in the central nervous system (CNS) in anatomical regions that show early involvement in PD (olfactory bulb and midbrain) and not in areas that are unaffected in the early stages of the disease. In addition, *parkin*-null mice displayed increased vulnerability to

inflammation-induced degeneration of nigral DA neurons when exposed to the same repeated i.p. LPS regimen used in these studies (Frank-Cannon, Tran et al. 2008). Importantly, these findings contrast the lack of increased susceptibility of *parkin*-null mice to oxidative neurotoxins such as MPTP, 6-OHDA and methamphetamine (Perez, Curtis et al. 2005; Thomas, von Coelln et al. 2007; Zhu, Maskri et al. 2007). Based on these findings, we conclude that Parkin and DJ-1 have non-overlapping roles in protecting the nigrostriatal pathway against a variety of specific neurotoxic stresses.

Figures

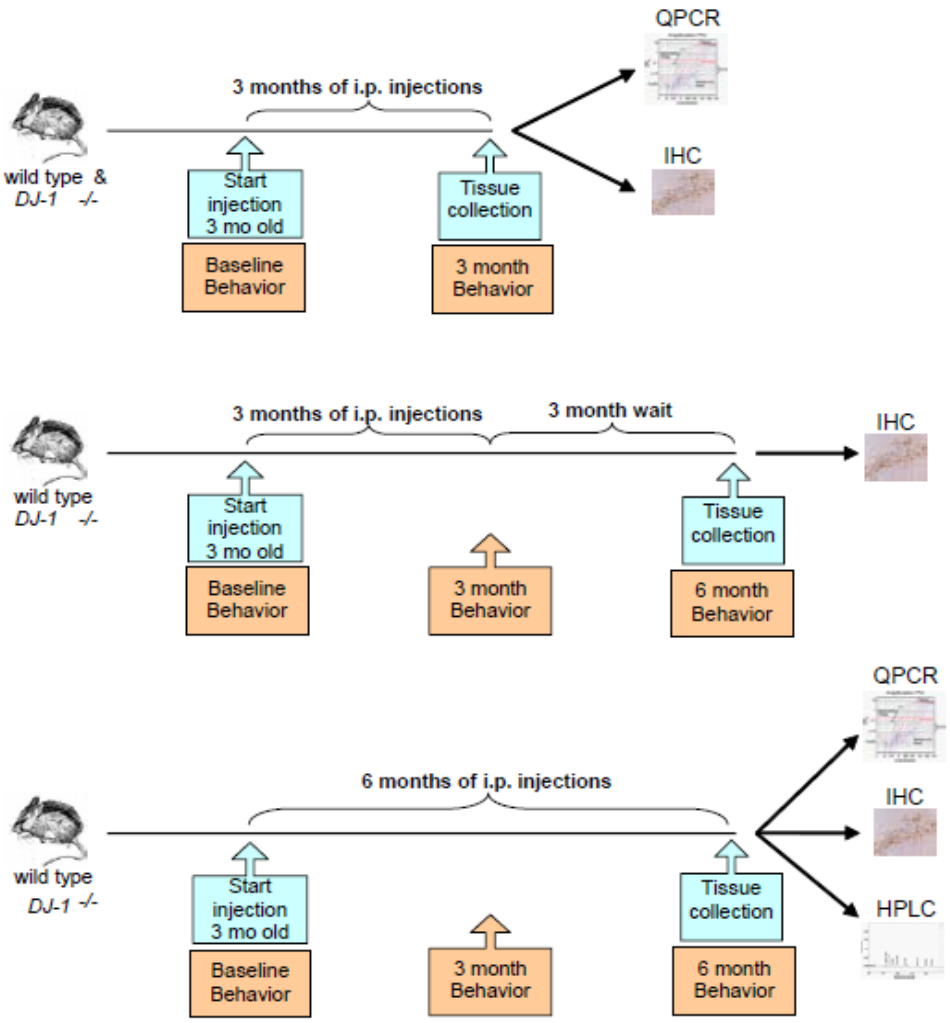

*Figure 5.1. Schematic of systemic LPS administration regimens and measurable outcomes***.** Wild type and *DJ-1*$^{-/-}$ mice were given low-dose LPS or an equivalent volume of saline vehicle twice a week intraperitoneally for the indicated times. Locomotor behavior was evaluated before and during the course of treatment. Groups of animals were sacrificed as indicated for biochemical and immunohistological analyses.

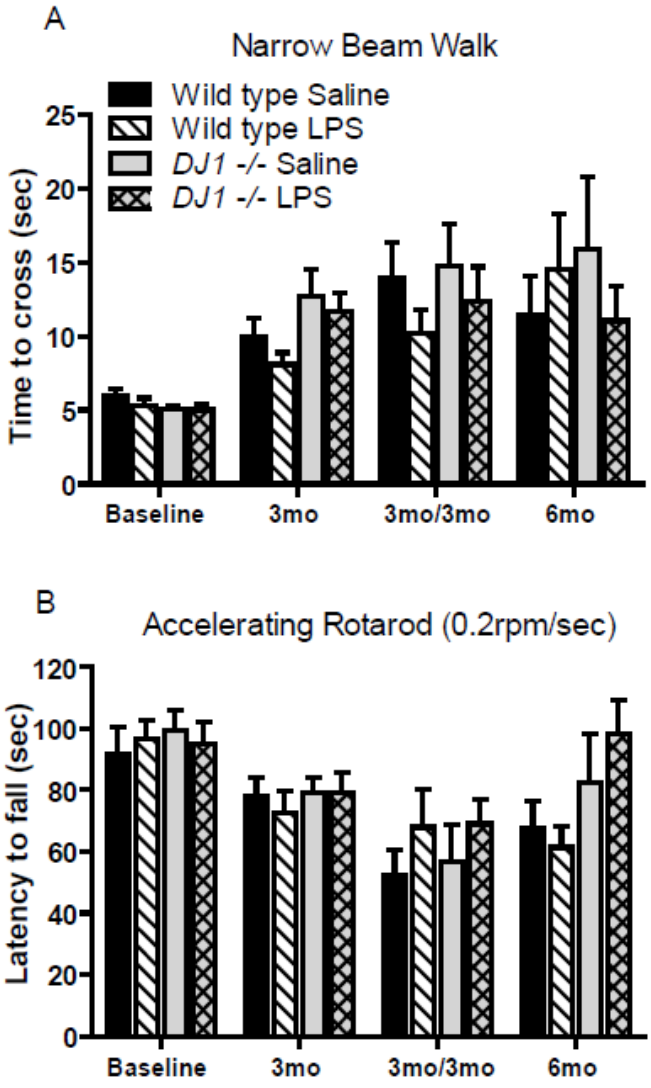

Figure 5.2. Fine-locomotor deficits in DJ-1$^{-/-}$ mice exposed to prolonged, serial lowdose systemic LPS. A, No significant differences were detected between genotypes or treatment groups on accelerating rotarod, suggesting no general malaise. Bars represent mean + SEM; n8 per group. *B, DJ-1$^{-/-}$* mice display significantly prolonged time to cross on narrow beam walk after LPS treatment regimens. Asterisks indicate significant

differences compared with saline-treated wild type and LPS-treated wild type group, whereas double asterisks indicate difference from all other groups. The triangle indicates a significant difference compared with LPS-treated wild type animals only.

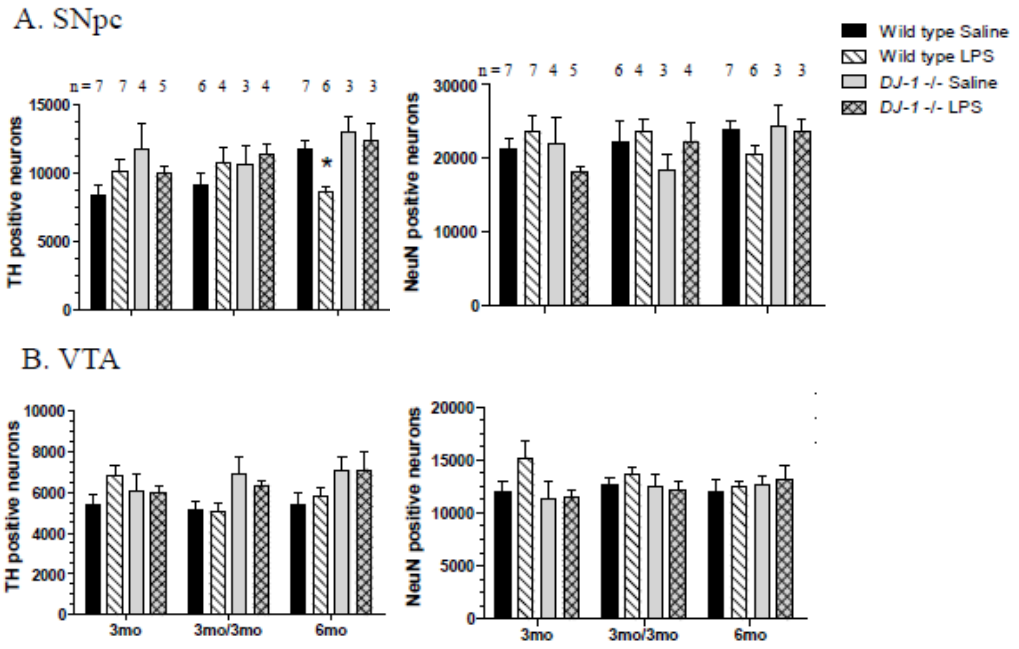

Figure 5.3. DJ-1$^{-/-}$ mice do not display increased vulnerability to nigral DA neuron loss induced by repeated low-dose systemic LPS compared to wild type mice. Unbiased stereological analysis indicates that DJ-1$^{-/-}$ mice exposed to 3 months of low-dose systemic LPS followed by a 3 month wait or mice exposed to 6 months of low-dose systemic LPS do not display a significant reduction of TH or NeuN immunopositive neurons in the SNpc. Error bars represent SEM, and the number of mice in each group is denoted in parentheses (n). Asterisks indicate significant differences compared with wild type, saline-treated animals by three-way ANOVA followed by Tukey's HSD post hoc test at $p < 0.05$.

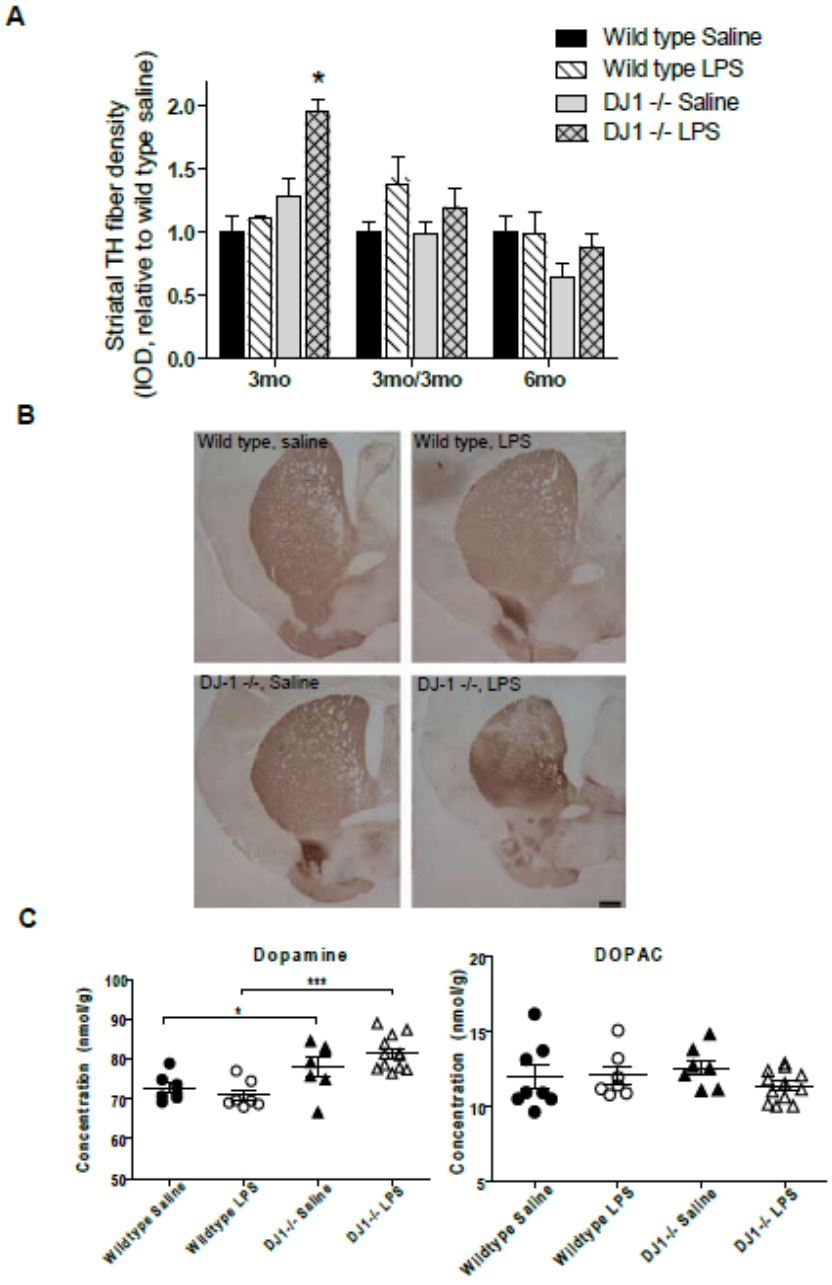

Figure 5.4. Repeated low-dose intraperitoneal LPS injections does not cause loss of striatal TH-immunopositive terminals or DA depletion in DJ-1-null or wild type mice. A, Densitometric analysis of striatal TH fiber density (see Materials and Methods) indicates

no significant differences between genotypes or treatment groups. Bars represent mean ± SEM; n = 7-12 animals per group. *B,* Representative striatal sections stained for TH from mice in the 6 month treatment groups. *C,* Striatal levels of DA and its metabolite DOPAC were measured by HPLC and electrochemical detection.

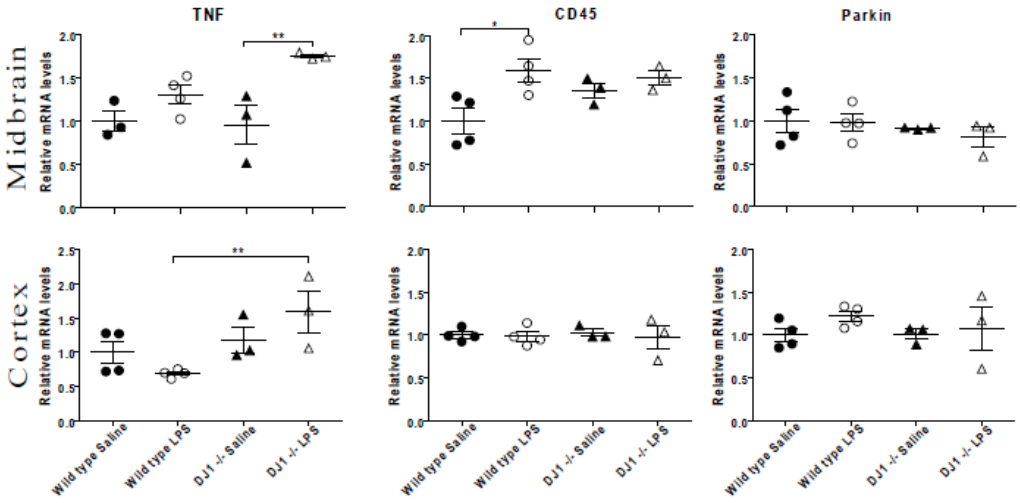

Figure 5.5. DJ-1-null and wild type mice display similar neuroinflammatory responses after repeated low-dose systemic LPS administration. Real-time QPCR analyses of microdissected midbrain tissue measured expression levels of neuroinflammation markers TNF and CD45 by QPCR in the ventral midbrain and cortex of mice treated with low-dose systemic LPS for 6 months. Parkin mRNA was also measured and found to be similar in both genotypes. Asterisks indicate significant difference wild typeas indicated. Bars represent mean $\pm$ SEM; n = 3– 4 animals per group. Two-way ANOVA was performed with Bonferroni's post hoc at *$p < 0.05$, **$p<0.01$.

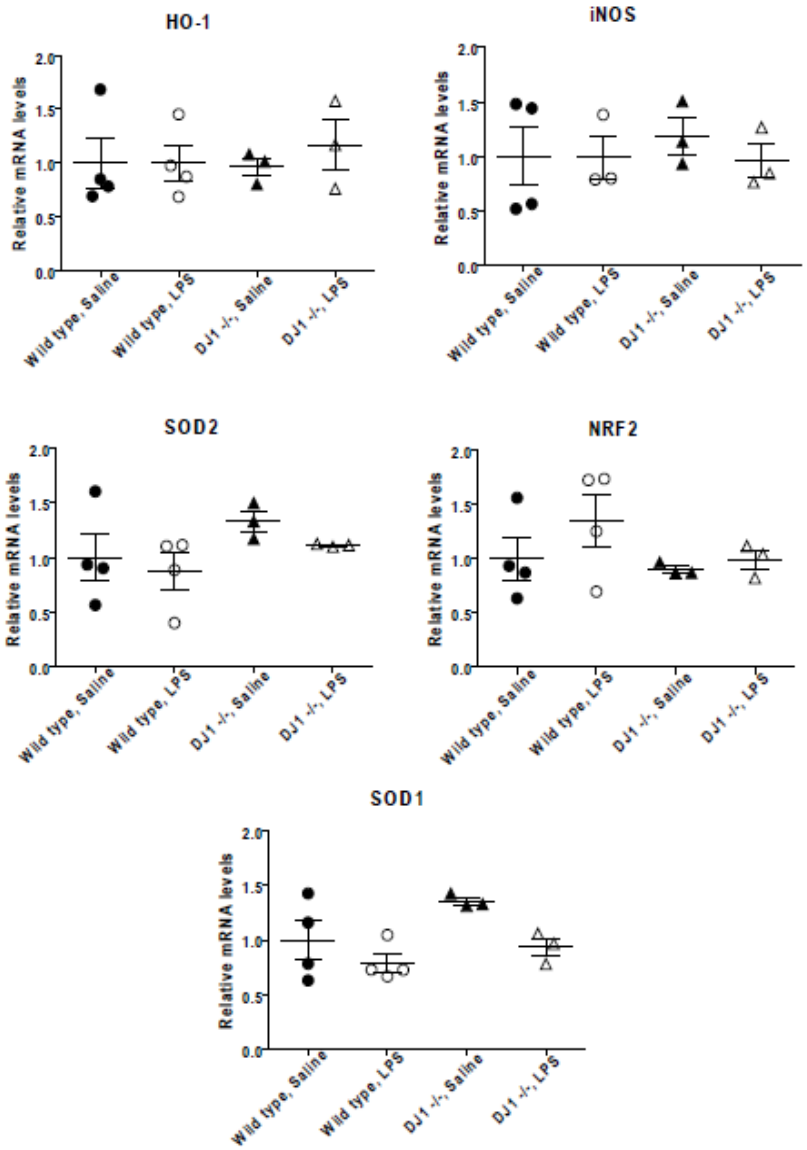

Figure 5.6. Oxidative stress responses to prolonged, serial administration of low-dose systemic LPS are similar in DJ-1-null and wild type mice. Real-time QPCR analyses of microdissected midbrain tissue measured expression levels of Nrf2, HO-1, NQO1, iNOS, SOD1, and SOD2.

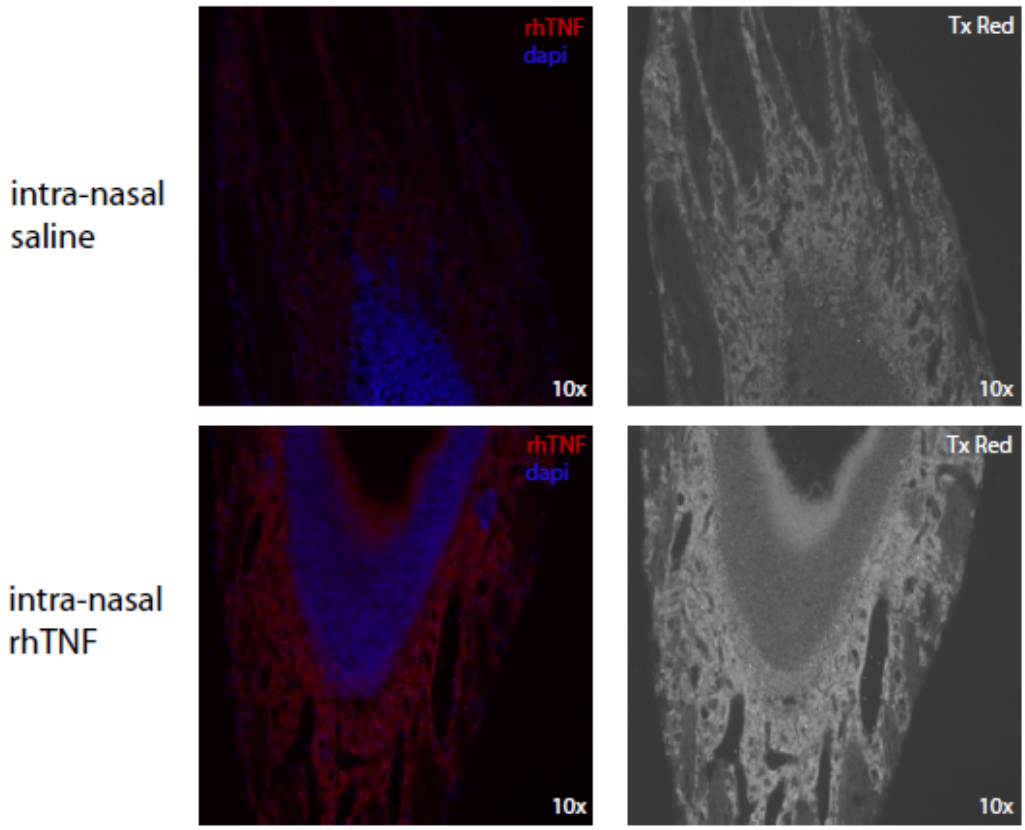

*Figure 5.7. Uptake and transport of rhodamine labeled hTNF into mouse nasal epithelial cells***.** Rhodamine-labeled TNF (Rh-TNF) was used to confirm uptake and transport of intranasally administered soluble TNF in nasal epithelia (NE) by immunofluorescence analyses of cryosectioned rostral and caudal tissues. Rhodamine-TNF fluorescence indicated detectable uptake and transport in rostral sections of NE by 12 hrs post administration.

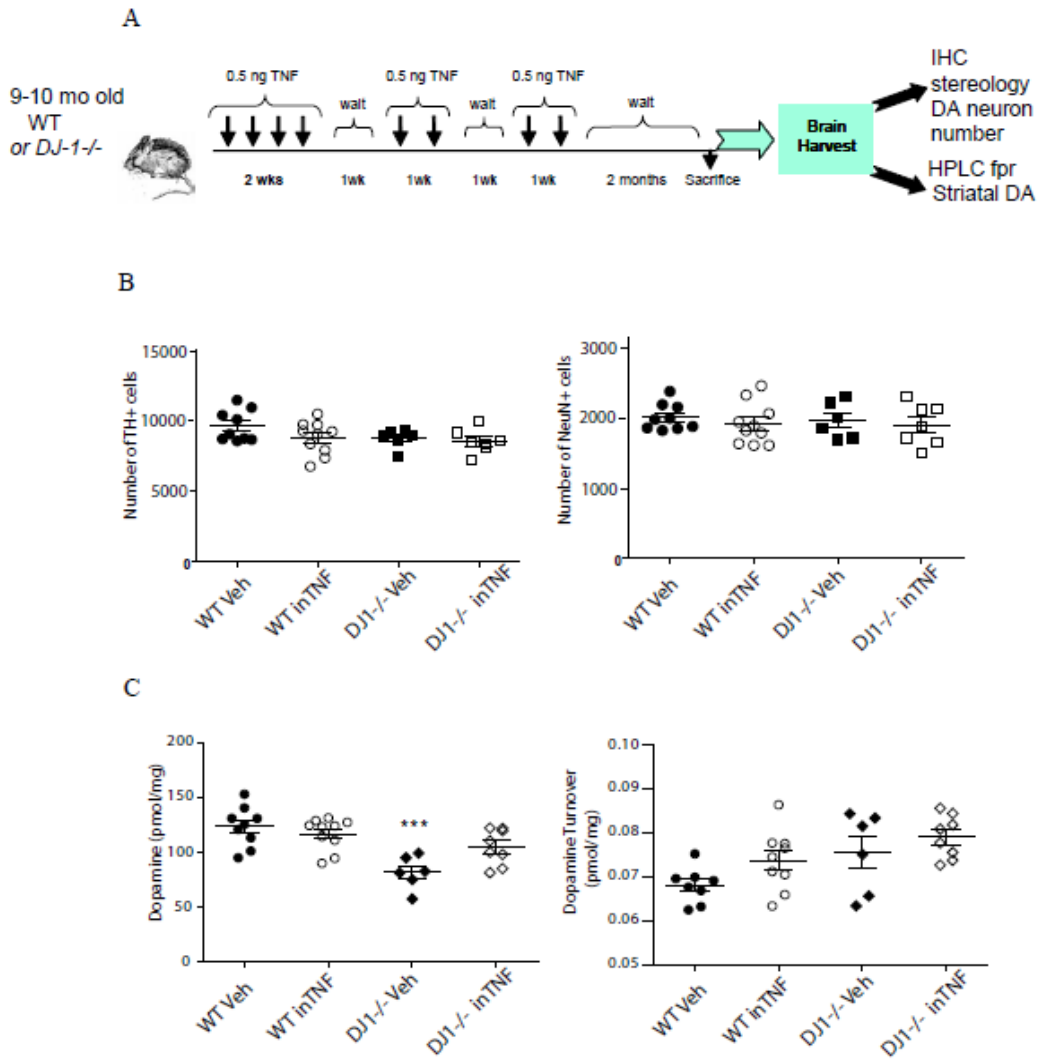

Figure 5.8. Schematic of intranasal TNF (inTNF) dosing paradigm in DJ-1-null and wild type mice and effects on nigral DA neuron number and striatal DA. A, Schematic of experimental design. Wild type and *DJ-1*-null mice were given soluble murine TNF at the indicated concentrations or an equivalent volume of saline vehicle intranasally for the indicated times. Groups of mice were sacrificed as indicated for biochemical (striatal DA

measurements by HPLC) and immunohistological analyses (unbiased stereological estimate of nigral DA neuron number). *B,* Unbiased stereological analysis indicates that DJ-$1^{-/-}$ mice exposed to inTNF do not display a significant reduction of TH or NeuN immunopositive neurons in the SNpc. Error bars represent SEM, n=6-10 animals per group. Two-way ANOVA indicated no significant differences. *C,* Striatal dopamine (DA) and DA metabolites were measured by HPLC and electrochemical detection. Error bars represent SEM, n=6-10 animals per group. Two- way ANOVA, Bonferroni's post hoc ***$p<0.001$.

CHAPTER SIX

Conclusion

PERSPECTIVES AND FUTURE DIRECTIONS

Chronic inflammation and disease

Inflammation was first described in the first century by Celsus as rubor (redness), calor (heat), dolor (pain) and tumor (swelling). The purpose of inflammation is to respond to foreign material and clear infections or debris and to provide a memory for future injuries. However, in cases of prolonged responses, these processes can lead to cellular damage. The effects of acute and chronic inflammation on the body have generally led to the conclusion that acute inflammation is necessary for initial recruitment of cells to initiate wound repair and release growth factors to aid in tissue maintenance. However, a sustained response beyond what is needed is often considered chronic inflammation. Inflammation is linked to the process of aging, and in the development and progression of disease. Studies have explored and found an association between people who experience chronic inflammatory diseases such as arthritis, atherosclerosis, and autoimmune disorders and the likelihood of developing neurodegenerative diseases such as AD or PD. Therefore, it is essential to understand how inflammatory activation and the body's response to inflammatory stimuli may contribute to the onset and progression of neuronal loss in PD.

Complex disease

Cell autonomous neuronal dysfunction has long been the focus of neurodegenerative diseases, because the neurons are the cell type most obviously affected; evidenced by the presence of intracytoplasmic neuronal inclusions and ultimately the loss of neurons. Recently the field has begun to explore the microenvironment, such as how microglial and astrocyte function and phenotype contribute to disease. We observed that Parkin levels are reduced by inflammation and that *parkin*$^{-/-}$ mice display increased cytokine and chemokine expression in the midbrain and in serum levels. Isolated microglia from *parkin*$^{-/-}$ mice also display increased CD45 surface expression, suggesting increased activation even in the absence of stimulation. Isolated *parkin*$^{-/-}$ microglia are not more cytotoxic to MN9D neuronal cells when treated with LPS, but co-culture of *parkin*$^{-/-}$ microglia and astrocytes resulted in transiently increased secretion of IL-1b, IL-6, IL-10, IL-12p70 and IFNg. These experiments examined cytokine secretion as the main mode of cytotoxicity to the neurons. Other microglial effector functions and the role of Parkin in other cell types in the brain are discussed below.

Our focus on the role of PD-linked genes in the increased cytotoxicity of microglia was supported by our studies showing that protective properties of CDDO-Me were primarily through anti-inflammatory effects on the microglia, more so than anti-oxidant actions in the neurons. We showed that blocking microglial proliferation and activation was correlated with decreased neuronal accumulation of reactive oxygen species (ROS) and overall viability. Importantly we observed that removing TNF in the conditioned medium

(CM) from LPS-stimulated BV2 microglia was enough to rescue MN9D cell death. These studies strongly support the role of microglia in neuronal toxicity.

Parkin-deficiency in the right cell type

Our studies investigating the role of *parkin*-deficiency in microglia showed that isolated microglia from *parkin*$^{-/-}$ mice are not more cytotoxic to MN9D cells in response to stimulation by LPS. Generating cellular stress in microglia through stimulation with LPS or TNF depends on the induction of inflammation at the receptor level, followed by downstream signaling and transcriptional expression of cytokines and chemokines. In contrast, induction of oxidative stress, which directly impairs the mitochondria, may require Parkin to function in a different cellular capacity than direct inflammatory stress mediated at the receptor level. Although we did not observe enhanced toxicity in *parkin*$^{-/-}$ microglia *in vitro*, we do not rule out the investigation of *parkin*$^{-/-}$ microglia *in vivo*. Generation of a lentivirus encoding a shRNA targeting Parkin would silence expression of Parkin protein in microglia and allow the investigation of Parkin loss of function in the physiological environment of the brain. In addition, we could further explore whether the loss of Parkin is more detrimental in neurons or microglia, by generating an adenovirus encoding shRNA to target Parkin since it is accepted that adenoviruses largely transduce neurons. *In vitro* experiments combining *parkin*$^{-/-}$ neurons and wild type microglia in co-culture, or vice versa, would also inform us of whether increased susceptibility to microglia-derived factors can be increased in neurons that do not express Parkin.

Astrocyte contribution to inflammation

Studying isolated microglia in culture has been criticized because the isolation process inevitably causes a heightened activation status. Although the response of the transgenic or mutant microglia are still compared to wild type microglia, the study of this cell type in a physiological state is underappreciated. Microglia grown in mixed glia cultures with astrocytes, or in the presence of neurons, exhibit different morphologies. Just as microglia communicate with neurons about the cellular environment, interactions exist between astrocytes and microglia to maintain the activation status. Astrocytes undergoing gliosis release Itgam, a ligand that binds lymphocyte function-associated antigen (LFA) on the microglia subsequently leading to activation (McGeer and McGeer 2008). Macrophage colony stimulating factor (M-CSF) is a cytokine that is commonly used when maintaining microglia in *in vitro* cultures to reduce microglial activation. Additionally, astrocyte production of monocyte chemotactic protein (MCP)-1 led to increased microglial proliferation in a transgenic mouse model of Alzheimer's disease (Wyss-Coray 2006). Based on these reports and others, it will be important to study the synergistic relationship between microglia and astrocytes in a more physiological environment.

In addition to understanding the interactions between microglia and astrocytes in co-cultures, investigating the inflammatory responses of astrocytes alone would also be of interest. Growing the *parkin*$^{-/-}$ microglia with astrocytes in co-culture may not have been the variable that resulted in the increased cytokine production from the *parkin*$^{-/-}$ microglia. In fact, the loss of parkin in the astrocytes may have specifically generated the

increased levels of cytokines. Astrocytes function to support neuronal health by releasing growth factors as well as removing neurotransmitter from the synaptic cleft to protect against excitotoxicity. However, it may not be as commonly known that astrocytes also express toll-like receptors and respond to stimulation by LPS. It was recently reported that *DJ1*$^{-/-}$ astrocytes release ten-fold more NO after LPS stimulation compared to wild type astrocytes (Waak, Weber et al. 2009). In addition, deletion of another PD-associated gene, *Nurr1*, in astrocytes resulted in relatively higher TNF and IL-1b expression by astrocytes than *Nurr1* deletion in microglia (Saijo, Winner et al. 2009). These data suggest that the role of Parkin in astrocytes may also be critical in handling inflammatory responses in the brain.

Microglia localization after injury

We reported that microglial proliferation in response to 6 months of low-dose peripheral LPS administration was similar in wild type and *parkin*$^{-/-}$ mice according to immunohistochemical analysis of CD45-labeled microglia (Frank-Cannon 2008). However, a striking observation in the *parkin*$^{-/-}$ mice is that the microglia were not localized to the SNpc, where we observed neuronal injury and loss, compared to microglia in LPS-treated wild type mice. Our *in vitro* experiment studying transwell migration of macrophages isolated from 20 month *parkin*$^{-/-}$ macrophages compared to wild type macrophages informed us that Parkin-related dysfunctions may be exacerbated with age. *parkin*$^{-/-}$ mice have increased GSH production (Solano, Menendez et al. 2006), a genetic compensation that allows the mice to generally perform functions such as clear ROS and migrate to signals of injury at a normal capacity. Nonetheless, the added

cellular damage induced by the aging process may override the genetic compensations, and the *parkin*$^{-/-}$ microglia may become unable to handle excess cellular stress. In fact, *in vitro* cultures of aged *parkin*$^{-/-}$ microglia were reported to be more sensitive to oxidative stress than aged wild type microglia (Solano, Casarejos et al. 2008). However, these findings could be confirmed and extended by studying additional microglial effector functions such as phagocytosis and migration and in an *in vivo* setting.

A recent publication elegantly showed the timely migration of microglia to a local injection of LPS or a microlesion caused by a laser (Nimmerjahn, Kirchhoff et al. 2005). With this understanding, and visualization of the dynamic movement of parenchymal microglia towards injury, we could examine the migratory behavior of microglia in young adult and aged *parkin*$^{-/-}$ mice compared to age-matched wild type mice.

Parkin in the TNF signaling pathway

Of interest is the robust increase of Parkin levels in the *TNF*$^{-/-}$ macrophages (**Figure 2.4**). Isolated microglia from *TNF*$^{-/-}$ mice show significant impairment of inflammatory activation, and reduced cytokine release. In the absence of the positive propagation of inflammatory signaling in these animals, we observe that Parkin levels are increased. Our hypothesis that cellular levels of Parkin need to be decreased in order for inflammatory activation to proceed may explain why we see increased levels of Parkin in macrophages that are genetically unable to activate inflammatory responses. Future directions in this aim would focus on the interaction of Parkin with proteins in the TNF signaling pathway. We would be interested in following up an observation generated from a PCR array in which TNF receptor-associated factor (Traf)-2 is upregulated two-fold in the absence of

Parkin (Appendix 1, 2). Of significance is that Parkin is still downregulated in *TNF*$^{-/-}$, *TNFR1*$^{-/-}$, and *TNFR2*$^{-/-}$ macrophages stimulated with LPS, which rules out the possibility that TNF-mediated autocrine activation led to downregulation of Parkin levels. In other words, even if the macrophage is unable to generate TNF or the TNF produced by the macrophage is unable to bind and signal through its own receptors, we still saw inflammation-induced decreases in Parkin.

The role of Parkin downstream of TNF is also interesting because TNF activation can signal survival or death pathways depending on the activation of TNFR1 or TNFR2 on the neuronal surface. TNFR1 activation largely leads to induction of caspases and subsequent apoptosis, while TNFR2 activation signals NF-κB and survival pathways in the neuron. Whether a cell lives or dies is determined by the relative strength and duration of these opposing signaling cascades (Aggarwal 2000; Chen and Goeddel 2002). Based on the observation that Parkin positively regulates NF-κB activation (Henn, Bouman et al. 2007), we postulate that loss of Parkin in neurons would lead to both decreased or delayed NF-κB and increased or unopposed caspase activation, which would result in neuronal death. PCR array analysis of the apoptotic and NF-κB signaling pathways in *parkin*$^{-/-}$ macrophages challenged with 1ug/mL LPS suggests that loss of Parkin increases apoptotic signaling (Appendix 1, 2).

Parkin regulation of mitochondria in microglia

The reports that Parkin protects mitochondrial respiration, morphology, and turnover are widely accepted. However, the intersection between Parkin interaction with the

mitochondria and mitochondrial function in immune cells like microglia and macrophages has not been explored. The identification of mitochondrial antiviral signaling (MAVS) protein linked mitochondria and innate immunity for the first time (Seth, Sun et al. 2005; Xu, Wang et al. 2005). To respond to viral infection, MAVS must localize to the mitochondrial membrane. However, in the absence of infection, turnover of MAVS protein in the cytosol might be necessary for the cell to remain inactivated. Parkin localizes to the mitochondria following oxidative stress as well as to mediate mitochondrial turnover. Parkin may interact with MAVS to indirectly shuttle MAVS to the mitochondria, or to ubiquitinate MAVS and lead to proteasome degradation. In either capacity, the absence of Parkin would increase MAVS localization and/or function at the mitochondria. Even so, MAVS activates expression of type I interferons only in response to viral infection (Seth, Sun et al. 2005; Xu, Wang et al. 2005), so cellular dysfunction would not be discovered unless challenged with an additional insult such as a viral infection. We observed that *parkin*$^{-/-}$ mice are more susceptible to exposure of the bacterial endotoxin, LPS (Frank-Cannon 2008). However, the function of Parkin in viral immunity and the response of *parkin*$^{-/-}$ mice to viral infection are unknown.

Parkin-deficiency and susceptibility to encephalitis

Although our paradigm of repeated peripheral LPS injections resulted in neuroinflammation and increased loss of DA neurons in the *parkin*$^{-/-}$ mice (Frank-Cannon 2008), we were curious whether a more physiological form of infection would also lead to increased nigral neuron loss in the SNpc. Based on the reports that bacterial and viral infections are associated with post encephalitic parkinsonism, we infected *parkin*$^{-/-}$ and

wild type mice with low levels of *Listeria monocytogenes* (LM), a gram positive bacteria. Our paradigm consisted of an initial tail vein injection of 200 colony forming units (CFU) of LM with an additional injection two months later. Based on our observation of significant DA neuron loss after a three month wait following removal of LPS stimulation, we waited three months after the second injection before we harvested the brains from the LM-infected mice. We did not observe increased nigral DA neuron loss in the SNpc of the *parkin*$^{-/-}$ mice after LM infection as determined by stereological analysis of TH-positive neurons on the SNpc. (Appendix 4). LM induced similar increases in the expression of CD45 and TNF in the midbrain of wild type and *parkin*$^{-/-}$ as measured by QPCR (Appendix 5), suggesting that our mild paradigm of infection was sufficient to cause neuroinflammation. Additionally, LM infection increased levels of IL-1b in the serum of the wild type, but not the *parkin*$^{-/-}$ mice, which already had elevated levels of IL-1b in the absence of infection (Appendix 6). We were able to induce neuroinflammation, but did not observe increased nigral DA neuron loss in the *parkin*$^{-/-}$ mice. One possible explanation is that the *parkin*$^{-/-}$ mice may be more susceptible to gram negative instead of gram positive bacterial infection, because as mentioned above, LM is gram positive. Additionally, although we were able to induce neuroinflammation, our model may not have been robust enough for the development of pathology.

Perspectives

The intersection between genes and environment and the development of disease is very intriguing. On the one hand, family members with the same mutations can develop disease symptoms at different ages. On the other hand, the exposure to environmental stimuli which can cause inflammation can lead to the development of autism, cancer, or neurodegenerative diseases; perhaps capitalizing on the cellular stresses and weaknesses from an individual's inherited mutations. We need a basic understanding not only of how disease-associated genes function in non-neuronal cell types, but also of how these genes function in response to different cellular stresses (or attacks on the immune system). By understanding the interactions between specific mutations and certain environmental insults, the field can begin to move towards developing specialized therapies to treat individuals more effectively.

CHAPTER SEVEN

Methodology

Animals

All mice were housed in a pathogen-free, climate controlled facility staffed with certified veterinarians in the Animal Resources Center at The University of Texas Southwestern Medical Center at Dallas and given food and water ad libitum. All animal studies were reviewed and approved by the Institutional Animal Care and Use Committee at The University of Texas Southwestern Medical Center at Dallas in accordance with the National Institutes of Health Guide for the Care and Use of Laboratory Animals. *parkin*$^{-/-}$ mice (Goldberg, Fleming et al. 2003) and *DJ-1*$^{-/-}$ mice (Goldberg, Pisani et al. 2005) were generated as previously described and have been backcrossed to strain C57BL/6 for over ten generations.

Systemic LPS administration paradigms

The regimen of LPS injections for our studies was chosen based on published protocols which have been shown to trigger a neuroinflammatory response and hasten appearance and progression of amyloid-associated burden in a transgenic mouse model of Alzheimer's disease (Kitazawa, Oddo et al. 2005). Young adult (6-13 week old) *parkin-/-* mice on a C57BL/6 background (backcrossed for over ten generations) and wild-type littermate mice were given either 7.5 x 10^5 EU/kg lipopolysaccharide (LPS) from *Escherichia coli* O111:B4 (Sigma-Aldrich, Saint Louis, MO, USA) or 0.9 % sodium chloride (vehicle control, Braun Medical, Inc, Irvine, CA, USA) injections

intraperitoneally (i.p.) twice a week for 2 months (n = 3 mice per group), 3 months (n = 11-12 mice per group), or 6 months (n = 11-12 mice per group) (**Figure 5.1**). An additional group was given systemic LPS or vehicle for 3 months followed by a 3-month wait period during which no additional i.p. injections were administered (n = 8 mice per group). Following the last i.p. injection, the animals were divided into two sets and processed for either immunohistochemistry or QPCR (**Figure 5.1**).

Intranasal TNF Administration

Murine soluble TNF (1-2 µl) was administered intranasally via an L-20 Pipetteman (Rainin) twice weekly for the time indicated in each set of experiments at one of two doses (T1= 0.5ng) and (T2= 5ng) in WT or *DJ-1*-null mice.

Behavior Testing

For all behavioral tests, mice (n = 8 per group) were evaluated at baseline (before i.p. injections began) and depending on the regimen again at 3 and 6 months after LPS or saline administration (**Figure 5.1**).

Open-field. Open-field behavior in a glass container (diameter, 24.5 cm) was recorded for 5 min for evaluation of time spent moving and number of rearing events by an investigator blinded to genotype and treatment history.

Narrow Beam walk. A narrow beam (1.1 cm diameter, 80.6 cm testing length) with a home cage at one end was used. Initial training prior to treatment consisted of 3 sessions of 3 trials per session for 4 consecutive days. Mice received additional training sessions at 3 months and 6 months after the start of treatment regimen consisting of 3 sessions of 3

trials per session on one day. Testing was conducted the day after training and consisted of one session of 3 trials. Average time to traverse the full length of the beam was determined and used for data analysis.

Accelerating rotarod. A base speed of 20 rpm with an acceleration of 0.2 rpm/second was used on the rotarod (Economex 0207-005 M, Columbus Instruments, Columbus, OH). Mice were trained prior to treatment in 3 sessions of 4 trials each for 4 consecutive days. Mice received additional training sessions at 3 months and 6 months after start of treatment consisting of 3 sessions of 4 trials per session on one day. Testing consisted of one session of 3 trials the day after training was completed. Latency to fall (seconds) was calculated and used for data analysis.

Tissue Harvest

Following the last i.p. injection, mice in the 2-month cohort (n = 3 mice per treatment group) were deeply anesthetized with halothane, decapitated, and the brain rapidly removed and microdissected into 4 regions on an ice-cold glass Petri dish: olfactory bulb (OB), cerebellum (CB), ventral midbrain (MB) and cortex (CX) then snap-frozen in liquid nitrogen and stored at -80ºC until processed for RNA extraction. For quantitative real time polymerase chain reaction (QPCR), mice in the 3-month, 3-month/3-month wait, and 6-month treatment cohort (n = 4 mice per treatment group) were deeply anesthetized with euthasol then intracardially perfused with 0.1 M phosphate buffered saline (PBS) pH 7.4 supplemented with 0.1 % glucose and 1 U/mL heparin prior to rapid whole brain removal. Microdissected tissue was snap-frozen or put in RNA*later* (Ambion, Austin, TX, USA) and stored at – 80 º until processed for QPCR. For

immunohistochemistry, mice in the 3-month, 3-month/3-month wait, and 6-month treatment cohort (n = 7 – 8 mice per group) were perfused with 0.1M PBS followed by 4 % paraformaldehyde in PBS (pH 7.4). Brains (in the skull) were post-fixed overnight in 4 % PFA. Brains were dissected out then cryoprotected for 24 hr in 20 % sucrose in 0.1 M PBS pH 7.4, embedded in Neg 50 (Richard Allen Scientific, Kalamazoo, MI), and frozen in dry ice-cooled isopentane.

Quantitative Real-time Polymerase Chain Reaction (QPCR)

QPCR was performed as previously described (Kurrasch, Huang et al. 2004). For QPCR total RNA was isolated from cultured cells or animal tissues using the Qiagen RNeasy isolation kit or RNA Stat-60 (Tel-Test, Inc., Friendswood, TX), respectively. After isolation RNA was treated with DNAse I (Invitrogen, Carlsbad, CA), and reverse transcribed using Superscript II RNase H- reverse transcriptase (Invitrogen) to obtain cDNA. QPCR was performed using SYBR Green Master Mix (ABI) on an Applied Biosystems Prism 7900HT sequence detection system as described (Kurrasch, Huang et al. 2004). Primers for each gene (available upon request) were designed using Primer Express Software (PerkinElmer Life Sciences, Wellesley, MA, USA) and validated by analysis of template titration and dissociation curves. Results for QPCR were normalized to the housekeeping gene cyclophilin B and evaluated by comparative C_T method (user bulletin No. 2, PerkinElmer Life Sciences). RNA levels in Chapter 2 are expressed relative to the wild-type saline-injected (vehicle) mice. Values in Chapter 3 represent the mean value of three separate samples +/- SEM, and data are representative of at least two independent experiments.

Immunohistochemistry

Coronal serial sections (30 μm thickness) were cut on a Leica CM 1850 cryostat and placed on Superfrost/Plus microscope slides (Fisher Scientific). Sections on slides were stored at -80° C until processed for immunohistochemistry.

Brightfield immunohistochemistry. Sections were stained for tyrosine hydroxylase (TH) using published protocols (Abbott and Jacobowitz 1995; Frank, Nunley et al. 2003). Sections were permeabilized in 0.3 % TritonX-100 in PBS pH 7.4. Endogenous peroxidases were quenched with 1 % H_2O_2 and non-specific binding was blocked with 5 % normal serum (goat or horse, Equitech-Bio, Inc., Kerrville, TX). Sections were incubated with primary antibodies against TH (rabbit polyclonal diluted 1:2000, Chemicon International, Temecula, CA, USA), or neuronal nuclear antigen (NeuN) (mouse monoclonal diluted 1:1000, Chemicon) overnight at room temperature followed by biotinylated secondary antibody (goat anti-rabbit or horse anti-mouse rat absorbed, or goat anti-rat IgG diluted 1:400, Vector Laboratories, Burlingame, CA, USA) and NeutrAvidin-HRP (diluted 1:5000, Pierce Biotechnology, Inc., Rockford, IL, USA). The tissue bound peroxidase activity was developed with a 0.024 % diaminobenzadine (DAB, Sigma), 0.006 % H_2O_2 in 0.05 M Tris-HCl buffer pH 7.6 for 20 min with or without nickel intensification. Tissue sections were dehydrated in a graded series of ethanols, immersed in xylene, and coverslipped with Permount (Fisher Scientific).

Fluorescence immunohistochemistry. Brain sections were stained for microglial markers using a standard immunofluorescence protocol (McCoy, Martinez et al. 2006). Auto-fluorescence was quenched in 0.2 M glycine in PBS pH 7.4, for 1 hr at room temperature.

Sections were then permeabilized in 0.3 % Triton X-100 with 1 % normal goat serum in 20 mM Tris-buffered saline (TBS) pH 7.4. Non-specific binding was blocked with species-appropriate 1% normal serum in TBS. Sections were incubated overnight at 4° C with rat monoclonal antibody made against mouse CD68 (diluted 1:150, Serotec, Raleigh, NC) and rabbit polyclonal anti-TH (diluted 1:250, Chemicon) followed by Alexa-488 goat anti-rabbit (Invitrogen) secondary antibody (Fab) or Alexa-594 goat anti-rat secondary antibody (each at 1:1000 dilution, Invitrogen) for 4 hr at room temperature. Antibodies were diluted in blocking buffer with 0.1 % Triton X-100. Washes were done in TBS with 0.2 % Triton X-100 (TBST). Following secondary antibody incubations, slides were rinsed briefly with dH_2O, then counterstained with Hoescht 33258 (at 1:20,000, Invitrogen) for 15 min, and coverslipped with aqueous mounting media with anti-fade (Biomeda Corp, Foster City, CA, USA).

Stereological Analysis

The optical fractionator probe of Stereoinvestigator software (MicroBrightField, Inc., Williston, VT, USA) was used to obtain an unbiased estimate of TH-positive and NeuN-positive neurons in the substantia nigra pars compacta (SNpc) and ventral tegmental area (VTA) as per the atlas of Paxinos (Paxinos 2001). Stereologic parameters were as follows: counting frame, 50 μm x 50 μm; optical dissector: 20 μm; grid size, 120 μm x 160 μm. For the population size estimate (number of sections per animal), a target coefficient of error (Gundersen's m = 1) of less than 0.10 was considered acceptable.

Striatal TH fiber density and densitometry

Coronal serial sections (30 μm thickness) were cut between Bregma -1.22 to 1.70 on a Leica CM 1850 cryostat and placed on Superfrost/Plus microscope slides (Fisher Scientific). Tissue sections were immunostained for TH and developed using DAB as described above. Images of striatum (caudate putamen) from 12 tissue sections per animal were taken with a Color digital camera (Model CX9000) mounted on a Nikon Eclipse 80i microscope. Exposure times were kept constant for all images. TH-positive fiber density was determined using background corrected integrated optical density (IOD) measurements for each section using an Alpha Innotech FluorChem FC2 imaging workstation and software. All sections for each animal were averaged and group means were used to compare between treatment groups.

Striatal DA and metabolite measurements.

Levels of striatal DA and its metabolites (DOPAC, HVA and 3-MT) were quantified by HPLC with electrochemical detection. Mice were euthanized by carbon dioxide asphyxiation and the striatum was immediately dissected on an ice-cold glass Petri dish, weighed and stored at -80 until analysis. Frozen brain tissue was sonicated in 49 volume/weight (mg of tissue) of 0.1 M perchloric acid containing 0.2 mM sodium metabisulfite and centrifuged at 20,000 rpm 20 minutes 4°C in a benchtop centrifuge to clear debris. 20 μL of cleared supernatant was injected onto a C18 HPLC column and separated by isocratic elution at a flow rate of 0.6 ml/min with MD-TM mobile phase (ESA Inc, Chelmsford, MA). Neurotransmitter monoamines and metabolites were

detected using a BAS electrochemical cell set to a potential of +800 mV and compared to external standards.

Statistics

Multiple-way analysis of variance (ANOVA) with significance level $\alpha = 0.05$ were used as indicated for each set of experimental data. Significant differences between groups were further evaluated using Tukey's HSD post hoc test. Kruskal-Wallis analysis was the nonparametric statistical test used for testing equality of population medians of integrated optical density measurements of striatal TH fiber density.

Reagents

Lipopolysaccharide (LPS) *E.coli* strain 0111:B4 was purchased from Sigma-Aldrich. Tumor necrosis alpha (TNF) was purchased from R&D Systems. CDDO-Im was provided by Michael Sporn (Dartmouth). Lyophilized stocks of the synthetic triterpenoid CDDO-Me (RTA 402) were stored at -20°C until they were dissolved in DMSO.

Cell culture

The murine BV2 microglia cell line was generated by Dr. Bistoni and colleagues by infecting primary microglial cell cultures with the v-raf/v-myc oncogene carrying retrovirus J2 (Blasi, Barluzzi et al. 1990). BV2 microglial cells were cultured in DMEM/F12 (Sigma-Aldrich) supplemented with 5% heat-inactivated fetal bovine serum (FBS, from Sigma-Aldrich) 1% penicillin/streptomycin, and 1% L-glutamine (Sigma-Aldrich). Cells were serially passaged when they reached 70% confluence. The murine

clonal hybrid cell line MN9D was developed by A. Heller and colleagues by somatic cell fusion of rostral mesencephalic tegmentum from E14 mice and the murine neuroblastoma cell line N18TG2 (Choi, Won et al. 1991). MN9D cells were grown in DMEM (Sigma-Aldrich) supplemented with 10% Fetal Clone III (from Hyclone) and 1% penicillin/streptomycin. Cells were serially passaged when they reached 70% confluence. To induce terminal neuron-like differentiation of MN9D cells, cells were incubated with 5 mM valproic acid in N2 (Invitrogen)-supplemented serum-free DMEM for 3 days.

Culture of primary microglia - Primary microglial cells were harvested from postnatal day 2-4 (P2-4) wild type C57BL/6 or *parkin* $^{-/-}$ mouse pups using previously published protocols (Floden and Combs 2007). Briefly, brain tissue was removed, finely minced with a razor, incubated in 0.25% trypsin (Sigma-Aldrich) containing 0.5% v/v DNaseI (Invitrogen) for 20 minutes at 37 ºC. After neutralization with DMEM/F12 media containing serum, cells were centrifuged, passed through a 40 μM filter (BD Falcon), and plated in cell culture flasks. Cells were fed every 3-4 days with fresh media (DMEM/F12 supplemented with 20% heat-inactivated fetal bovine serum (Sigma-Aldrich), 1% penicillin-streptomycin, and 1% L-glutamine). After 14-18 days *in vitro*, microglia were isolated from cultures by mechanical agitation (150 rpm, 40 min at 37 °C). The cultures were checked for purity and found to contain greater than 95% microglia as determined by cell-type specific expression of CD68 and less than 5% astrocytes as determined by GFAP immunoreactivity.

Culture of primary macrophages - Murine peritoneal macrophages were obtained by eliciting an acute peripheral inflammatory reaction with intraperitoneal (i.p.) injection of thioglycolate (Venkateswaran, Repa et al. 2000). Briefly, adult mice were given an i.p. injection of 3% Brewer's yeast thioglycolate in normal saline. Three days later peritoneal exudates were recovered, pelleted and resuspended in culture media (high glucose DMEM supplemented with 10 % FBS (Atlanta Biologicals), 1% penicillin/streptomycin, and 1% L-glutamine). Six hours after the initial plating, cells were washed twice with PBS to remove non-adherent cells and growth medium was replenished to the homogeneous population of macrophages.

Immunoblot analysis - Cells were treated with LPS as indicated and washed once with PBS before harvesting with RIPA lysis buffer. Cell lysates were centrifuged at 10,000 rpm for 5 min at 4°C, and the supernatants stored at -80 °C until use. To ensure equal loading, protein concentrations were determined using BCA protein assay (Pierce). Cell lysate proteins were resolved on 10% SDS-PAGE gels (Bio-Rad) and transferred onto PDVF membranes (Millipore). Immunoblotting was performed using anti-Parkin (PARK8, Covance) and anti-alpha tubulin (Calbiochem) antibodies. Membranes were stripped with 0.2 M glycine, 1% SDS and 0.1% Tween-20, pH 2.2) and re-probed as necessary.

Generation of parkin reporter plasmids

Sequences containing the 5'-flanking region of the mouse parkin gene were amplified by PCR with the Phusion DNA polymerase kit (New England Biolabs). Mouse genomic DNA isolated from a C57BL/6 mouse was used as the template. The PCR products were

purified, subjected to restriction digestion, and subcloned into the multiple cloning site of the promoterless pGL4 vector (Promega, pGL4.10) upstream of a synthetic luciferase coding sequence. The pGL4-tk-Renilla Luciferase vector, in which Renilla luciferase is constitutively expressed under the control of the thymidine kinase (tk) promoter, was obtained from Promega (pGL4.74). The integrity of each plasmid was confirmed by DNA sequencing.

Electroporation of reporter plasmids and luciferase assays

Electroporation was performed using the Amaxa Nucleofector II (Lonza). One μg of the indicated pGL4-Parkin luciferase plasmid or the empty pGL4 plasmid, and 0.4 μg of Renilla luciferase were electroporated into BV2 cells as per the manufacturer's instructions. Electroporation of 0.5 μg GFP was used to estimate the electroporation efficiency which was found to be ~30% by fluorescence microscopy. Cells were treated with TNF or LPS as indicated 24 hours after electroporation. After an overnight stimulation, cell were washed with PBS and lysed in 70 μl of Passive Lysis Buffer (Promega) at room temperature. Firefly and Renilla luciferase activities were measured in a 96-well plate format with the Dual-Luciferase Reporter Assay System (Promega). Data are expressed as the normalized value of firefly luciferase activity/Renilla luciferase activity.

PCR array

Inflammatory cytokine and chemokine PCR arrays were performed on a 96-well plate format as per the manufacturer's instructions (SA Biosciences). Gene expression values are expressed as fold-changes over the indicated condition.

Multiplexed high-sensitivity immunoassays

Serum from 8 month old mice was collected in **Figure 2.5** to measure the production of seven inflammatory mediators (IFN-γ, IL-1β, IL-6, IL-10, IL-12, KC/CXCL1, and TNF) using a high-sensitivity multiplexed immunoassay per the manufacturer's instructions (Meso-Scale Discovery). In **Figure 4.3**, BV2 cells were plated at 500,000 cells/well in a 6-well plate in DMEM containing 5% FBS and switched to serum-free media before pre-treatment with CDDO-Me or DMSO vehicle and subsequent stimulation of LPS as indicated. Conditioned Medium (CM) was collected to measure the production of the seven cytokines listed above.

Immunocytochemistry

Immunocytochemical analyses were performed as described previously (Lee, McCoy et al. 2008). Microglia and macrophages were incubated with primary antibody overnight at 4 ºC at the dilutions indicated for anti-Iba1 (Abcam), 1:150; anti-CD45 (Serotec), 1:500; Hoechst 33258 (Invitrogen), 1:20,000. Fluorescence images were captured on an Olympus CK40 microscope with a CoolSnap CCD ES monochromatic camera and Metamorph imaging software.

Caspase activation assay

Primary peritoneal macrophages were harvested from wild type and *parkin*$^{-/-}$ mice as described above and seeded in a 96-well plate format. Caspase activation was measured in resting cells or after stimulation with TNF, LPS, or etanercept for 1 hour before incubation with a caspase substrate as per manufacturer's instructions (Roche). Cleaved

substrate is proportional to the concentration of activated caspase, and was quantified by a standard curve. Homogeneous caspase activation (caspases 2, 3, 6, 7, 8, 9 and 10) was measured at 521nm in a BMG Fluostar fluorimeter.

Aggregation of amyloid beta peptide

Aβ 1–42 peptide was synthesized by Dr. Haydn Ball in the Protein Chemistry Core at UT Southwestern. Aggregation into fibrillar form was achieved by resuspending the peptide at final concentration of 100 μM into phosphate-buffered saline and incubating it at 37°C for 48 hrs. Thioflavin T fluorescence (LeVine 1999) and Congo Red binding in vitro was used to confirm fibril formation (Lorenzo and Yankner 1994).

Microglial activation assays

In **Figure 4.1**, rat embryonic ventral mesencephalon primary cultures were harvested from E14 pups, mechanically dissociated and seeded as micro-islands (25 uL of $1 \times 10_6$ cells/mL) on 4-chamber slides precoated with poly-D-lysine and laminin (BD Bioscience) in DMEM/F12 with 1% penicillin/streptomycin, glutamine, and non-essential amino acid and containing 10% fetal bovine serum (Atlanta Biologicals) and 10 ng/mL FGF-2 (R&D Systems, Minneapolis, MN). Culture media was changed after 2 days in vitro and cells were treated at day 5 in vitro with indicated compounds in DMEM containing 2.5% FBS and lacking FGF-2. Cells were fixed at 2 days post-treatment in 4% paraformaldehyde in PBS (pH 7.4) and stained with an antibody against activation marker F4/80 (1:60 dilution Serotec,Raleigh, NC) to quantify number of activated

microglia. Each condition was done in triplicate; 20 random sites were visited per well; data was plotted as the average number of F4/80-positive microglia per field.

Oligonucleotide microarrays

BV2 cells were plated at 500,000 cells/well in a 6-well plate in DMEM with 5% FBS and switched to serum-free media before pre-treatment with CDDO-Me or DMSO vehicle and subsequent stimulation with LPS as indicated. RNA was harvested as detailed above and levels of inflammation-related gene expression were detected on an oligonucleotide array as per manufacturer's instructions (Superarray Bioscience Corporation, Frederick, MD). Data analyses were performed using the Scatter Plot data analysis tool in the SuperArray GEArray Analysis Suite. The Scatter Plot displays the fold difference in the relative expression levels of genes between groups. Seven housekeeping genes were used for normalization. The control group was assigned to the X-Axis, and the treated group was assigned to the Y-Axis. An arbitrary boundary of 1.5-fold regulation in either direction was selected. If the fold increase was greater than boundary value, the gene names are shown in red with a plus (+) sign, and are located above the upper line. The further the sign is from the upper line, the greater the fold difference. If the fold decrease is greater than the boundary value, the genes are shown in green with a minus (-) sign, and are located below the lower line. The further the sign is from the lower line, the greater the fold difference. Black signs mean the fold change is not significant.

Intracellular reactive oxygen species (ROS) imaging

Rat embryonic ventral mesencephalon neuron/glia cultures were prepared as published previously (McCoy, Martinez et al. 2006). At 5 days in vitro (5 DIV), they were incubated with 3 μM DCFDA (Invitrogen) in serum-free growth medium for 40 min to quantify intracellular reactive oxygen species (ROS) production by fluorescence imaging. The next day, cells were treated with the vehicle, 1 μM fibrillar amyloid beta (Aβ) 42 peptide plus or minus 10 ng/mL LPS in the presence or absence of CDDO-Me as indicated for 24 hrs. Fluorescence images were captured on an Olympus CK40 microscope with a CoolSnap CCD ES monochromatic camera with a FITC filter in place. Quantification of fluorescence intensity was performed using intensity threshold analysis of digital images on an Alpha Innotech ChemiImager 4400 (Alpha Innotech, San Leandro, CA). MN9D dopaminergic cells were plated at 50,000 cells per well in DMEM containing 10% FBS in 24 well plates. The following day cultures were differentiated in N2 supplemented serum-free DMEM containing 5 mM valproic acid. 48 hours following differentiation MN9D cells were incubated with 3 uM DCFDA in serum free DMEM for 40 min, and then returned to differentiation media. Six hours after DCFDA loading, MN9D cells were treated with 10 nM CDDO-Me (or DMSO vehicle) for 16–20 hrs before 30 minute stimulation with either TNF or conditioned media from LPS and CDDO-Me treated BV2 microglial cultures. BV2 microglial cultures for these experiments were plated in DMEM containing 5% FBS at 800,000 cells per well in a 6-well plate. Cultures were permitted to adhere to the plastic and then were pretreated with 10 nM CDDO-Me (or DMSO vehicle) for 16–18 hrs prior to stimulation with 10 ng/mL LPS (or saline vehicle). The following day conditioned media from BV2 cultures was

removed and centrifuged at 1200 × g for 4 min before addition to DCFDA-loaded, differentiated MN9D dopaminergic cultures. Fluorescence images were captured on an Olympus CK40 microscope with a CoolSnap CCD ES monochromatic camera with a FITC filter in place. Quantification of ROS accumulation was performed by counting DCFDA-positive cell bodies in four fields per condition under 20× magnification (equivalent to approximately 50% of the plated area per well) in two independent experiments. DCFDA positive cells ranged between 38 and 420 per field depending on experiment and treatment. Values for treatment conditions in each experiment were expressed as fold increase in DCFDA positive cells per field relative to DMSO vehicle, saline treated control, and averaged between independent experiments.

Cell survival/neuroprotection assays

MN9D dopaminergic cells (grown as described above), were terminally differentiated with 5 mM valproic acid in N2-supplemented serum-free DMEM 3 days prior to neuroprotection studies with CDDO-Me. MN9D cell viability was measured using the CellTiter 96 AQ$_{ueous}$ Assay reagent (Promega, Madison, WI). This reagent uses the tetrazolium compound (3-(4,5-dimethylthiazol-2-yl)-5-(3-carboxymethoxyphenyl)-2-(4-sulfophenyl)-2H-tetrazolium, inner salt; MTS) and the electron coupling reagent, phenazine methosulfate (PMS). MTS is chemically reduced into soluble formazan in metabolically active cells. MN9D cell viability was assayed by measurement of formazan absorbance at 492 nm in multi-titer 96-well plates at 492 nm during the last 2–4 hrs of a three-day incubation with soluble TNF or a two-day incubation with BV2 conditioned media in target-effector assays in which the BV2 microglia cell line was used as the

effector cell and the MN9D dopaminergic ells as the target cell. Specifically, conditioned medium (CM) from LPS-treated BV2 microglia was transferred to MN9D cell cultures to induce inflammation-induced death in a dose-dependent manner.

Phagocytosis assays

BV2 microglia were plated at a density of 50,000 cells/well in a 96-well plate and switched to serum-free media 24 hr later for stimulation as indicated with LPS (10 ng/mL) and/or fAβ (1 μM), in the presence or absence of CDDO-Me (10 nM). After 24 hr stimulation, phagocytosis was measured by exposing the cultures to fluorescently labeled E. coli particles (Invitrogen) for 2 hr. Cells were incubated with trypan blue and rinsed with PBS to remove non-internalized particles prior to measuring fluorescence at 480 nm excitation and 520 nm emission on a Fluoroskan multiwell plate reader.

APPENDIX A

	WT LPS/WT SAL	PK LPS/PK SAL	PK SAL/WT SAL	PK LPS/WT LPS
Symbol	**Test / Control Sample**	**Test / Control Sample**	**Test / Control Sample**	**Test / Control Sample**
Traf1	**68.45**	**67.15**	1.16	1.14
Cd40	**45.27**	**58.96**	1.09	1.42
Tnf	**41.02**	**45.16**	1.33	1.47
Tnfsf10	**12.28**	**12.13**	1.94	1.92
Cd70	**7.46**	**39.66**	**-3.44**	1.54
Bnip3	**7.15**	**6.00**	-1.07	-1.28
Fasl	**6.49**	**2.90**	1.00	**-2.23**
Casp7	**5.35**	**3.43**	1.55	-1.01
Birc3	**4.93**	**4.56**	1.15	1.06
Cflar	**4.56**	**6.31**	-1.25	1.11
Fas	**4.49**	**4.06**	1.12	1.01
Casp4	**4.16**	**4.63**	1.04	1.15
Nol3	**3.81**	1.78	1.64	-1.31
Tnfrsf11b	**3.48**	**2.30**	1.78	1.18
Gapdh	**2.77**	**2.52**	1.04	-1.05
Naip2	**2.66**	**2.78**	1.03	1.07
Traf2	**2.30**	**4.06**	-1.43	1.23
Casp14	**2.07**	-1.37	1.00	**-2.83**
Traf3	1.96	**2.07**	-1.02	1.03
Bcl2l2	1.78	**2.16**	1.01	1.23
Fadd	-1.25	-1.56	1.23	-1.01
Cd40lg	-1.31	**-3.57**	**3.19**	1.17
Casp9	-1.87	**-2.21**	1.13	-1.05
Trp53inp1	-1.97	**-2.08**	1.06	1.01
Bnip3l	**-2.20**	**-2.38**	1.00	-1.08
Card10	**-2.42**	-1.94	-1.21	1.03
Gusb	**-2.47**	**-2.49**	1.04	1.03
Bag3	**-2.61**	**-2.42**	1.04	1.13
Tsc22d3	**-3.38**	**-3.65**	-1.05	-1.13
Bok	**-4.27**	**-4.80**	1.31	1.16
Tnfsf12	**-5.32**	**-4.94**	1.03	1.12
Nme5	**-6.45**	**-6.64**	-1.02	-1.05
Trp73	**-7.79**	-1.40	-1.57	**3.55**
Birc5	**-8.09**	**-11.02**	1.29	-1.06
Casp12	**-10.96**	**-4.24**	-1.17	**2.22**
Il10	**-11.26**	**-8.04**	-1.09	1.29

Appendix 1. Apoptosis PCR array (SA Biosciences) using mRNA samples from isolated peritoneal macrophages treated with 1ug/mL LPS for 48 hrs.

		WT LPS_WT SAL	PK LPS_PK SAL
Symbol	**Function**	**Test Sample /Control Sample**	**Test Sample /Control Sample**
Cd40	Signals microglial activation TNF-receptor superfamily	45.27	58.96
Cd70	Activate NfkB Llgand for CD27	7.46	39.66
Fasl	Signals apoptosis	6.49	2.90
Traf2	TNF receptor adaptor protein Recruits IAP	2.30	4.06
Cd40lg	Signals microglial activation	-1.31	-3.57
Il10	Cytokine; inhibits synthesis of pro-inflammatory cytokines	-11.26	-8.04
Casp7	Executioner of apoptosis	5.35	3.43
Cflar	NFkB-dependent antiapoptotic gene CASP8, FADD-like apoptosis regulator	4.56	6.31
Nol3	Apoptosis repressor	3.81	1.78
Trp73	Induction of apoptosis Downregulated by NFkB	-7.79	-1.40
Birc5	Inhibits caspase activation	-8.09	-11.02
Casp12	Inflammatory caspase Inhibit NFkb activation	-10.96	-4.24
Tnf	Cytokine	41.02	45.16
Gapdh	Housekeeping gene	2.77	2.52

Appendix 2. Quantitative PCR (QPCR) validation of results from Apoptosis PCR array (SA Biosciences) using newly designed and validated primers for the genes listed above. QPCR was performed on mRNA samples from isolated peritoneal macrophages treated with 1ug/mL LPS for 48 hrs.

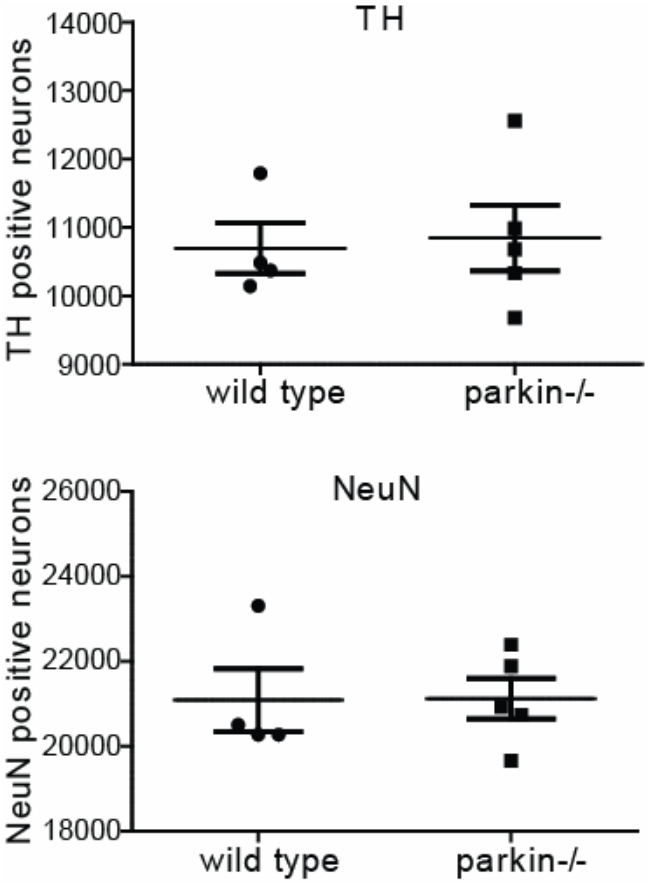

Appendix 3. *Listeria monocytogenes (LM) infection does not increase nigral DA neuron loss in parkin*$^{-/-}$ *mice compared to neuronal counts in LM-infected wild type mice.* Animals were given initial tail vein injections of 200 CFU of LM and a booster injection of 2,000 CFU of LM 2 months later. Animals were sacrificed 3 months after the second injection by transcardial perfusion. Brains were removed, frozen, sectioned, and stained for immunoreactivity against DA neuron marker tyrosine hydroxylase (TH) and pan-neuronal marker NeuN. Unbiased stereological analysis of neuronal numbers revealed no increased susceptibility of Parkin loss in DA neuron loss in the SNpc after LM infection.

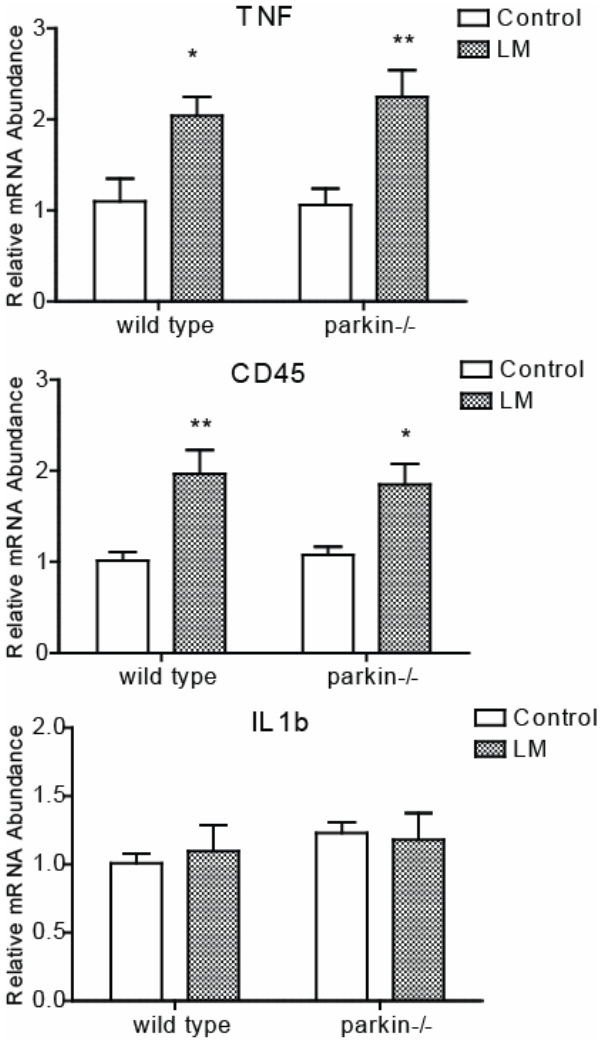

Appendix 4. Cytokine expression is comparable in the midbrain of wild type and parkin$^{-/-}$ mice infected with LM. Midbrain tissue was collected at the end of the study, 5 months after initial infection, to determine levels of cytokine expression by QPCR. Analysis was performed by two-way ANOVA followed by Bonferroni's post hoc where * $p< 0.05$ and ** $p<0.01$; significance compared to untreated wild type.

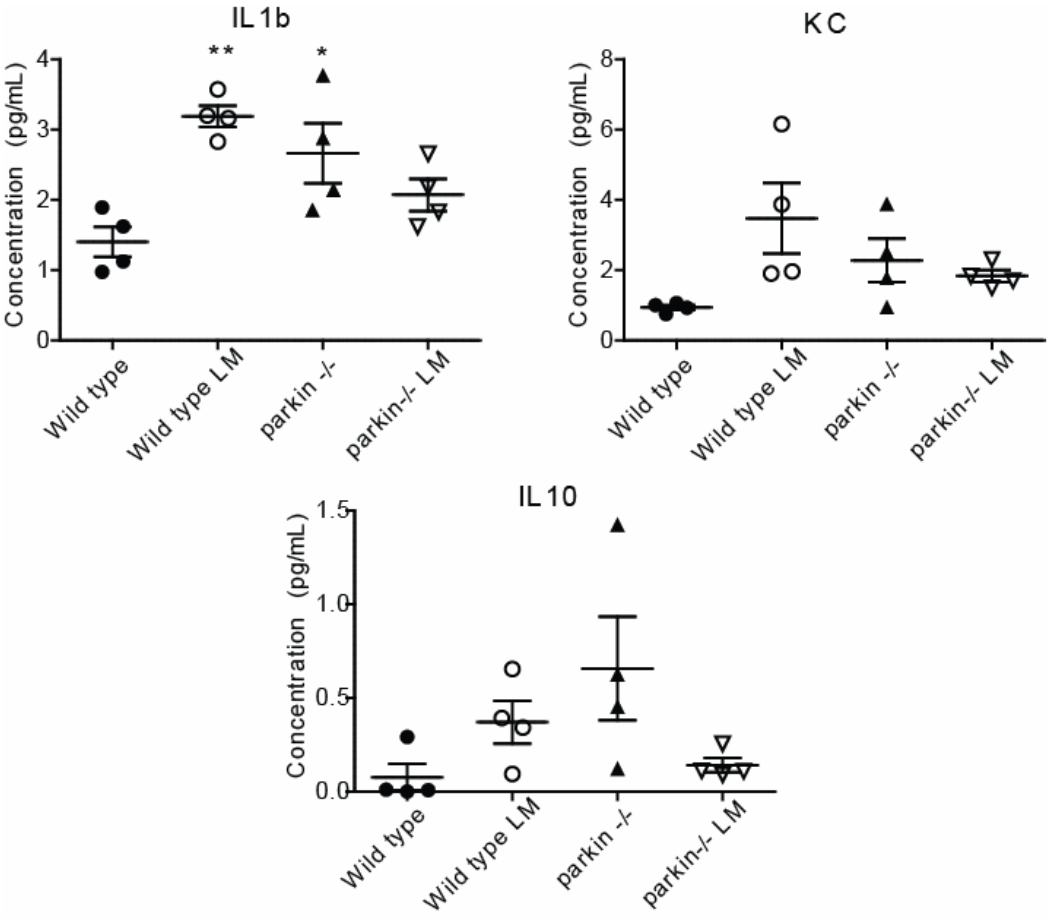

Appendix 5. Cytokine levels in the serum of parkin$^{-/-}$ mice are not elevated after LM infection compared to wild type. Blood was collected 4 months after initial infection to determine levels of cytokine production. Cytokine levels were determined by a 7-multianalyte ELISA (MesoScale Discovery). Analysis was performed by two-way ANOVA followed by Bonferroni's post hoc where * $p< 0.05$ and ** $p<0.01$ compared to untreated wild type animals.

BIBLIOGRAPHY

Abbas, N., C. B. Lucking, et al. (1999). "A wide variety of mutations in the parkin gene are responsible for autosomal recessive parkinsonism in Europe. French Parkinson's Disease Genetics Study Group and the European Consortium on Genetic Susceptibility in Parkinson's Disease." Hum Mol Genet **8**(4): 567-574.

Abbott, L. C. and D. M. Jacobowitz (1995). "Developmental expression of calretinin-immunoreactive unipolar brush-like cells and an afferent pathway to the embryonic and early postnatal mouse cerebellum." Anat Embryol (Berl) **191**(6): 541-559.

Abeliovich, A., Y. Schmitz, et al. (2000). "Mice lacking alpha-synuclein display functional deficits in the nigrostriatal dopamine system." Neuron **25**(1): 239-252.

Aggarwal, B. B., Samanta, A., and Feldmann, M. (2000). TNF Receptors. Cytokine Reference. J. J. a. F. Oppenheim, M. London, Academic Press**:** pp. 1620-1632.

Ahmad, R., D. Raina, et al. (2006). "Triterpenoid CDDO-Me blocks the NF-kappaB pathway by direct inhibition of IKKbeta on Cys-179." J Biol Chem **281**(47): 35764-35769.

Ascherio, A., H. Chen, et al. (2006). "Pesticide exposure and risk for Parkinson's disease." Ann Neurol **60**(2): 197-203.

Asehnoune, K., D. Strassheim, et al. (2004). "Involvement of reactive oxygen species in Toll-like receptor 4-dependent activation of NF-kappa B." J Immunol **172**(4): 2522-2529.

Auluck, P. K., H. Y. Chan, et al. (2002). "Chaperone suppression of alpha-synuclein toxicity in a Drosophila model for Parkinson's disease." Science **295**(5556): 865-868.

Avraham, E., R. Rott, et al. (2007). "Phosphorylation of Parkin by the cyclin-dependent kinase 5 at the linker region modulates its ubiquitin-ligase activity and aggregation." J Biol Chem **282**(17): 12842-12850.

Banati, R. B., S. E. Daniel, et al. (1998). "Glial pathology but absence of apoptotic nigral neurons in long-standing Parkinson's disease." Mov Disord **13**(2): 221-227.

Bandopadhyay, R., A. E. Kingsbury, et al. (2004). "The expression of DJ-1 (PARK7) in normal human CNS and idiopathic Parkinson's disease." Brain **127**: 420-430.

Bartels, A. L. and K. L. Leenders (2007). "Neuroinflammation in the pathophysiology of Parkinson's disease: evidence from animal models to human in vivo studies with [11C]-PK11195 PET." Mov Disord **22**(13): 1852-1856.

Batchelor, P. E., G. T. Liberatore, et al. (1999). "Activated macrophages and microglia induce dopaminergic sprouting in the injured striatum and express brain-derived neurotrophic factor and glial cell line-derived neurotrophic factor." J Neurosci **19**(5): 1708-1716.

Betarbet, R., T. B. Sherer, et al. (2000). "Chronic systemic pesticide exposure reproduces features of Parkinson's disease." Nat Neurosci **3**(12): 1301-1306.

Blackinton, J., R. Kumaran, et al. (2009). "Post-transcriptional regulation of mRNA associated with DJ-1 in sporadic Parkinson disease." Neurosci Lett **452**(1): 8-11.

Blasi, E., R. Barluzzi, et al. (1990). "Immortalization of murine microglial cells by a v-raf/v-myc carrying retrovirus." J Neuroimmunol **27**(2-3): 229-237.

Block, M. L., L. Zecca, et al. (2007). "Microglia-mediated neurotoxicity: uncovering the molecular mechanisms." Nat Rev Neurosci **8**(1): 57-69.

Blum-Degen, D., T. Muller, et al. (1995). "Interleukin-1 beta and interleukin-6 are elevated in the cerebrospinal fluid of Alzheimer's and de novo Parkinson's disease patients." Neurosci Lett **202**(1-2): 17-20.

Boillee, S., K. Yamanaka, et al. (2006). "Onset and progression in inherited ALS determined by motor neurons and microglia." Science **312**(5778): 1389-1392.

Bonifati, V., B. A. Oostra, et al. (2004). "Unraveling the pathogenesis of Parkinson's disease--the contribution of monogenic forms." Cell Mol Life Sci **61**(14): 1729-1750.

Bonifati, V., P. Rizzu, et al. (2003). "Mutations in the DJ-1 gene associated with autosomal recessive early-onset parkinsonism." Science **299**(5604): 256-259.

Braak, H., U. Rub, et al. (2003). "Idiopathic Parkinson's disease: possible routes by which vulnerable neuronal types may be subject to neuroinvasion by an unknown pathogen." J Neural Transm **110**(5): 517-536.

Bryant, C. and K. A. Fitzgerald (2009). "Molecular mechanisms involved in inflammasome activation." Trends Cell Biol **19**(9): 455-464.

Canet-Aviles, R. M., M. A. Wilson, et al. (2004). "The Parkinson's disease protein DJ-1 is neuroprotective due to cysteine-sulfinic acid-driven mitochondrial localization." Proc Natl Acad Sci U S A **101**(24): 9103-9108.

Carson, M. J., C. R. Reilly, et al. (1998). "Mature microglia resemble immature antigen-presenting cells." Glia **22**(1): 72-85.

Casarejos, M. J., J. Menendez, et al. (2006). "Susceptibility to rotenone is increased in neurons from parkin null mice and is reduced by minocycline." J Neurochem **97**(4): 934-946.

Cassarino, D. S., E. M. Halvorsen, et al. (2000). "Interaction among mitochondria, mitogen-activated protein kinases, and nuclear factor-kappaB in cellular models of Parkinson's disease." J Neurochem **74**(4): 1384-1392.

Chen, G. and D. V. Goeddel (2002). "TNF-R1 signaling: a beautiful pathway." Science **296**(5573): 1634-1635.

Chen, H., E. Jacobs, et al. (2005). "Nonsteroidal antiinflammatory drug use and the risk of Parkinson's disease." Annals of Neurology **59**: 988-989.

Chen, H., S. M. Zhang, et al. (2003). "Nonsteroidal anti-inflammatory drugs and the risk of Parkinson disease." Arch Neurol **60**(8): 1059-1064.

Choi, H. K., L. A. Won, et al. (1991). "Immortalization of embryonic mesencephalic dopaminergic neurons by somatic cell fusion." Brain Res **552**(1): 67-76.

Chung, K. K., B. Thomas, et al. (2004). "S-nitrosylation of parkin regulates ubiquitination and compromises parkin's protective function." Science **304**(5675): 1328-1331.

Chung, K. K., Y. Zhang, et al. (2001). "Parkin ubiquitinates the alpha-synuclein-interacting protein, synphilin-1: implications for Lewy-body formation in Parkinson disease." Nat Med **7**(10): 1144-1150.

Clark, I. E., M. W. Dodson, et al. (2006). "Drosophila pink1 is required for mitochondrial function and interacts genetically with parkin." Nature **441**(7097): 1162-1166.

Clarke, D. J. and R. L. Branton (2002). "A role for tumor necrosis factor alpha in death of dopaminergic neurons following neural transplantation." Exp Neurol **176**(1): 154-162.

Colton, C. A. (2009). "Heterogeneity of microglial activation in the innate immune response in the brain." J Neuroimmune Pharmacol **4**(4): 399-418.

Conway, K. A., J. D. Harper, et al. (1998). "Accelerated in vitro fibril formation by a mutant alpha-synuclein linked to early-onset Parkinson disease." Nat Med **4**(11): 1318-1320.

Costello, S., M. Cockburn, et al. (2009). "Parkinson's disease and residential exposure to maneb and paraquat from agricultural applications in the central valley of California." Am J Epidemiol **169**(8): 919-926.

Croisier, E., L. B. Moran, et al. (2005). "Microglial inflammation in the parkinsonian substantia nigra: relationship to alpha-synuclein deposition." J Neuroinflammation **2**: 14.

D'Agata, V., W. Zhao, et al. (2000). "Cloning and distribution of the rat parkin mRNA." Brain Res Mol Brain Res **75**(2): 345-349.

Dale, R. C., A. J. Church, et al. (2004). "Encephalitis lethargica syndrome: 20 new cases and evidence of basal ganglia autoimmunity." Brain **127**(Pt 1): 21-33.

Darios, F., O. Corti, et al. (2003). "Parkin prevents mitochondrial swelling and cytochrome c release in mitochondria-dependent cell death." Hum Mol Genet **12**(5): 517-526.

Dawson, T. M., V. L. Dawson, et al. (1992). "A novel neuronal messenger molecule in brain: the free radical, nitric oxide." Ann Neurol **32**(3): 297-311.

De Pablos, R. M., A. J. Herrera, et al. (2005). "Dopamine-dependent neurotoxicity of lipopolysaccharide in substantia nigra." Faseb J **19**(3): 407-409.

Deng, H., M. W. Dodson, et al. (2008). "The Parkinson's disease genes pink1 and parkin promote mitochondrial fission and/or inhibit fusion in Drosophila." Proc Natl Acad Sci U S A **105**(38): 14503-14508.

Dick, A. D., A. L. Ford, et al. (1995). "Flow cytometric identification of a minority population of MHC class II positive cells in the normal rat retina distinct from CD45lowCD11b/c+CD4low parenchymal microglia." Br J Ophthalmol **79**(9): 834-840.

Dinkova-Kostova, A. T., K. T. Liby, et al. (2005). "Extremely potent triterpenoid inducers of the phase 2 response: correlations of protection against oxidant and inflammatory stress." Proc Natl Acad Sci U S A **102**(12): 4584-4589.

Dooms, H., E. Kahn, et al. (2004). "IL-2 induces a competitive survival advantage in T lymphocytes." J Immunol **172**(10): 5973-5979.

Dourmashkin, R. R. (1997). "What caused the 1918-30 epidemic of encephalitis lethargica?" J R Soc Med **90**(9): 515-520.

Fahn, S. (2003). "Description of Parkinson's disease as a clinical syndrome." Ann N Y Acad Sci **991**: 1-14.

Farrer, M., P. Chan, et al. (2001). "Lewy bodies and parkinsonism in families with parkin mutations." Ann Neurol **50**(3): 293-300.

Farrer, M. J. (2006). "Genetics of Parkinson disease: paradigm shifts and future prospects." Nat Rev Genet **7**(4): 306-318.

Ferger, B., A. Leng, et al. (2004). "Genetic ablation of tumor necrosis factor-alpha (TNF-alpha) and pharmacological inhibition of TNF-synthesis attenuates MPTP toxicity in mouse striatum." J Neurochem **89**(4): 822-833.

Fine, S. M., R. A. Angel, et al. (1996). "Tumor necrosis factor alpha inhibits glutamate uptake by primary human astrocytes. Implications for pathogenesis of HIV-1 dementia." J Biol Chem **271**(26): 15303-15306.

Floden, A. M. and C. K. Combs (2007). "Microglia repetitively isolated from in vitro mixed glial cultures retain their initial phenotype." J Neurosci Methods **164**(2): 218-224.

Ford, A. L., A. L. Goodsall, et al. (1995). "Normal adult ramified microglia separated from other central nervous system macrophages by flow cytometric sorting. Phenotypic differences defined and direct ex vivo antigen presentation to myelin basic protein-reactive CD4+ T cells compared." J Immunol **154**(9): 4309-4321.

Forno, L. S. (1996). "Neuropathology of Parkinson's disease." J Neuropathol Exp Neurol **55**(3): 259-272.

Frank-Cannon, T. C., T. Tran, et al. (2008). "Parkin deficiency increases vulnerability to inflammation-related nigral degeneration." J Neurosci **28**(43): 10825-10834.

Frank-Cannon, T. C., Tran, T., Ruhn, K.A., Martinez, T.N., Hong, J., Marvin, M., Hartley, M., Treviño, I., O'Brien, D.E, Casey, B. Goldberg, M.S., Tansey, M.G. (2008). "Parkin deficiency increases vulnerabiity to inflammation-related nigral degeneration " J Neurosci **28**(43).

Frank, T. C., M. C. Nunley, et al. (2003). "Fluoro-jade identification of cerebellar granule cell and purkinje cell death in the alpha1A calcium ion channel mutant mouse, leaner." Neuroscience **118**(3): 667-680.

Frink, M., Y. C. Hsieh, et al. (2007). "Keratinocyte-derived chemokine plays a critical role in the induction of systemic inflammation and tissue damage after trauma-hemorrhage." Shock **28**(5): 576-581.

Gao, H. M., P. T. Kotzbauer, et al. (2008). "Neuroinflammation and oxidation/nitration of alpha-synuclein linked to dopaminergic neurodegeneration." J Neurosci **28**(30): 7687-7698.

Gerhard, A., N. Pavese, et al. (2006). "In vivo imaging of microglial activation with [11C](R)-PK11195 PET in idiopathic Parkinson's disease." Neurobiol Dis **21**(2): 404-412.

Ghosh, S., M. J. May, et al. (1998). "NF-kappa B and Rel proteins: evolutionarily conserved mediators of immune responses." Annu Rev Immunol **16**: 225-260.

Giasson, B. I., J. E. Duda, et al. (2000). "Oxidative damage linked to neurodegeneration by selective alpha-synuclein nitration in synucleinopathy lesions." Science **290**(5493): 985-989.

Goetz, C. G. (1986). "Charcot on Parkinson's disease." Mov Disord **1**(1): 27-32.

Goldberg, M. S., S. M. Fleming, et al. (2003). "Parkin-deficient mice exhibit nigrostriatal deficits but not loss of dopaminergic neurons." J Biol Chem **278**(44): 43628-43635.

Goldberg, M. S., A. Pisani, et al. (2005). "Nigrostriatal dopaminergic deficits and hypokinesia caused by inactivation of the familial Parkinsonism-linked gene DJ-1." Neuron **45**(4): 489-496.

Greene, J. C., A. J. Whitworth, et al. (2003). "Mitochondrial pathology and apoptotic muscle degeneration in Drosophila parkin mutants." Proc Natl Acad Sci U S A **100**(7): 4078-4083.

Griffin, W. S. (2006). "Inflammation and neurodegenerative diseases." Am J Clin Nutr **83**(2): 470S-474S.

Gu, W. J., N. Abbas, et al. (2000). "Cloning of rat parkin cDNA and distribution of parkin in rat brain." J Neurochem **74**(4): 1773-1776.

Hald, A. and J. Lotharius (2005). "Oxidative stress and inflammation in Parkinson's disease: is there a causal link?" Exp Neurol **193**(2): 279-290.

Hamaue, N., A. Ogata, et al. (2006). "Brain catecholamine alterations and pathological features with aging in Parkinson disease model rat induced by Japanese encephalitis virus." Neurochem Res **31**(12): 1451-1455.

Hattori, N., T. Kitada, et al. (1998). "Molecular genetic analysis of a novel Parkin gene in Japanese families with autosomal recessive juvenile parkinsonism:

evidence for variable homozygous deletions in the Parkin gene in affected individuals." Ann Neurol **44**(6): 935-941.

Hawkes, C. H., B. C. Shephard, et al. (1997). "Olfactory dysfunction in Parkinson's disease." J Neurol Neurosurg Psychiatry **62**(5): 436-446.

Hayashi, S., K. Wakabayashi, et al. (2000). "An autopsy case of autosomal-recessive juvenile parkinsonism with a homozygous exon 4 deletion in the parkin gene." Mov Disord **15**(5): 884-888.

Henn, I. H., L. Bouman, et al. (2007). "Parkin mediates neuroprotection through activation of IkappaB kinase/nuclear factor-kappaB signaling." J Neurosci **27**(8): 1868-1878.

Hershko, A. and A. Ciechanover (1998). "The ubiquitin system." Annu Rev Biochem **67**: 425-479.

Hirsch, E. C., S. Hunot, et al. (2005). "Neuroinflammatory processes in Parkinson's disease." Parkinsonism Relat Disord **11 Suppl 1**: S9-S15.

Hiscott, J., H. Kwon, et al. (2001). "Hostile takeovers: viral appropriation of the NF-kappaB pathway." J Clin Invest **107**(2): 143-151.

Honda, T., B. V. Rounds, et al. (1999). "Novel synthetic oleanane triterpenoids: a series of highly active inhibitors of nitric oxide production in mouse macrophages." Bioorg Med Chem Lett **9**(24): 3429-3434.

Honda, T., B. V. Rounds, et al. (2000). "Synthetic oleanane and ursane triterpenoids with modified rings A and C: a series of highly active inhibitors of nitric oxide production in mouse macrophages." J Med Chem **43**(22): 4233-4246.

Honda, T., B. V. Rounds, et al. (1998). "Design and synthesis of 2-cyano-3,12-dioxoolean-1,9-dien-28-oic acid, a novel and highly active inhibitor of nitric oxide production in mouse macrophages." Bioorg Med Chem Lett **8**(19): 2711-2714.

Hunot, S., N. Dugas, et al. (1999). "FcepsilonRII/CD23 is expressed in Parkinson's disease and induces, in vitro, production of nitric oxide and tumor necrosis factor-alpha in glial cells." J Neurosci **19**(9): 3440-3447.

Huynh, D. P., D. R. Scoles, et al. (2000). "Parkin is associated with actin filaments in neuronal and nonneural cells." Ann Neurol **48**(5): 737-744.

Huynh, D. P., D. R. Scoles, et al. (2003). "The autosomal recessive juvenile Parkinson disease gene product, parkin, interacts with and ubiquitinates synaptotagmin XI." Hum Mol Genet **12**(20): 2587-2597.

Imai, Y., M. Soda, et al. (2001). "An unfolded putative transmembrane polypeptide, which can lead to endoplasmic reticulum stress, is a substrate of Parkin." Cell **105**(7): 891-902.

Imai, Y., M. Soda, et al. (2000). "Parkin suppresses unfolded protein stress-induced cell death through its E3 ubiquitin-protein ligase activity." J Biol Chem **275**(46): 35661-35664.

Inoue, K. (2002). "Microglial activation by purines and pyrimidines." Glia **40**(2): 156-163.

Inoue, K. (2007). "UDP facilitates microglial phagocytosis through P2Y6 receptors." Cell Adh Migr **1**(3): 131-132.

Irizarry, M. C., T. W. Kim, et al. (1996). "Characterization of the precursor protein of the non-A beta component of senile plaques (NACP) in the human central nervous system." J Neuropathol Exp Neurol **55**(8): 889-895.

Ischiropoulos, H. and J. S. Beckman (2003). "Oxidative stress and nitration in neurodegeneration: cause, effect, or association?" J Clin Invest **111**(2): 163-169.

Isomaki, P., J. M. Clark, et al. (2005). "Pathways of T cell activation and terminal differentiation in chronic inflammation." Curr Drug Targets Inflamm Allergy **4**(3): 287-293.

Itier, J. M., P. Ibanez, et al. (2003). "Parkin gene inactivation alters behaviour and dopamine neurotransmission in the mouse." Hum Mol Genet **12**(18): 2277-2291.

Ito, D., Y. Imai, et al. (1998). "Microglia-specific localisation of a novel calcium binding protein, Iba1." Brain Res Mol Brain Res **57**(1): 1-9.

Jang, H., D. Boltz, et al. (2009). "Highly pathogenic H5N1 influenza virus can enter the central nervous system and induce neuroinflammation and neurodegeneration." Proc Natl Acad Sci U S A **106**(33): 14063-14068.

Jankovic, J. (2008). "Parkinson's disease: clinical features and diagnosis." J Neurol Neurosurg Psychiatry **79**(4): 368-376.

Janssens, S. and R. Beyaert (2002). "A universal role for MyD88 in TLR/IL-1R-mediated signaling." Trends Biochem Sci **27**(9): 474-482.

Jellinger, K. A. (2009). "Formation and development of Lewy pathology: a critical update." J Neurol **256 Suppl 3**: 270-279.

Jenner, P. (2003). "Oxidative stress in Parkinson's disease." Ann Neurol **53 Suppl 3**: S26-36; discussion S36-28.

Jeong, J. Y., K. U. Kim, et al. (1997). "Tosylphenylalanine chloromethyl ketone inhibits TNF-alpha mRNA synthesis in the presence of activated NF-kappa B in RAW 264.7 macrophages." Immunology **92**(2): 267-273.

Jiang, J., H. Cai, et al. (1993). "Conversion of a dorsal-dependent silencer into an enhancer: evidence for dorsal corepressors." EMBO J **12**(8): 3201-3209.

Josephs, K. A., J. E. Parisi, et al. (2002). "Alpha-synuclein studies are negative in postencephalic parkinsonism of von Economo." Neurology **59**(4): 645-646.

Junn, E., W. H. Jang, et al. (2009). "Mitochondrial localization of DJ-1 leads to enhanced neuroprotection." J Neurosci Res **87**(1): 123-129.

Kahle, P. J., M. Neumann, et al. (2000). "Subcellular localization of wild-type and Parkinson's disease-associated mutant alpha -synuclein in human and transgenic mouse brain." J Neurosci **20**(17): 6365-6373.

Kaltschmidt, C., B. Kaltschmidt, et al. (1994). "Transcription factor NF-kappa B is activated in microglia during experimental autoimmune encephalomyelitis." J Neuroimmunol **55**(1): 99-106.

Karin, M. and Y. Ben-Neriah (2000). "Phosphorylation meets ubiquitination: the control of NF-[kappa]B activity." Annu Rev Immunol **18**: 621-663.

Karin, M. and E. Gallagher (2009). "TNFR signaling: ubiquitin-conjugated TRAFfic signals control stop-and-go for MAPK signaling complexes." Immunol Rev **228**(1): 225-240.

Kawai, T., O. Adachi, et al. (1999). "Unresponsiveness of MyD88-deficient mice to endotoxin." Immunity **11**(1): 115-122.

Kim, R. H., P. D. Smith, et al. (2005). "Hypersensitivity of DJ-1-deficient mice to 1-methyl-4-phenyl-1,2,3,6-tetrahydropyrindine (MPTP) and oxidative stress." Proc Natl Acad Sci U S A **102**(14): 5215-5220.

Kitada, T., S. Asakawa, et al. (1998). "Mutations in the parkin gene cause autosomal recessive juvenile parkinsonism." Nature **392**(6676): 605-608.

Kitada, T., S. Asakawa, et al. (2000). "Molecular cloning, gene expression, and identification of a splicing variant of the mouse parkin gene." Mamm Genome **11**(6): 417-421.

Kitazawa, M., S. Oddo, et al. (2005). "Lipopolysaccharide-induced inflammation exacerbates tau pathology by a cyclin-dependent kinase 5-mediated pathway in a transgenic model of Alzheimer's disease." J Neurosci **25**(39): 8843-8853.

Klein, R. L., R. D. Dayton, et al. (2006). "Parkin is protective for substantia nigra dopamine neurons in a tau gene transfer neurodegeneration model." Neurosci Lett **401**(1-2): 130-135.

Koenigsknecht-Talboo, J. and G. E. Landreth (2005). "Microglial phagocytosis induced by fibrillar beta-amyloid and IgGs are differentially regulated by proinflammatory cytokines." J Neurosci **25**(36): 8240-8249.

Kremlev, S. G. and C. Palmer (2005). "Interleukin-10 inhibits endotoxin-induced pro-inflammatory cytokines in microglial cell cultures." J Neuroimmunol **162**(1-2): 71-80.

Kreutzberg, G. W. (1996). "Microglia: a sensor for pathological events in the CNS." Trends Neurosci **19**(8): 312-318.

Kulms, D., Schwarts, T., (2006). NFkappaB and Cytokines. Vitamins & Hormones Interleukins. L. Gerlad, Academic Press**:** pp. 283-300.

Kurrasch, D. M., J. Huang, et al. (2004). "Quantitative real-time PCR measurement of regulators of G-protein signaling (RGS) mRNA levels in mouse tissues." Methods in Enzymology **389**: 3-15.

Lai, A. Y. and K. G. Todd (2008). "Differential regulation of trophic and proinflammatory microglial effectors is dependent on severity of neuronal injury." Glia **56**(3): 259-270.

Lang, A. E. and A. M. Lozano (1998). "Parkinson's disease. First of two parts." N Engl J Med **339**(15): 1044-1053.

LaVoie, M. J., B. L. Ostaszewski, et al. (2005). "Dopamine covalently modifies and functionally inactivates parkin." Nat Med **11**(11): 1214-1221.

Lawson, L. J., V. H. Perry, et al. (1990). "Heterogeneity in the distribution and morphology of microglia in the normal adult mouse brain." Neuroscience **39**(1): 151-170.

Ledesma, M. D., C. Galvan, et al. (2002). "Astrocytic but not neuronal increased expression and redistribution of parkin during unfolded protein stress." J Neurochem **83**(6): 1431-1440.

Lee, J. K., M. K. McCoy, et al. (2008). "Regulator of G-protein signaling 10 promotes dopaminergic neuron survival via regulation of the microglial inflammatory response." J Neurosci **28**(34): 8517-8528.

Lee, J. K., T. Tran, et al. (2009). "Neuroinflammation in Parkinson's Disease." J Neuroimmune Pharmacol.

Leroy, E., R. Boyer, et al. (1998). "The ubiquitin pathway in Parkinson's disease." Nature **395**(6701): 451-452.

LeVine, H., 3rd (1999). "Quantification of beta-sheet amyloid fibril structures with thioflavin T." Methods Enzymol **309**: 274-284.

Li, H. M., T. Niki, et al. (2005). "Association of DJ-1 with chaperones and enhanced association and colocalization with mitochondrial Hsp70 by oxidative stress." Free Radic Res **39**(10): 1091-1099.

Liao, S. L. and C. J. Chen (2001). "Differential effects of cytokines and redox potential on glutamate uptake in rat cortical glial cultures." Neurosci Lett **299**(1-2): 113-116.

Liu, B., L. Du, et al. (2000). "Naloxone protects rat dopaminergic neurons against inflammatory damage through inhibition of microglial activation and superoxide generation." J Pharmacol Exp Ther **293**(2): 607-617.

Liu, B. and J. S. Hong (2003). "Role of microglia in inflammation-mediated neurodegenerative diseases: mechanisms and strategies for therapeutic intervention." J Pharmacol Exp Ther **304**(1): 1-7.

Liu, B., L. Qin, et al. (2001). "Femtomolar concentrations of dynorphins protect rat mesencephalic dopaminergic neurons against inflammatory damage." J Pharmacol Exp Ther **298**(3): 1133-1141.

Liu, J. (1995). "Pharmacology of oleanolic acid and ursolic acid." J Ethnopharmacol **49**(2): 57-68.

Liu, Y., L. Qin, et al. (2003). "Dextromethorphan protects dopaminergic neurons against inflammation-mediated degeneration through inhibition of microglial activation." J Pharmacol Exp Ther **305**(1): 212-218.

Lorenzo, A. and B. A. Yankner (1994). "Beta-amyloid neurotoxicity requires fibril formation and is inhibited by congo red." Proc Natl Acad Sci U S A **91**(25): 12243-12247.

Lucking, C. B., A. Durr, et al. (2000). "Association between early-onset Parkinson's disease and mutations in the parkin gene. French Parkinson's Disease Genetics Study Group." N Engl J Med **342**(21): 1560-1567.

McCoy, M. K., T. N. Martinez, et al. (2006). "Blocking soluble tumor necrosis factor signaling with dominant-negative tumor necrosis factor inhibitor attenuates loss of dopaminergic neurons in models of Parkinson's disease." J Neurosci **26**(37): 9365-9375.

McCoy, M. K., K. A. Ruhn, et al. (2008). "Intranigral lentiviral delivery of dominant-negative TNF attenuates neurodegeneration and behavioral deficits in hemiparkinsonian rats." Mol Ther **16**(9): 1572-1579.

McGeer, P. L., S. Itagaki, et al. (1988). "Reactive microglia are positive for HLA-DR in the substantia nigra of Parkinson's and Alzheimer's disease brains." Neurology **38**(8): 1285-1291.

McGeer, P. L. and E. G. McGeer (2004). "Inflammation and neurodegeneration in Parkinson's disease." Parkinsonism Relat Disord **10 Suppl 1**: S3-7.

McGeer, P. L. and E. G. McGeer (2004). "Inflammation and the degenerative diseases of aging." Ann N Y Acad Sci **1035**: 104-116.

McGeer, P. L. and E. G. McGeer (2007). "Glial reactions in Parkinson's disease." Mov Disord.

McGeer, P. L. and E. G. McGeer (2008). "Glial reactions in Parkinson's disease." Mov Disord **23**(4): 474-483.

McGeer, P. L., C. Schwab, et al. (2003). "Presence of reactive microglia in monkey substantia nigra years after 1-methyl-4-phenyl-1,2,3,6-tetrahydropyridine administration." Ann Neurol **54**(5): 599-604.

McNaught, K. S., D. P. Perl, et al. (2004). "Systemic exposure to proteasome inhibitors causes a progressive model of Parkinson's disease." Ann Neurol **56**(1): 149-162.

Miller, D. W., R. Ahmad, et al. (2003). "L166P mutant DJ-1, causative for recessive Parkinson's disease, is degraded through the ubiquitin-proteasome system." Journal of Biological Chemistry **278**: 36588-36595.

Mitsumoto, A. and Y. Nakagawa (2001). "DJ-1 is an indicator for endogenous reactive oxygen species elicited by endotoxin." Free Radical Research **35**: 885-893.

Mizuno, Y., N. Hattori, et al. (2001). "Familial Parkinson's disease. Alpha-synuclein and parkin." Adv Neurol **86**: 13-21.

Mogi, M., M. Harada, et al. (1996). "Interleukin (IL)-1 beta, IL-2, IL-4, IL-6 and transforming growth factor-alpha levels are elevated in ventricular cerebrospinal fluid in juvenile parkinsonism and Parkinson's disease." Neurosci Lett **211**(1): 13-16.

Mogi, M., M. Harada, et al. (1994). "Tumor necrosis factor-alpha (TNF-alpha) increases both in the brain and in the cerebrospinal fluid from parkinsonian patients." Neurosci Lett **165**(1-2): 208-210.

Molina-Holgado, F., R. Grencis, et al. (2001). "Actions of exogenous and endogenous IL-10 on glial responses to bacterial LPS/cytokines." Glia **33**(2): 97-106.

Moore, D. J., V. L. Dawson, et al. (2003). "Genetics of Parkinson's disease: what do mutations in DJ-1 tell us?" Ann Neurol **54**(3): 281-282.

Morett, E. and P. Bork (1999). "A novel transactivation domain in parkin." Trends Biochem Sci **24**(6): 229-231.

Mortiboys, H., K. J. Thomas, et al. (2008). "Mitochondrial function and morphology are impaired in parkin-mutant fibroblasts." Ann Neurol **64**(5): 555-565.

Mosley, R. L., E. J. Benner, et al. (2006). "Neuroinflammation, Oxidative Stress and the Pathogenesis of Parkinson's Disease." Clin Neurosci Res **6**(5): 261-281.

Mrak, R. E. and W. S. Griffin (2005). "Glia and their cytokines in progression of neurodegeneration." Neurobiol Aging **26**(3): 349-354.

Mrak, R. E. and W. S. Griffin (2007). "Common inflammatory mechanisms in Lewy body disease and Alzheimer disease." J Neuropathol Exp Neurol **66**(8): 683-686.

Nagatsu, T. and M. Sawada (2005). "Inflammatory process in Parkinson's disease: role for cytokines." Curr Pharm Des **11**(8): 999-1016.

Nakajima, K. and S. Kohsaka (2004). "Microglia: neuroprotective and neurotrophic cells in the central nervous system." Curr Drug Targets Cardiovasc Haematol Disord **4**(1): 65-84.

Nakajima, K., Y. Tohyama, et al. (2001). "Ability of rat microglia to uptake extracellular glutamate." Neurosci Lett **307**(3): 171-174.

Narendra, D., A. Tanaka, et al. (2008). "Parkin is recruited selectively to impaired mitochondria and promotes their autophagy." J Cell Biol **183**(5): 795-803.

Nimmerjahn, A., F. Kirchhoff, et al. (2005). "Resting microglial cells are highly dynamic surveillants of brain parenchyma in vivo." Science **308**(5726): 1314-1318.

Ogata, A., K. Tashiro, et al. (1997). "A rat model of Parkinson's disease induced by Japanese encephalitis virus." J Neurovirol **3**(2): 141-147.

Olzmann, J. A., K. Brown, et al. (2004). "Familial Parkinson's disease-associated L166P mutation disrupts DJ-1 protein folding and function." Journal of Biological Chemistry **279**: 8506-8515.

Ouchi, Y., E. Yoshikawa, et al. (2005). "Microglial activation and dopamine terminal loss in early Parkinson's disease." Ann Neurol **57**(2): 168-175.

Palacino, J. J., D. Sagi, et al. (2004). "Mitochondrial dysfunction and oxidative damage in parkin-deficient mice." J Biol Chem **279**(18): 18614-18622.

Park, J., G. Lee, et al. (2009). "The PINK1-Parkin pathway is involved in the regulation of mitochondrial remodeling process." Biochem Biophys Res Commun **378**(3): 518-523.

Park, J., S. B. Lee, et al. (2006). "Mitochondrial dysfunction in Drosophila PINK1 mutants is complemented by parkin." Nature **441**(7097): 1157-1161.

Pavese, N., A. Gerhard, et al. (2006). "Microglial activation correlates with severity in Huntington disease: a clinical and PET study." Neurology **66**(11): 1638-1643.

Paxinos, G., Franklin, K.B.J. (2001). The Mouse Brain in Stereotaxic Coordinates. San Diego, CA, Academic Press.

Perez, F. A., W. R. Curtis, et al. (2005). "Parkin-deficient mice are not more sensitive to 6-hydroxydopamine or methamphetamine neurotoxicity." BMC Neurosci **6**: 71.

Persson, M., M. Brantefjord, et al. (2005). "Lipopolysaccharide increases microglial GLT-1 expression and glutamate uptake capacity in vitro by a mechanism dependent on TNF-alpha." Glia **51**(2): 111-120.

Pham, T. T., F. Giesert, et al. (2009). "DJ-1-deficient mice show less TH-positive neurons in the ventral tegmental area and exhibit non-motoric behavioural impairments." Genes Brain Behav.

Polymeropoulos, M. H., C. Lavedan, et al. (1997). "Mutation in the alpha-synuclein gene identified in families with Parkinson's disease." Science **276**(5321): 2045-2047.

Poole, A. C., R. E. Thomas, et al. (2008). "The PINK1/Parkin pathway regulates mitochondrial morphology." Proc Natl Acad Sci U S A **105**(5): 1638-1643.

Pramstaller, P. P., M. G. Schlossmacher, et al. (2005). "Lewy body Parkinson's disease in a large pedigree with 77 Parkin mutation carriers." Ann Neurol **58**(3): 411-422.

Rail, D., C. Scholtz, et al. (1981). "Post-encephalitic Parkinsonism: current experience." J Neurol Neurosurg Psychiatry **44**(8): 670-676.

Ransohoff, R. M. and V. H. Perry (2009). "Microglial physiology: unique stimuli, specialized responses." Annu Rev Immunol **27**: 119-145.

Rentzos, M., C. Nikolaou, et al. (2009). "Circulating interleukin-10 and interleukin-12 in Parkinson's disease." Acta Neurol Scand **119**(5): 332-337.

Reynolds, A., C. Laurie, et al. (2007). "Oxidative stress and the pathogenesis of neurodegenerative disorders." Int Rev Neurobiol **82**: 297-325.

Rezai-Zadeh, K., D. Gate, et al. (2009). "CNS infiltration of peripheral immune cells: d-day for neurodegenerative disease?" J Neuroimmune Pharmacol **4**(4): 462-475.

Rimaniol, A. C., S. Haik, et al. (2000). "Na+-dependent high-affinity glutamate transport in macrophages." J Immunol **164**(10): 5430-5438.

Rubio de la Torre, E., B. Luzon-Toro, et al. (2009). "Combined kinase inhibition modulates parkin inactivation." Hum Mol Genet **18**(5): 809-823.

Saijo, K., B. Winner, et al. (2009). "A Nurr1/CoREST pathway in microglia and astrocytes protects dopaminergic neurons from inflammation-induced death." Cell **137**(1): 47-59.

Samii, A., M. Etminan, et al. (2009). "NSAID use and the risk of Parkinson's disease: systematic review and meta-analysis of observational studies." Drugs Aging **26**(9): 769-779.

Sanchez-Pernaute, R., A. Ferree, et al. (2004). "Selective COX-2 inhibition prevents progressive dopamine neuron degeneration in a rat model of Parkinson's disease." J Neuroinflammation **1**(1): 6.

Seth, R. B., L. Sun, et al. (2005). "Identification and characterization of MAVS, a mitochondrial antiviral signaling protein that activates NF-kappaB and IRF 3." Cell **122**(5): 669-682.

Sha, D., L. S. Chin, et al. (2010). "Phosphorylation of parkin by Parkinson disease-linked kinase PINK1 activates parkin E3 ligase function and NF-kappaB signaling." Hum Mol Genet **19**(2): 352-363.

Shavali, S., C. K. Combs, et al. (2006). "Reactive macrophages increase oxidative stress and alpha-synuclein nitration during death of dopaminergic neuronal cells in co-culture: relevance to Parkinson's disease." Neurochem Res **31**(1): 85-94.

Shen, J. and M. R. Cookson (2004). "Mitochondria and dopamine: new insights into recessive parkinsonism." Neuron **43**(3): 301-304.

Sherer, T. B., R. Betarbet, et al. (2002). "An in vitro model of Parkinson's disease: linking mitochondrial impairment to altered alpha-synuclein metabolism and oxidative damage." J Neurosci **22**(16): 7006-7015.

Sherer, T. B., J. H. Kim, et al. (2003). "Subcutaneous rotenone exposure causes highly selective dopaminergic degeneration and alpha-synuclein aggregation." Exp Neurol **179**(1): 9-16.

Shimura, H., N. Hattori, et al. (2000). "Familial Parkinson disease gene product, parkin, is a ubiquitin-protein ligase." Nat Genet **25**(3): 302-305.

Shimura, H., N. Hattori, et al. (1999). "Immunohistochemical and subcellular localization of Parkin protein: absence of protein in autosomal recessive juvenile parkinsonism patients." Ann Neurol **45**(5): 668-672.

Shimura, H., M. G. Schlossmacher, et al. (2001). "Ubiquitination of a new form of alpha-synuclein by parkin from human brain: implications for Parkinson's disease." Science **293**(5528): 263-269.

Shoji, H., M. Watanabe, et al. (1993). "Japanese encephalitis and parkinsonism." J Neurol **240**(1): 59-60.

Shults, C. W. (2006). "Lewy bodies." Proc Natl Acad Sci U S A **103**(6): 1661-1668.

Silvestri, L., V. Caputo, et al. (2005). "Mitochondrial import and enzymatic activity of PINK1 mutants associated to recessive parkinsonism." Hum Mol Genet **14**(22): 3477-3492.

Solano, R. M., M. J. Casarejos, et al. (2008). "Glial dysfunction in parkin null mice: effects of aging." J Neurosci **28**(3): 598-611.

Solano, R. M., J. Menendez, et al. (2006). "Midbrain neuronal cultures from parkin mutant mice are resistant to nitric oxide-induced toxicity." Neuropharmacology **51**(2): 327-340.

Spillantini, M. G., R. A. Crowther, et al. (1998). "alpha-Synuclein in filamentous inclusions of Lewy bodies from Parkinson's disease and dementia with lewy bodies." Proc Natl Acad Sci U S A **95**(11): 6469-6473.

Streit, W. J. (2002). "Microglia as neuroprotective, immunocompetent cells of the CNS." Glia **40**(2): 133-139.

Streit, W. J. (2006). "Microglial senescence: does the brain's immune system have an expiration date?" Trends Neurosci **29**(9): 506-510.

Streit, W. J. and Q. S. Xue (2009). "Life and death of microglia." J Neuroimmune Pharmacol **4**(4): 371-379.

Supakar, P. C., M. H. Jung, et al. (1995). "Nuclear factor kappa B functions as a negative regulator for the rat androgen receptor gene and NF-kappa B

activity increases during the age-dependent desensitization of the liver." J Biol Chem **270**(2): 837-842.

Taira, T., Y. Saito, et al. (2004). "DJ-1 has a role in antioxidative stress to prevent cell death." EMBO Report **5**: 213-218.

Tansey, M. G., M. K. McCoy, et al. (2007). "Neuroinflammatory mechanisms in Parkinson's disease: potential environmental triggers, pathways, and targets for early therapeutic intervention." Exp Neurol **208**(1): 1-25.

Tansey, M. G. a. W.-C., T. (2008). Cytokines in CNS Inflammation and Disease. Central Nervous System Diseases and Inflammation. T. E. C. Lane, M.; Bergmann, C.; Wyss-Coray, T. . New York, Springer**:** 59-106.

Tao, X. and L. Tong (2003). "Crystal structure of human DJ-1, a protein associated with early onset Parkinson's disease." J Biol Chem **278**(33): 31372-31379.

Taubenberger, J. K., A. H. Reid, et al. (1997). "Initial genetic characterization of the 1918 "Spanish" influenza virus." Science **275**(5307): 1793-1796.

Thimmulappa, R. K., R. J. Fuchs, et al. (2007). "Preclinical evaluation of targeting the Nrf2 pathway by triterpenoids (CDDO-Im and CDDO-Me) for protection from LPS-induced inflammatory response and reactive oxygen species in human peripheral blood mononuclear cells and neutrophils." Antioxid Redox Signal **9**(11): 1963-1970.

Thimmulappa, R. K., C. Scollick, et al. (2006). "Nrf2-dependent protection from LPS induced inflammatory response and mortality by CDDO-Imidazolide." Biochem Biophys Res Commun **351**(4): 883-889.

Thomas, B., R. von Coelln, et al. (2007). "MPTP and DSP-4 susceptibility of substantia nigra and locus coeruleus catecholaminergic neurons in mice is independent of parkin activity." Neurobiol Dis **26**(2): 312-322.

Tomas-Camardiel, M., I. Rite, et al. (2004). "Minocycline reduces the lipopolysaccharide-induced inflammatory reaction, peroxynitrite-mediated nitration of proteins, disruption of the blood-brain barrier, and damage in the nigral dopaminergic system." Neurobiol Dis **16**(1): 190-201.

Trinh, K., K. Moore, et al. (2008). "Induction of the phase II detoxification pathway suppresses neuron loss in Drosophila models of Parkinson's disease." J Neurosci **28**(2): 465-472.

Valente, E. M., P. M. Abou-Sleiman, et al. (2004). "Hereditary early-onset Parkinson's disease caused by mutations in PINK1." Science **304**(5674): 1158-1160.

Vallabhapurapu, S. and M. Karin (2009). "Regulation and function of NF-kappaB transcription factors in the immune system." Annu Rev Immunol **27**: 693-733.

van der Brug, M. P., J. Blackinton, et al. (2008). "RNA binding activity of the recessive parkinsonism protein DJ-1 supports involvement in multiple cellular pathways." Proc Natl Acad Sci U S A **105**(29): 10244-10249.

Venkateswaran, A., J. J. Repa, et al. (2000). "Human white/murine ABC8 mRNA levels are highly induced in lipid-loaded macrophages. A transcriptional role for specific oxysterols." J Biol Chem **275**(19): 14700-14707.

Waak, J., S. S. Weber, et al. (2009). "Regulation of astrocyte inflammatory responses by the Parkinson's disease-associated gene DJ-1." FASEB J **23**(8): 2478-2489.

Wahner, A. D., J. S. Sinsheimer, et al. (2007). "Inflammatory cytokine gene polymorphisms and increased risk of Parkinson disease." Arch Neurol **64**(6): 836-840.

Wang, J. Y., L. L. Wen, et al. (2006). "Dual effects of antioxidants in neurodegeneration: direct neuroprotection against oxidative stress and indirect protection via suppression of glia-mediated inflammation." Curr Pharm Des **12**(27): 3521-3533.

Wang, M., T. Suzuki, et al. (2001). "Developmental changes in the expression of parkin and UbcR7, a parkin-interacting and ubiquitin-conjugating enzyme, in rat brain." J Neurochem **77**(6): 1561-1568.

Wersinger, C. and A. Sidhu (2002). "Inflammation and Parkinson's disease." Curr Drug Targets Inflamm Allergy **1**(3): 221-242.

Wersinger, C. and A. Sidhu (2006). "An inflammatory pathomechanism for Parkinson's disease?" Curr Med Chem **13**(5): 591-602.

Whitton, P. S. (2007). "Inflammation as a causative factor in the aetiology of Parkinson's disease." Br J Pharmacol **150**(8): 963-976.

Wyss-Coray, T. (2006). "Inflammation in Alzheimer disease: driving force, bystander or beneficial response?" Nat Med **12**(9): 1005-1015.

Xu, J., N. Zhong, et al. (2005). "The Parkinson's disease-associated DJ-1 protein is a transcriptional co-activator that protects against neuronal apoptosis." Hum Mol Genet **14**(9): 1231-1241.

Xu, L. G., Y. Y. Wang, et al. (2005). "VISA is an adapter protein required for virus-triggered IFN-beta signaling." Mol Cell **19**(6): 727-740.

Yamada, T., P. L. McGeer, et al. (1992). "Lewy bodies in Parkinson's disease are recognized by antibodies to complement proteins." Acta Neuropathol **84**(1): 100-104.

Yamaguchi, H. and J. Shen (2007). "Absence of dopaminergic neuronal degeneration and oxidative damage in aged DJ-1-deficient mice." Mol Neurodegener **2**: 10.

Yamamoto, A., A. Friedlein, et al. (2005). "Parkin phosphorylation and modulation of its E3 ubiquitin ligase activity." J Biol Chem **280**(5): 3390-3399.

Yamamura, Y., N. Hattori, et al. (2000). "Autosomal recessive early-onset parkinsonism with diurnal fluctuation: clinicopathologic characteristics and molecular genetic identification." Brain Dev **22 Suppl 1**: S87-91.

Yang, W., L. Chen, et al. (2007). "Paraquat induces dopaminergic dysfunction and proteasome impairment in DJ-1-deficient mice." Hum Mol Genet **16**(23): 2900-2910.

Yang, Y., S. Gehrke, et al. (2006). "Mitochondrial pathology and muscle and dopaminergic neuron degeneration caused by inactivation of Drosophila Pink1 is rescued by Parkin." Proc Natl Acad Sci U S A **103**(28): 10793-10798.

Yao, D., Z. Gu, et al. (2004). "Nitrosative stress linked to sporadic Parkinson's disease: S-nitrosylation of parkin regulates its E3 ubiquitin ligase activity." Proc Natl Acad Sci U S A **101**(29): 10810-10814.

Yore, M. M., K. T. Liby, et al. (2006). "The synthetic triterpenoid 1-[2-cyano-3,12-dioxooleana-1,9(11)-dien-28-oyl]imidazole blocks nuclear factor-kappaB activation through direct inhibition of IkappaB kinase beta." Mol Cancer Ther **5**(12): 3232-3239.

Zetterstrom, R. H., L. Solomin, et al. (1997). "Dopamine neuron agenesis in Nurr1-deficient mice." Science **276**(5310): 248-250.

Zhang, J., D. R. Goodlett, et al. (2005). "Quantitative proteomic analysis of age-related changes in human cerebrospinal fluid." Neurobiol Aging **26**(2): 207-227.

Zhang, L., V. L. Dawson, et al. (2006). "Role of nitric oxide in Parkinson's disease." Pharmacol Ther **109**(1-2): 33-41.

Zhang, L., M. Shimoji, et al. (2005). "Mitochondrial localization of the Parkinson's disease related protein DJ-1: implications for pathogenesis." Hum Mol Genet **14**(14): 2063-2073.

Zhang, Y., J. Gao, et al. (2000). "Parkin functions as an E2-dependent ubiquitin-protein ligase and promotes the degradation of the synaptic vesicle-associated protein, CDCrel-1." Proc Natl Acad Sci U S A **97**(24): 13354-13359.

Zhao, C., Z. Ling, et al. (2007). "TNF-alpha knockout and minocycline treatment attenuates blood-brain barrier leakage in MPTP-treated mice." Neurobiol Dis **26**(1): 36-46.

Zhu, X. R., L. Maskri, et al. (2007). "Non-motor behavioural impairments in parkin-deficient mice." Eur J Neurosci **26**(7): 1902-1911.